ABSTRACT

MAURER, CHRISTINE CAROL. Field Study and Modeling of an Unglazed Transpired Solar Collector System. (Under the direction of Richard R. Johnson.)

An unglazed transpired solar collector (UTC) consists of a perforated metal cladding mounted on the south side of a structure. Outdoor air is drawn through the collector for low temperature heating including preheating ventilation air, preheating combustion air, and crop drying. While UTC systems are more commonly used in the Northeast U.S. and Canada, they have not been installed as much in the southeast because of the short heating season.

The NC Solar Center installed a data acquisition system to monitor the performance of a UTC system at a manufacturing facility in North Carolina. The main objectives of this project were to evaluate the performance of the components of the system and determine the energy collected and potential monetary savings from the system. The case study was used to understand the principles behind operation of these collectors and compare the monitoring results to previous models of collector performance. A simulation of a UTC system was built in TRNSYS and used to look at the potential for transpired collectors in warmer climates than where UTCs are typically installed.

A heat transfer analysis was done to look at the possibility of the collector causing additional heat gain to the building in the summer. The results show that it is possible that the collector causes unwanted heat gain in the summer. Additional investigation could be done to characterize the flow conditions in bypass mode and validate theory with experimental data.

Despite the short heating season, some industrial or commercial buildings could still benefit from the technology. The success of the technology depends on site characteristics and building conditions; therefore, transpired collector systems must be considered on a case

by case basis. Even if the system works well, space heating is only a minor portion of the energy used in industrial facilities in North Carolina.

FIELD STUDY AND MODELING OF AN UNGLAZED TRANSPIRED SOLAR COLLECTOR SYSTEM

by
CHRISTINE C. MAURER

A thesis submitted to the Graduate Faculty of
North Carolina State University
in partial fulfillment of the
requirements for the Degree of
Master of Science

MECHANICAL AND AEROSPACE ENGINEERING

Raleigh

2004

APPROVED BY:

_____ _____

_____
Chair of Advisory Committee

PERSONAL BIOGRAPHY

Christine Carol (CC) Maurer was born on November 30, 1976 in Livingston, NJ. She was raised in Greensboro, NC and graduated from Walter Hines Page High School in 1994. She completed a Bachelor of Science degree in Environmental Studies with a focus on Pollution Control at the University of North Carolina at Asheville in 2000. While at the University of North Carolina at Asheville (UNCA), she worked as a lab assistant at the Environmental Quality Institute, a research facility for pollutants in drinking water and stream water. She also interned with a local non-profit organization to analyze the energy efficiency projects on the UNCA campus.

. She began at the NC Solar Center in May 2001 to research moisture control practices in crawlspaces in the southeast in conjunction with Advanced Energy Corporation. She began taking classes towards a Master of Science Degree in Mechanical Engineering in 2002 and started working on this thesis project monitoring the performance and effectiveness of a transpired solar collector system at an industrial facility in North Carolina. While at the Solar Center, she has also assisted fellow Solar Center engineers with field work on photovoltaic and solar thermal systems and has worked on renewable energy demonstration projects at the NCSU Solar House.

CC has recently become involved with the NC State Sustainability Coalition and aspires to increase energy efficiency and renewable energy awareness and implementation on NC State campus. In her free time, CC enjoys sewing and building projects, playing the guitar, gardening, biking, and taking advantage of any opportunity to be outdoors in the sunshine.

ACKNOWLEDGEMENTS

Thank you to my parents and sister for all their love and support. I could not have made it through this project without their inspirational talks.

Thank you also to my coworkers at the NC Solar Center, especially Shawn Fitzpatrick and Kurt Creamer for all their technical advice and help doing the monitoring project. They have been great mentors while at the Solar Center. Also, thank you to Carole Coble for her interesting conversations while sharing office space at the NC Solar House for the last three years.

I would like to thank Dr. Richard Johnson for his patience and advice on approaching problems that arose throughout my thesis. Thanks also to Dr. Herbert Eckerlin for all his years of dedication to the Solar House and Solar Center and for helping me through my first teaching experience. I also must thank Will Hooker for inspiring me and helping me grow in both my personal and academic life while here at NC State.

TABLE OF CONTENTS

LIST OF TABLES vi

LIST OF FIGURES vii

NOMENCLATURE viii

1 INTRODUCTION 1

1.1 Background and Description of Transpired Collector Systems 1
1.2 Study Objectives 2

2 LITERATURE REVIEW AND BACKGROUND ON TRANSPIRED COLLECTORS 4

2.1 Heat Transfer Theory 4
2.2 Laboratory Experiments and Computer Modeling 5
2.3 Demonstration Projects and Validation Testing 8

3 MONITORING STUDY 10

3.1 Details about the Intek Solarwall® System 10
3.2 Monitoring Equipment Description 13
3.3 Calculations for Monitoring Data 17
3.4 Empirical Equations of Heat Transfer 19
3.5 Pressure Drop Estimation through Collector and Plenum 25
3.5.1 Example Pressure Drop Calculation 28
3.6 Results from Monitoring Data 29
3.6.1 Temperatures Measurements 30
3.6.2 Experimental and Empirical Efficiency Comparison 34
3.7 Economic Evaluation 37

4 TRNSYS SIMULATION 38

4.1 Energy balance for TRNSYS simulation 39
4.2 TRNSYS Simulation Results 46

5 HEAT TRANSFER ANALYSIS OF PLENUM DURING BYPASS CONDITIONS 57

5.1 Case One: A Sunlit Wall 57
5.2 Case Two: South Facing Wall with Transpired Collector 60
5.3 Results from Heat Transfer Analysis during Bypass Conditions 63

6 ECONOMIC ANALYSIS AND APPLICATION IN NC 66

6.1 Economics 66
6.2 Application in North Carolina 68

7 DISCUSSION 70

7.1 Monitoring Results 70
7.2 TRNSYS Analysis 71
7.3 Heat Transfer During Bypass Conditions 72
7.4 Economics and Application in North Carolina 73

8 CONCLUSIONS 74

REFERENCES 76

APPENDIX A 78

APPENDIX B.....**87**

APPENDIX C **90**

LIST OF TABLES

TABLE 3.2.1: SENSOR DESCRIPTION FOR DATA ACQUISITION SYSTEM....14
TABLE 3.2.1: SENSOR DESCRIPTION FOR DATA ACQUISITION SYSTEM (CONT'D) 15
TABLE 3.3.1: DEFINITION OF VARIABLES USED IN CALCULATIONS OF SOLAR RADIATION ON A TILTED SURFACE. .18
TABLE 3.5.1 PARAMETERS USED TO PREDICT STATIC PRESSURE 28
TABLE 4.2.1 LIST OF PARAMETER VALUES IN TRNSYS SIMULATION 48
TABLE 4.2.2 LIST OF INPUT VALUES IN TRNSYS SIMULATION 48
TABLE 4.2.3: COMPARISON OF POTENTIAL HEAT GAIN AND ENERGY SAVINGS BETWEEN NEW AND SUMMERS TRNSYS COMPONENT MODEL. 49
TABLE 5.3.1: PARAMETERS USED IN HEAT TRANSFER ANALYSIS OF PLENUM DURING BYPASS CONDITIONS 64
TABLE 5.3.2: ACTUAL DATA USED IN HEAT TRANSFER ANALYSIS OF PLENUM DURING BYPASS CONDITIONS 64
TABLE 6.1.1 YEARLY MONETARY SAVINGS FROM THE ENERGY SAVED BY USING UTC SYSTEM OVER CONVENTIONAL GAS HEATING 67

LIST OF FIGURES

FIGURE 1.1.1 DIAGRAM OF BASIC COMPONENTS IN TRANSPIRED SOLAR COLLECTOR SYSTEM. 1
FIGURE 3.1.1 (LEFT) TRANSPIRED COLLECTOR MOUNTED ON SOUTH SIDE OF FABRIC WAREHOUSE 11
FIGURE 3.1.2 (LEFT) AIR DISTRIBUTION FAN AND FLEXIBLE FABRIC DUCT WHICH DELIVERS AIR AT CEILING. 11
FIGURE 3.1.3 (RIGHT) ORIGINAL FAN CONTROLS WHICH REGULATE OUTLET TEMPERATURE WITH MODULATING DAMPER. 11
FIGURE 3.2.1 (ABOVE): WARM AIR DISTRIBUTION DUCT WITH SENSORS TO MEASURE AIR FLOW AND TEMPERATURE. 14
FIGURE 3.2.2 (RIGHT): DATA ACQUISITION SYSTEM WITH TRANSPIRED COLLECTOR IN BACKGROUND. 14
FIGURE 3.3.1 FLOWS IN FAN MIXING CHAMBER 17
FIGURE 3.4.1 BASIC ENERGY BALANCE ON TRANSPIRED COLLECTOR. 20
FIGURE 3.6.1 TEMPERATURES OF FAN INLETS FROM THE WALL AND CEILING, FAN OUTLET, AND AMBIENT OUTDOOR 31
FIGURE 3.6.2 TEMPERATURES RISE IN COLLECTOR COMPARED TO SOLAR INSOLATION. 32
FIGURE 3.6.3 TEMPERATURE DIFFERENCE BETWEEN CEILING AND AMBIENT INDOOR NEAR FLOOR LEVEL. 33
FIGURE 3.6.4 TEMPERATURE ON BOTH FAN OUTLETS 33
FIGURE 3.6.5 EFFICIENCY VERSUS SOLAR RADIATION INCIDENT ON THE TRANSPIRED COLLECTOR 35
FIGURE 3.6.6 EFFICIENCY VERSUS MEASURED PLATE TEMPERATURE, AMBIENT TEMPERATURE, AND SOLAR INSOLATION 36
FIGURE 3.6.7: MEASURED AND MODELED INSTANTANEOUS EFFICIENCY VERSUS WIND SPEED 36
FIGURE 4.1.1: ENERGY BALANCE ON THE COLLECTOR AND THE WALL. 39
FIGURE 4.1.2: ENERGY BALANCE ON A BUILDING WITH VENTILATION SYSTEM 41
FIGURE 4.1.3: ENERGY BALANCE ON A BUILDING WITH TRANSPIRED COLLECTOR VENTILATION SYSTEM 43
FIGURE 4.1.4: REDEFINED ENERGY BALANCE ON A BUILDING WITH TRANSPIRED COLLECTOR VENTILATION SYSTEM TO SHOW AUXILIARY HEATING 45
FIGURE 4.2.1: COMPARISON OF POTENTIAL HEAT GAIN AND ENERGY SAVINGS FOR NEGLECTED CONVECTIVE LOSSES (CF=0) AND FOR THE INCLUSION OF CONVECTIVE LOSSES THROUGH THE COLLECTOR (CF=5) AT A RECOMMENDED FLOW RATE 51
FIGURE 4.2.2: COMPARISON OF POTENTIAL HEAT GAIN AND ENERGY SAVINGS FOR NEGLECTED CONVECTIVE LOSSES (CF=0) AND FOR THE INCLUSION OF CONVECTIVE LOSSES AT A LOWER THAN RECOMMENDED FLOW RATE 51
FIGURE 4.2.3: POTENTIAL HEAT GAIN AND ENERGY SAVINGS CHANGING MAXIMUM FLOW THROUGH THE COLLECTOR WITH THE MINIMUM FLOW CONSTANT 53
FIGURE 4.2.4: POTENTIAL HEAT GAIN AND ENERGY SAVINGS CHANGING FLOW THROUGH THE COLLECTOR 53
FIGURE 4.2.5: ENERGY SAVINGS DEPENDENT ON ROOM TEMPERATURE 54
FIGURE 4.2.8: SOLAR FRACTION FOR THE POTENTIAL HEAT GAIN AND ENERGY SAVINGS FROM TRANSPIRED COLLECTOR SYSTEM 56
FIGURE 5.1.1: RESISTANCE ANALOGY NETWORK FOR THE HEAT TRANSFER THROUGH WALL EXPOSED TO SOLAR RADIATION. 58
FIGURE 5.2.1: RESISTANCE ANALOGY NETWORK FOR THE HEAT TRANSFER THROUGH WALL WITH TRANSPIRED COLLECTOR 60
FIGURE 6.1.1 ESTIMATED LIFE CYCLE SAVINGS BASED ON FIRST YEAR FUEL SAVINGS FOR TRANSPIRED COLLECTOR SYSTEM 68

NOMENCLATURE

a = experimentally determined constant by Van Decker = 1.733

A = the plate surface area minus the hole area (m^2)

A_C = Collector area used for life cycle cost (m^2)

A_p=Projected area of collector (ft^2 or m^2)

A_{plen} =Cross sectional area of plenum (m^2 or ft^2)

A_d = Cross sectional area of duct (ft^2 or m^2)

A_s = Surface area of collector (ft^2 or m^2)

A_{wall} = wall area = projected area of collector

c = experimentally determined constant by Van Decker = 0.004738

C_A = Cost of equipment dependent on collector area ($)

C_E = Cost of equipment not dependent on collector area ($)

C_f = Corrugation factor

$C_{F1}L\mathcal{F}$ = Cost of fuel times the heating load and solar fraction ($)

C_p = Specific heat of air (0.24 BTU/lbm/R or 1007 J/kg/K)

D = hole diameter (m)

D_{plen} = Plenum depth (m)

e = experimentally determined constant by Van Decker = 0.2273

f = experimentally determined constant by Van Decker = 0.02136

f = frictional constant

F_{cs} = View factor from collector to sky = 0.5

F_{cg} = View factors from collector to ground = 0.5

g = gravitational constant (9.81 m/s^2 or 32.2 ft/s^2)

Gr = Grashoff number

h_{avg} = average distance air travels in plenum (m)

h_r = the linearized radiation heat loss coefficient (W/m^2K)

h_c = convection heat transfer coefficient for losses from collector (W/m^2K)

$h_{conv,w\text{-}a}$ =forced convective heat transfer coefficient between wall and air in plenum (W/m^2K)

$h_{conv,nat,\ in}$ = convective heat transfer coefficient from wall to air in room (W/m^2K)

$h_{conv,nat,out}$ = natural convective heat transfer coefficient from wall to air in plenum (W/m^2K)

$h_{conv,for,out}$ = forced convective heat transfer coefficient from wall to air outside(W/m^2K)

$h_{conv,plen}$ = convective heat transfer coefficient from wall to air in plenum for bypass conditions (W/m^2K)

$h_{conv,\ loss,\ tot}$ = total convective heat transfer coefficient between wall and outside air (W/m^2K)

h_o = ASHRAE recommended total convective heat transfer coefficient between wall and outside air (W/m^2K)

$h_{rad,loss}$ = the linearized radiation heat loss coefficient for wall to outside (W/m^2K)

h_{c-w}= the linearized radiation heat loss coefficient from collector to wall (W/m^2K)

H= collector height (m)

I_T = Solar radiation incident on tilted collector (W/m^2 or $BTU/hr/ft^2$)

k = thermal conductivity (W/mK)

L = length (height) of collector for heat transfer analsysis

LCS=Life Cycle Savings ($)

L_{loc} = longitude of location

L_{st} = Standard longitude

$\dot{m}_{ceil}$ = mass flow of recirculated air into fan from ceiling (lbm/s or kg/s)

$\dot{m}_{tot}$ = mass flow rate of the fan outlet (lbm/s or kg/s)

$\dot{m}_{\min}$ = minimum amount of air flow through the collector (kg/s)

$\dot{m}_{coll}$ or $\dot{m}_{wall}$ = mass flow into fan from wall or collector (lbm/s or kg/s)

NTU= Number of transfer units

Nu_D = Empirical Nusselt number for a transpired collector

Nu_L = Nusselt number based on collector height (definition varies for different cases)

P = hole pitch in meters

P_1 = ratio of life cycle cost savings to first year fuel cost savings

P_2 = ratio of life cycle expenditures incurred because of additional capital investment

P_{abs} = absolute Pressure (inches water column)

P_{amb} = ambient pressure (1013 mbar)

Per_{plen} = perimeter of plenum (m)

P_{fan} = estimated fan power (W)

Pr = Prandtl number

ΔP_{acc} = Pressure drop in plenum due to acceleration of the air (Pa)

ΔP_{buoy} = Pressure drop in plenum due to buoyancy (Pa)

ΔP_{coll} = Pressure drop in transpired collector (Pa)

ΔP_{fric} = Pressure drop in plenum due to friction (Pa)

ΔP_{tot} = Total pressure drop in transpired collector and plenum (Pa)

Ra_L = Rayleigh number (definition varies for different cases)

Re_L = Reynolds number based on collector height and wind

Re_b = Reynolds number based on hole velocity and pitch

Re_W = Reynolds number based on wind and pitch

Re_D = Reynolds number on hole velocity and diameter

Re_h = Reynolds number based on hole velocity and diameter

Re_s = Reynolds number based on suction velocity and pitch

R_{cond} = Conductive resistance through wall (m^2K/W)

R_{loss} = Total heat loss resistance from wall to outside air (m^2K/W)

R_{plen} = Total heat loss resistance from wall to plenum air (m^2K/W)

R_{rad} = Radiative resistance from wall to surroundings (m^2K/W)

$Q_{aux,tran}$ = Auxiliary heating required for building with transpired collector (W)

$Q_{bldg,base}$ = heating required for a building with no transpired collector system (W)

$Q_{bldg,load}$ = Heat load on the building from not including ventilation (W)

$Q_{bldg,loss}$ = heat loss from building (W)

$Q_{cond,diff}$ =Difference in heat conduction through the south wall due to transpired collector (W)

$Q_{cond,tran}$ = heat loss from building by conduction through wall with a transpired collector (W)

$Q_{conv,loss}$ = convective heat loss (BTU/hr or W)

$Q_{conv,c-a}$ = convective heat transfer from collector to air (BTU/hror W)

$Q_{conv,w-a}$= convective heat transfer between wall and air (BTU/hr or W)

$Q_{cond,wall}$ = conduction through from room to plenum through inside wall (BTU/hr or W)

Q_{del} = measured heat delivered to the building from the transpired collector (W or BTU/hr)

$Q_{in,abs}$ = solar radiation absorbed by the collector (BTU/hr or W)

Q_{int} = internal heat gain to the building (W)

$Q_{rad,w\text{-}c}$ = radiative heat transfer between wall and collector (BTU/hr or W)

$Q_{rad,loss}$ = radiative heat loss (BTU/hr or W)

Q_{save} = Energy savings (W)

$\dot{Q}_{out}$ = Volumetric airflow from fan outlet (cfm)

S= plenum depth (m)

t = plate thickness (m)

T_{amb} = Temperature of ambient air (K)

$T_{avg,wall}$ = Average temperature of heat loss for the wall (K)

T_{avg}= the average temperature for heat loss

T_{ceil} = temperature of air entering fan from ceiling (^oF)

T_{coll} = Surface temperature of collector (K)

T_{dp} = Dew point temperature (C)

T_{gr} = Ground temperature (K or R)

t_{hr} = hour from midnight (hr)

T_{mix} = Temperature of mixed air (K)

T_{out} = Temperature of outlet air (R or K)

$T_{out,coll}$= temperature of air leaving collector and entering fan from collector (^oF)

$T_{out,fanl}$= temperature of air leaving fan and entering room (^oF)

T_{plen} = Plenum air temperature (K)

T_{recirc} = Recirculated air temperature (K)

T_{room} =Inside room temperature (K)

T_{sky} = Sky temperature (K or R)

T_{solair} = Solar air temperature (K)

T_{sup} = Supply temperature needed to maintain constant building temperature

T_{sur} = the average temperature of the surroundings (K)

$T_{wall,1}$ = Outer wall temperature for case 1 (K)

$T_{wall,2}$ = Outer wall temperature for case 2 (K)

$T_{wall,o}$ = temperature of outer inside wall surface (K)

U_{wall} = overall heat transfer coefficient for the wall behind transpired collector (W/m^2K)

U_{cond} = overall heat transfer coefficient for the wall behind transpired collector including convection to room(W/m^2K)

$(UA)_{wall}$ = overall heat transfer coefficient area product for the wall behind transpired collector (W/K)

$(UA)_b$ = overall heat transfer coefficient area product for the building (W/m^2K)

U_{coll} =the overall heat transfer coefficient of the collector based on the log mean temperature difference (W/m^2K)

U_∞ = wind speed (m/s)

V_{out}= Outlet velocity (m/s)

V_{plen} = suction face velocity in (ft /s or m/s) defined by flow rate through the collector divided by projected collector area)

V_h = the hole velocity (m/s)

$V_{plen,max}$ = maximum velocity in plenum (m/s)

$V_{plen,avg}$ = average velocity in plenum (m/s)

$\dot{W}_{in}$ = work into fan that is not used to move air (heat added to system) (W or BTU/hr)

W_{coll} = Collector width (m)

Greek Symbols

α_{coll} = absorptivity of collector

α = thermal diffusivity

βc = collector tilt

β = volumetric thermal expansion coefficient (1/K)

ε_{HX} = heat exchange effectiveness of collector

ε_T = total heat exchange effectiveness as defined by Van Decker (2001)

ε_f = front of plate effectiveness

ε_h = hole effectiveness

ε_b = back of plate effectiveness

ε_{coll} = Collector surface emissivity

ε_{wall} = inner wall emissivity

γ_{VD}= Reynold's number ratio defined by Van Decker (2001)

γ_c = azimuth angle of collector

γ = fraction of total air supply from outdoors (through collector)

η = efficiency of collector

η_{fan} = efficiency of collector

ρ_{out} = density of air at outlet (kg/m^3 or lbm/ft^3

ρ_g = ground reflectivity

ρ_{avg} = average density of air in the collector (kg/m^3)

ϕ = latitude of location

σ = plate porosity

σ_{sb} = Stefan Boltzman Constant = 5.67×10^{-8} W/m^2K^4

ν is the kinematic viscosity (m^2/s or ft^2/s)

ζ = dimensionless pressure term

1 Introduction

1.1 Background and Description of Transpired Collector Systems

Over the last fifteen years, there has been a substantial amount of research to develop transpired solar collectors by both Conserval Engineering, Inc. and the National Renewable Energy Laboratory. The transpired collector is the general term describing a perforated metal cladding mounted on the south side of a structure which provides low temperature heating. There are several applications for these collectors including preheating ventilation air, preheating combustion air, and crop drying. In the United States and Canada, transpired collector (also called Solarwall®) installations have been primarily used for pre-heating ventilation air in locations with long heating seasons. Long-term monitoring of installed transpired solar collectors has been conducted for all these applications in Canada, Colorado, Europe, and Indonesia.

The basic components of this make-up air heating system include the transpired collector mounted on the south side of the building and the air distribution and control system as shown in Figure 1.1.1. The perforated collector is made of a thin gauge sheet of corrugated aluminum. The unglazed collector is painted black to maximize solar

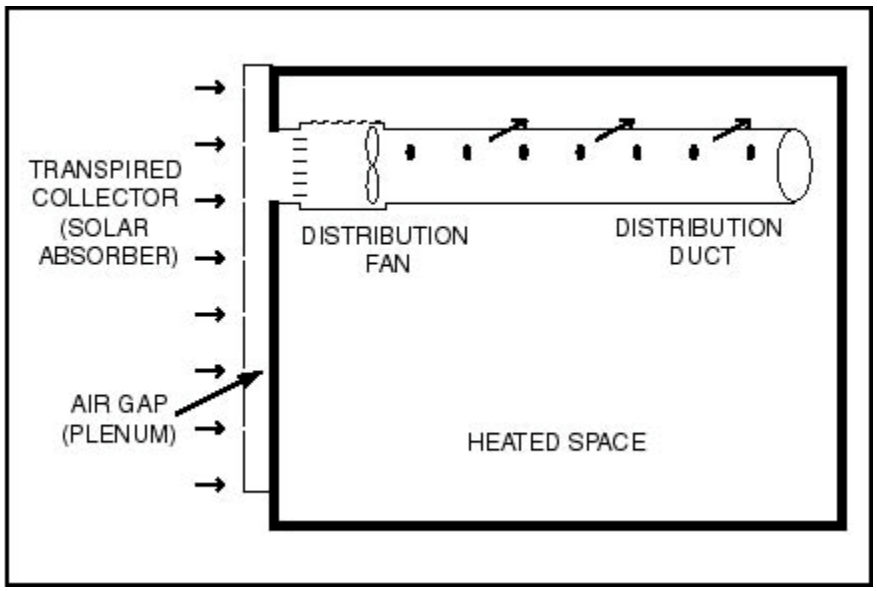

Figure 1.1.1 Diagram of basic components in transpired solar collector system.

absorption. Currently, Conserval Engineering now produces two Solarwall® products which have slotted perforations on a square layout.

If year round ventilation is required, then a summer bypass damper is typically included to avoid heating the ventilation air during the warm season. The bypass damper located at the fan inlet will allow outside air to enter the ventilation system without entering the collector. A control would open this damper based on the ambient outdoor temperature. A typical configuration would be to bypass the collector when the ambient temperature is above 18^{o}C (64.4^{o}F) (Brunger 1999).

The air distribution system usually has a constant speed distribution fan, a recirculation damper, a flexible perforated distribution duct, a control system, and possibly an inline conventional heater. The recirculation damper is controlled by an adjustable thermostat at the fan outlet to attempt to deliver air at a constant temperature. This air is distributed through the holes in the flexible fabric duct at the ceiling. Distributing the air at the ceiling is supposed to destratify the air within the building by pushing warm air toward the floor. The fan system also creates a positive pressure in the building forcing colder air at floor level out of the building. According to Conserval Engineering, the air-make up system design can result in temperature differences between floor and ceiling of less than 2^{o}F (Hollick 1990). If an inline heater is used, the Solarwall® becomes a preheater to a conventional gas fired air makeup unit and it is not necessary to have a recirculation damper.

1.2 Study Objectives

The North Carolina Solar Center is responsible for outreach to the public about solar technologies and their application. The Center has an industrial and commercial program to assist in evaluating the potential for integrating renewable energy systems into these sectors. Certain areas in the southeast may benefit from installing transpired air collector systems. However, the short heating season could make the benefit of the technology marginal from an economic standpoint. The objective of this thesis was to determine whether UTCs are appropriate for the climate in North Carolina. In North Carolina, this technology has been installed at two buildings: one is at Intek Fabrics, a manufacturing facility in Aberdeen and the other is on a fire station in Willow Spring. In January 2003, the North Carolina Solar

Center installed a monitoring system on the transpired collector system at Intek to evaluate its performance.

The purpose of the monitoring project was to evaluate the overall performance of the components of the system, calculate actual heat delivered to the building, and determine the potential monetary savings from the heat gained through the system. The monitored results were used as a case study to understand and evaluate certain components of an unglazed transpired collector (UTC) system. Using previous models, a simulation of a UTC system was built in TRNSYS. This simulation was used to extend the lessons learned from monitoring project to the bigger picture of transpired collectors and their application in North Carolina.

North Carolina has a relatively short heating season and often there is more concern about cooling a building in this climate. The addition of the UTC to the south façade of a building may increase the heat gain through the south wall during the cooling season. Therefore, a heat transfer analysis was done to investigate whether the addition of the collector could increase the cooling load of the building during the summer.

2 Literature Review and Background on Transpired Collectors

2.1 Heat Transfer Theory

Research and investigation into using UTC for solar heating systems first appears in 1990. Christensen *et al.* (1991) compared cost and thermal performance of three types of advanced concepts for solar water and air heating systems to a conventional drainback solar water heating system. A transpired collector was one of these advanced active solar heating systems and was modeled with a steady state efficiency model in the TRNSYS computer program. Because of the transpiration, the convection losses were assumed to be zero and radiation losses dependent on the collector temperature. The results for simulation of the air preheating system estimated the solar fraction, the fraction of total heating provided by the solar collector, to be 0.20. It was noted that this is a low solar fraction, but these systems could still provide a large energy savings.

Heat transfer mechanisms for the unglazed transpired collector have typically been modeled by assuming a flat plate collector with homogenous suction. A review of the heat loss theory applied to the transpired collector was presented by Kutscher *et al* (1993) and Kutscher and Christensen (1993). They provided a simple heat balance on the collector. An equation for the radiation was developed based on the collector temperature, sky temperature, and ground temperature. Convective heat loss including laminar forced convection, laminar free convection, and turbulent forced convection were included in the models.

Schlichting (1979) examined flow over flat plate with suction which was summarized by Kutscher *et al.* (1993). Homogenous suction causes the velocity and thermal boundary layer thicknesses to remain essentially constant over the length of the plate. At the plate edge, the boundary layer thickness asymptotically approaches this constant value. For the transpired collector, the free stream velocity over the plate is the wind. While the boundary layer thickness does not depend on the free stream velocity, it does depend on suction velocity. To prevent the transition to turbulence, a minimum value of suction velocity must

be maintained. For the transpired collector, suction velocity,V_s, is defined as the ratio of flow delivered to collector area. Based on Schlichting's work, Kutscher *et al.*(1993) showed that the minimum suction velocity for stability at typical wind speeds is much less than the operating suction velocity for the transpired collector.

The thermal boundary layer thickness is also asymptotic as the heat conducted into the boundary layer is removed by convection. In theory, the starting length of the plate where the boundary layer has not reached the asymptotic region is the only area where convective loss would be considered. Kutscher *et al.* (1993) projected that for the typical parameters for the transpired collector, these convective losses are small for a large collector. A similar analysis was done for the laminar free convection. Again, for typical suction velocities, heat losses would be negligible from free convection.

To estimate convective heat loss under turbulent flow conditions, experimental data was used. Experimental data did not exist for the typical suction flow rate to free stream velocity (wind) ratio that would be typical for a transpired collector. However, Kutscher *et al.* (1993) estimated the turbulent losses using data from Verrolet *et al.* (1972). For the turbulent boundary layer, the conclusion was that the heat loss was higher than for the laminar boundary layer, but it was still insignificant.

Kutscher *et al* (1993) used the derived equations to develop a predictive model for thermal performance. They found that efficiency is nearly constant and independent of wind speed for suction velocities greater than 0.05 m/s. The temperature rise in the collector increases as the velocity decreases, but the overall efficiency decreases. This article also addressed the importance of the pressure drop across the collector in assuring uniform flow and balancing this with associated fan power.

2.2 Laboratory Experiments and Computer Modeling

Once the heat exchange effectiveness of the collector is known, it is straightforward to predict the efficiency. Following is a review of several papers which develop equations for effectiveness experimentally. Kutscher (1994) performed laboratory experiments on a small test collector to determine heat exchange effectiveness for the collector noting that important parameters include suction flow rate, crosswind speed, hole pitch, and hole

diameter. An equation to predict pressure drop was also found to help design the collectors to have uniform flow.

Van Decker et al (1996) investigated heat exchange effectiveness more thoroughly for three dimensional flow. They determined effectiveness experimentally for plates with circular holes on either a square or triangular layout over a range of wind speeds. A model was developed to look at three heat transfer mechanisms: on the front of the plate, in the hole, and on the back side of the plate. They were able to model the heat exchange effectiveness as a function of suction velocity, porosity, hole diameter, plate thermal conductivity, wind speed and air properties. Van Decker and Hollands (1999) and Van Decker et al (2001) extended the correlation for the effectiveness to no-wind conditions circular holes on a square or triangular pitch.. The effectiveness was broken into heat transfer form the front of the plate, in the hole, and at the back of the plate.

Arulandanam (1999) used a CFD code to determine the heat exchange effectiveness for circular holes on a square pitch. The model, however, was only developed under no-wind conditions and excluding heat transfer at the back of the plate. A correlation for the Nusselt number was found based on the non-dimensional variables: the hole Reynolds number, porosity, non-dimensional plate thickness, and a term called plate admittance.

Gunnewiek *et al* (1996) developed a two dimensional Computational Fluid Dynamics (2-D CFD) model. The objective of Gunnewiek's work was to understand flow distribution problems in large collectors. To examine the important parameters on suction velocity profile, they looked at different collector heights, height to depth ratios, incident solar radiation, ratio of flow rate delivered to collector area (suction velocity), plate hydraulic impedence, and heat exchange effectiveness. This model only simulated flow in the plenum for the case where wind speed was almost zero. The most significant finding was that for suction velocities less than 0.0125 flow reversal can occur. Also, they found that heat transfer at the back of the plate (plenum) is more significant for non-uniform flow. Gunnewiek *et al* (2002) extended their previous study to include the effects of wind on flow inside the plenum. Based on these results, the recommended minimum suction velocity to prevent reverse flow was raised to 0.017 m/s for long buildings with wind normal to collector, 0.026 m/s for cubical buildings with wind normal to collector, and 0.039 m/s for cubical building with a wind at 45^{o} incidence angle to the collector.

Wind effects were addressed also by Fleck *et al.* through a field study on a UTC. Detailed measurements were made on the wind speed and direction to characterize the flow of boundary layer and the free stream air. Results showed that there is a lot of turbulence outside the boundary layer and they concluded that the model of a laminar boundary layer smaller than the perforation diameter may not be appropriate. Conclusions of the effect of wind direction were not made. The implications of this study will be discussed more in Section 3.4.

Dymond and Kutscher (1995 and 1997) worked to develop a computer model where geometric configurations could be varied and used to design collectors. They used a pipe network model. The model included all significant heat transfer mechanisms and four pressure drops in the system: pressure drop through the collector, friction inside the collector plenum, buoyancy pressure drop, and acceleration pressure drop. The program they developed was named TCFLOW and was used by Conserval Engineering in the design of their collectors. To validate their model, they compared the output for face velocity and surface temperature to digitized IR thermography of the unglazed collector at the National Renewable Energy Laboratory Waste Handling Facility. They found that this model did a reasonable job of predicting the temperature profile over the absorber.

Summers (1995) created a TRNSYS simulation of a UTC system based upon an empirical heat transfer from Kutscher. The simulation also included the reduced and recovered heat loss in the transpired collector plenum on the south wall of a building. The results of this simulation were compared with data from the National Solar Test Facility. Prediction of temperature rise in collector versus incident solar radiation compared well with Summers' TRNSYS simulation and NSTF curve fit for suction velocities of 0.035 m/s and 0.02 m/s, but over predicted for the lower suction velocity of 0.005m/s.

Simulated values were also compared with monitored data from the General Motors battery plant. The monitored active solar efficiency and reduced wall heat loss compared well with the predicted TRNSYS model, but the model under predicted the recaptured wall loss. A sensitivity analysis showed that energy savings correlates most with collector absorptivity and area.

2.3 Demonstration Projects and Validation Testing

In 1989, the International Energy Agency launched Solar Heating and Cooling Task 14. The Air Systems working group under this task decided to focus on solar air heating applications for commercial and industrial facilities. The final report from this working group (Brunger 1999) included results from monitoring of several demonstration projects. Conclusions from three projects are presented here: Ford of Canada-Oakville Assembly Plant (1990), General Motors, Oshawa, Canada (1991-1993), and NREL Waste Handling Facility (1992-1994).

Monitoring of the Ford of Canada-Oakville Assembly Plant showed over 70% instantaneous efficiency, monthly efficiency of over 55%, and a temperature rise on sunny day over 12^{o}C (21.6^{o}F). Results also showed that performance is maximized with perforated collector airflows of over 120 m^3/h per m^2 of collector area (6.56 cfm/ft^2 or 0.0333m/s). The second year of monitoring showed better performance due to both system upgrades and lower wind speeds. Performance was improved was by manually closing and securing the bypass damper and tightening the fan belts.

The system at the General Motors Battery Plant in Oshawa, Canada was installed in 1991 and included an overhanging canopy which helped maintain uniform flow. It was monitored over three heating seasons and upgrades were made during these three years. One improvement was replacing the air distribution system with a fan that would increase airflow to operate closer to design values and consume less electricity. Several observations were made from the monitoring of this system. High airflow can help overcome some of the efficiency loss due to higher wind speed (defined as above 1.2 m/s). Almost all of the low wind speed instantaneous efficiency values were over 60% and there was a significant number that were above 80%.

The NREL Waste Handling Facility requires unusually high ventilation rates because it is used to store explosives and general hazardous waste. Average daily efficiency of collector from September to April of the first monitoring season was found to be 68%. Due to high uncertainty in results, data with solar radiation of less than 1500Wh/m^2day were not included in the analysis. Improvements were made to the data acquisition system and the heating system was monitored again in the first three months of 1994. Instantaneous raw

collector efficiency results contained values above 100%. These unreasonable numbers were attributed to variations in solar radiation due to cloud cover. Therefore, a reduced collector efficiency was determined using a finite difference method to model the heat transfer into and out of the regular concrete wall. Including the heat transfer from the wall made the efficiency more reasonable and below 100%.

Further, plotting the ambient temperature and solar radiation on the same graph also revealed an interesting result. The days with lower efficiency occur on days when the ambient temperature is higher than the previous day. The conclusion was that the thermal mass of building is absorbing some of the energy of the collector and reduces the measured energy of collector. Because of these variations, the author recommends that collector efficiency should be evaluated over a week or month.

3 Monitoring Study

3.1 Details about the Intek Solarwall® System

The Solarwall® system on the fabric warehouse was installed at Intek in 1998 and has therefore been in operation for five heating seasons. The estimated cost of installation from Conserval Engineering was $56,127 including material shipping and labor. The warehouse is about 15' taller than the adjacent spinning room. The solar collector was retrofitted to this top section of wall on the south side of the warehouse as shown in Figure 3.1.1. The south elevation and construction detail of the Solarwall® system at Intek is included in Appendix B. The warehouse is approximately 45' wide and 210' long with a ceiling height of 38'. The collector on the wall is 0.032" thick aluminum painted black. Its dimensions are 14'3" tall by 210'6" wide. The aluminum was perforated to have 0.6% open area (porosity). The holes are 1/16" or 0.0625" (1.6mm) diameter. The hole spacing is 0.648" (16.5 mm) apart horizontally 0.80" (20 mm) apart vertically. The collector was mounted vertically and did not have a canopy. There was not a summer bypass damper built into the collector.

Two 24" Energy Jet Fans (Model # EJ24S) delivered the warm air to the room through two flexible ducts with 4" perforations. The fans were approximately 105' apart on center. A picture of one fan box and flexible duct is shown in Figure 3.1.2. The control system included a Johnson Controls A350P temperature sensor and a Belimo NF24-SR US damper control (Figure 3.1.3). These controls operated to maintain a preset outlet temperature through the automated damper system. There was a damper both to the wall and the ceiling connected through a linkage. There was one shaft that turned both dampers; as one closed the other would open. If the transpired collector could not provide warm enough air, then the system recirculated air from the ceiling.

Figure 3.1.1 (left) Transpired collector mounted on south side of fabric warehouse

Figure 3.1.2 (left) Air distribution fan and flexible fabric duct which delivers air at ceiling.
Figure 3.1.3 (right) Original fan controls which regulate outlet temperature with modulating damper.

Conserval Engineering provided an energy savings analysis in April 1998 for design of the makeup air system. There are some assumptions in their analysis that are important to mention. It was designed to operate seven months of the years for 24 hours a day (144 hours a week). This schedule was different from actual operation. The projected mixed air temperature setting was 50°F, which is the temperature Solar Center engineers found as the setting on the control system. The desired room temperature was 60°F. Although a bypass damper was not included in the final installation, it was designed to open when the ambient temperature reached 68°F.

When the Solar Center first contacted Intek about monitoring the Solarwall® system, plant workers indicated that they did not really use the solar air make up system. They did not usually turn the system on in the winter because they perceived that the system delivered cold air. They also complained that when the system did deliver warm air, it would remain at ceiling level. The air was distributed straight into the room (not as a preheater to a conventional heating system). Because the control temperature was set to 50°F, at night the system would bring in air colder than room temperature. As a solution to this problem, Solar Center engineers installed a new control system in February 2003. This control system turned on the distribution system based on the Solarwall® plenum temperature. These controls guaranteed that the system would operate on days when there was enough solar insolation to warm up the air, allow us to collect data during the day, and keep the warehouse workers comfortable. Originally, the new control system was programmed to turn on the fans when the plenum temperature reached 80°F and off when it reached 70°F. Because this setting significantly reduced the hours the system would run, it was changed to turn on at 75°F and off at 65°F. This control system is still not ideal. There is no way to bypass the collector, turn the system off automatically, or guarantee a constant amount of make-up air. The new control system operates well on cold sunny days of winter, but not properly on cloudy days or marginal heating days of spring. Any system installed in North Carolina's climate should include a bypass damper that would open when the ambient outdoor temperature or indoor temperature rises above a comfortable level.

3.2 Monitoring Equipment Description

To monitor the long term performance and capture real-time data, the Solar Center installed a data acquisition system at the Intek manufacturing facility. This data system allowed useful information to be collected on the performance of the system under a variety of conditions. In order to choose flow monitoring equipment properly, initial measurements were made on the air velocity in the distribution duct prior to installing a full data acquisition system. The velocity of the flow was measured with an Alnor Velometer at the following specified radius from the center of the 24" diameter duct: 0.316R, 0.548R, 0.707R, 0.837R, and 0.949R. These measurements were used to determine the average velocity in the duct and estimate the average flow rate. Then, two Air Monitor 24" Fan-Evaluator flow measuring stations were installed downstream from the fan outlet and coupled with two Omega PX-277 differential pressure transmitters to determine outlet air flow. The flow measuring device and temperature sensors in the distribution duct are shown in Figure 3.2.1.

Other measurements sensors included a LI-COR pyranometer to measure total horizontal solar radiation and a NRG Max 40 cup anemometer for wind speed. Campbell Scientific T108 thermistors were used to measure air temperature at the fan inlet from the wall, fan inlet from the ceiling, and fan outlet. Type T thermocouples measured surface temperature of the transpired collector as well as temperature in the plenum between the aluminum collector and south wall of the building. These thermocouples were mounted about halfway up the collector, five to six feet from the bottom. Table 3.2.1 provides a summary of all sensors connected to the data acquisition system and the location of temperature sensors are shown in Figure 3.2.3.

The heart of this system consisted of a Campbell Scientific (CSI) CR10X datalogger and an AM 16/32 multiplexer. The system was powered by a 12 Volt DC battery charged by a Solarex 20 Watt PV Module through a Sun Selector charge controller. The enclosure for the datalogger, wind meter, and PV power source are shown in Figure 3.2.2. Data was downloaded through a CSI DC112 modem. The Campbell Scientific software PC208W was used to build and compile a program for the datalogger and also to communicate with the datalogger. Measurements of all sensors were made every thirty seconds. Every fifteen minutes these measurements were averaged and this data was recorded. Most sensors were

installed on January 7th and 8th, 2003. Data collection began on January 14th, 2003 and continued until February 7th with the old control system. Then, one fan was shut off for the next week while the new controls were installed. Data collection began February 15th with the new controls and continued until March 11th. At this time, most days were warm enough that heating ventilation air was not necessary.

Figure 3.2.1 (above): Warm air distribution duct with sensors to measure air flow and temperature.
Figure 3.2.2 (right): Data acquisition system with transpired collector in background.

Table 3.2.1: Sensor description for Data Acquisition System

Sensor ID	Sensor Placement Description	Manufacturer Description
T1081	Temperature sensor Fan 1 Inlet from wall	CSI T108 Thermistor
T1082	Temperature sensor Fan 1 Inlet from ceiling	CSI T108 Thermistor
T1083	Temperature sensor Fan 1 outlet	CSI T108 Thermistor
T1084	Temperature sensor Fan 2 inlet from wall	CSI T108 Thermistor
T1085	Temperature sensor fan 2 inlet from ceiling	CSI T108 Thermistor
T1086	Temperature sensor Fan 2 outlet	CSI T108 Thermistor
T107	Multiplexer Temperature Sensor	CSI T107 Thermistor
T500	Outdoor ambient temperature sensor	CSI 500 RH/Temperature Probe
RH500	Relative Humidity Sensor	CSI 500 RH/Temperature Probe
Fan-E	Outlet from Fan 1 and 2 (7 feet downstream from fan discharge)	Air Monitor Corporation 24" Round Fan-Evaluator

PX277-1	Differential pressure transmitter Fan 1	Omega PX 277 DPT
PX277-2	Differential pressure transmitter Fan 2	Omega PX 277 DPT

Table 3.2.1: Sensor description for Data Acquisition System (Cont'd)

TC1	Thermocouple Solarwall® Surface 1 (Middle)	Omega Bolt-On Washer Type T Thermocouple
TC2	Thermocouple Solarwall® Surface 2 (Under Fan 1)	Omega Bolt-On Washer Type T Thermocouple
TC3	Thermocouple Solarwall® Surface 3 (End)	Omega Bolt-On Washer Type T Thermocouple
TC4	Thermocouple Solarwall® Plenum 1 (Middle)	Omega Type T Probe Thermocouple
TC5	Thermocouple Solarwall® Plenum 2 (Under Fan 1)	Omega Type T Probe Thermocouple
TC6	Thermocouple Solarwall® Plenum 3 (End)	Omega Type T Probe Thermocouple
TC7	Differential Thermocouple for Fan 1	Omega Type T Probe Thermocouple
TC8	Differential Thermocouple for Fan 2	Omega Type T Probe Thermocouple
TC9	Thermocouple: Ambient Indoor Temperature	Omega Type T Probe Thermocouple
Wind	Outdoor Wind Speed	NRG Max 40 Cup Anemometer
SoRad	Horizontal Solar Radiation	LI-Cor 200 Pyranometer

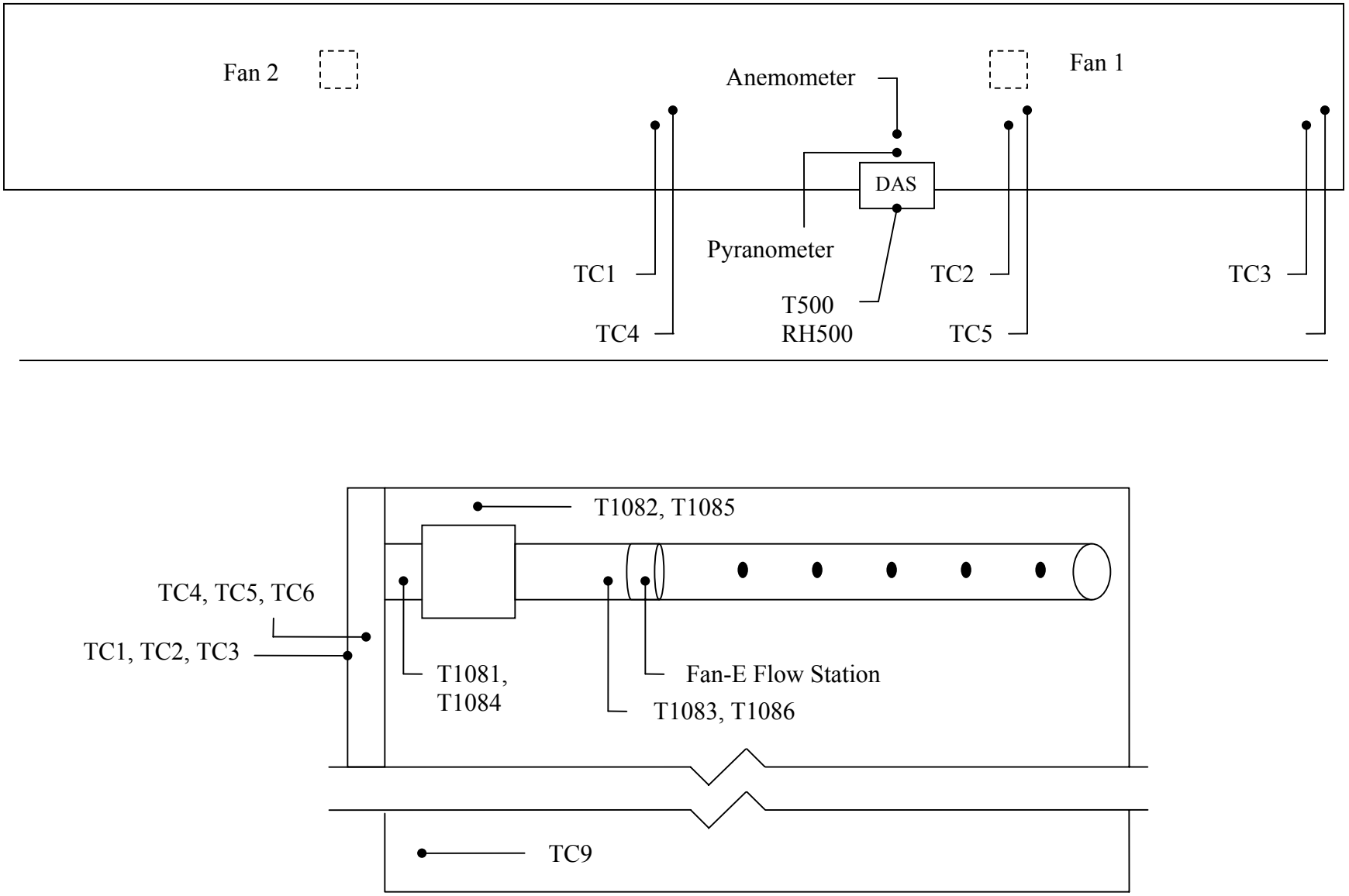

Figure 3.2.3: Top: South side elevation of Solarwall and sensor placement for data acquisition system; Bottom: Cross sectional view of sensor placement

3.3 Calculations for monitoring data

To determine the direct heat gain to the warehouse, it was necessary to measure the airflow delivered to the building by each fan. Since the pressure and temperature of this air are measured, the ideal gas equation of state was used to determine the density. A Fan Evaluator Flow Station from Air Monitor Corporation was used to measure the static pressure in the duct and the total pressure at equal area cross-sections. The difference between these values gives the velocity pressure, directly related to the velocity of the air. The velocity of the outlet air is related to the pressure in the following manner:

$$V_{out,fan} = \left[\frac{2 * g * P_{abs}}{0.1922 * \rho_{out}} \right]^{1/2} \qquad (3.3.1)$$

1 inch water = 0.19223 lbf/ft^2

For the control system used in most of the study, the measured velocity pressure value can be used to determine fan outlet flow velocity, V_{out}, and hence the volumetric flow rate, Q_{out} and the mass flow rate using equation 3.3.2.

$$\dot{m}_{tot} = \rho_{out} \dot{Q}_{out,fan} = \rho_{out} A_d V_{out,fan} \qquad (3.3.2)$$

Examining the actual amount of fresh air heated by the solar collector with the original control system is more complicated because some of the air is recirculated. To determine accurately how much air is coming from the wall versus the ceiling, a thermodynamic balance on the air entering and leaving the fan box fan can be used to determine the relative contributions of air flow from the ceiling and the wall.

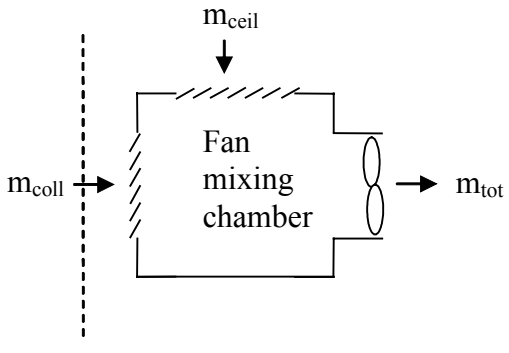

$$\dot{m}_{coll} + \dot{m}_{ceil} = \dot{m}_{tot} \qquad (3.3.3)$$

$$\dot{W}_{in} + \dot{m}_{coll} T_{out,coll} + \dot{m}_{ceil} T_{ceil} = \dot{m}_{tot} T_{out,fan} \qquad (3.3.4)$$

Figure 3.3.1 Flows in fan mixing chamber

Measurements of solar radiation were made with a Li-Cor pyranometer on a horizontal surface. Because the transpired collector was mounted vertically, these measurements had to be converted to incident radiation on a vertical surface. All calculations were based on equations from Duffie and Beckman (1991). For the anistropic sky model for radiation on a tilted surface, Table 3.3.1 shows the values used for all calculations

Table 3.3.1: Definition of variables used in calculations of solar radiation on a tilted surface.

Latitude:	$\phi = 35.145^{o}$N
Longitude:	$L_{LOC} = 79.425^{o}$W
Standard Longitude:	$L_{ST} = 75^{o}$W
Azimuth Angle:	$\gamma_c = 17.0^{o}$
Tilt Angle:	$\beta_c = 0^{o}$ (horizontal)
	$\beta_c = 90^{o}$ (vertical)
Ground Reflectivity:	$\rho_g = 0.35$

It would have been more accurate to take solar radiation measurements on the vertical plane of the collector. A pyranometer capable measuring solar radiation in the plane of the collector was not available for long-term monitoring in this study. However, verification of the vertical solar radiation model was done with an Eppley PSP. Simultaneous measurements of solar radiation in the vertical and horizontal plane were made and these results were used to estimate the ground reflectivity.

Next, the heat delivered to the building is determined. The ambient outdoor temperature, T_{amb}, and fan outlet temperature, $T_{out,fan}$ were measured with thermistors. The heat delivered to the building, Q_{del}, (W or BTU/hr) is simply:

$$Q_{del} = \dot{m}_{tot} C_p (T_{out,fan} - T_{amb}) \qquad (3.3.5)$$

where C_p is constant over the given range of air temperature and equal to 0.24 BTU/lbm-^{o}F or 1007 J/kg-K.

Instantaneous collector efficiency, η, can be defined as the heat delivered to the building compared to the available solar energy incident on the collector.

$$\eta = \frac{Q_{del}}{I_T A_p} \tag{3.2.7}$$

3.4 Empirical equations of heat transfer

The National Renewable Energy Laboratory and the National Solar Test Facility have done numerous studies on the small scale transpired collector models in the laboratory. A basic analysis can be started with an energy balance on the collector where heat delivered by the collector is equal to the incoming solar energy minus the radiative and convective heat losses. Since the conservation of energy is a fundamental physical equation, it can be applied to both small scale test collectors and large scale operational collectors. For simplicity, to analyze data from the monitoring study, any additional heat transfer through the wall of the building is not included in the heat balance. This additional heating is negligible during times of high solar radiation. It will be included in the TRNSYS model in Section 4. The heat balance for a transpired collector is shown in figure 3.4.1 and defined by equation 3.4.1.

$$\rho_{avg} C_p V_s A_P \varepsilon_{HX} (T_{coll} - T_{amb}) = I_T A_P \alpha_{coll} - Q_{rad,loss} - Q_{conv,loss} \tag{3.4.1}$$

with a heat exchange effectiveness defined as the temperature rise in the collector compared to the maximum possible temperature rise.

$$\varepsilon_{HX} = \frac{T_{out,coll} - T_{amb}}{T_{coll} - T_{amb}} \tag{3.4.2}$$

Because the radiative and convective losses are unknown, laboratory tests were conducted at NREL to find correlations for the heat exchange effectiveness. These correlations were strictly based on design parameters such as porosity and size of the collector, suction velocity through

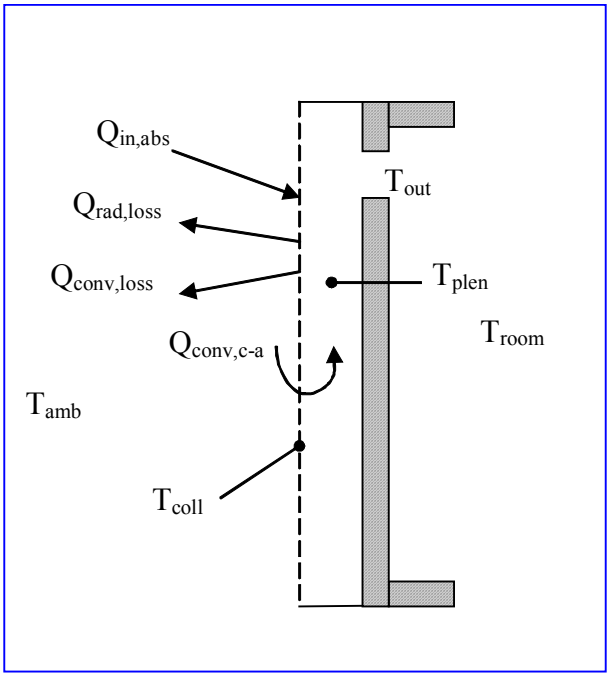

Figure 3.4.1 Basic energy balance on transpired collector.

the collector (depends on flow rate and collector size), and density and specific heat of air. The collector efficiency can be easily determined once the heat exchange effectiveness of the transpired collector is known (Brunger 1999). Heat exchange effectiveness affects plate surface temperature and thus radiative heat loss. The collector efficiency can be characterized by the following equations:

$$\eta = \frac{\dot{m}_{coll} C_p \varepsilon_{HX} (T_{coll} - T_{amb})}{I_c A_p} = \frac{\alpha_{coll}}{\frac{[1 + (h_r + h_c) A_s}{\dot{m}_{coll} C_p \varepsilon_{HX}}} \tag{3.4.3}$$

The radiation heat loss coefficient is:

$$h_r = \frac{\varepsilon_{coll} \sigma_{sb} (T_{coll}{}^4 - F_{cs} T_{sky}{}^4 - F_{cg} T_{gnd}{}^4)}{(T_{coll} - T_{amb})} \tag{3.4.4}$$

$$T_{sky} = T_{amb} \left[0.711 + 0.0056 T_{dp} + 0.000073 T_{dp}{}^2 + 0.013 \cos(15 t_{hr}) \right]^{1/4} \tag{3.4.5}$$

When the surface temperature is close to the sky and ground temperature, it is a common assumption to use an average temperature (Duffie 1991). The linearized radiative heat loss coefficient becomes: (Kutscher 1992)

$$h_r = \frac{4\varepsilon_{coll}\sigma_{sb}T_{avg}^{3}(T_{coll}-T_{sur})}{(T_{coll}-T_{amb})} \tag{3.4.6}$$

$$T_{sur}^{4} = 0.5(T_{sky}^{4}+T_{gr}^{4}) \tag{3.4.7}$$

The ground temperature is assumed to be equal to the ambient temperature.

Heat loss due to the wind must also be addressed and is normally a large concern for unglazed collectors. Kutscher (1993) showed the derivation of a forced convective heat loss coefficient. The solution assumes the suction surface is homogenous and the boundary layer developed over the plate surface is for unidirectional laminar flow. Because suction stabilizes the boundary layer, the velocity and thermal boundary layer thicknesses for this case are asymptotic. The thickness of the boundary layer is proportional to heat loss on the downwind edge of the collector. Therefore, maintaining the stability of the boundary layer is essential to optimal performance of the transpired collector. Initial investigations of transpired collectors are based on these assumptions. Kutscher's solution to the momentum and energy equations yielded the following heat loss coefficient from the collector to the air on the front side of the plate.

$$h_c = C_f[0.82\frac{U_\infty \nu}{V_s H}\rho_{avg}C_p] \tag{3.4.8}$$

It is necessary to recognize the challenges to the convective heat transfer coefficient solution. Recently, the effect of wind on flow distribution has been studied more in depth both in a parametric study and a field study. Airflow around buildings complicates the laminar boundary layer assumption. Gunnewiek *et al* (2002) built on previous work done in 1996 to analyze the flow distribution inside the plenum of a transpired collector using computational fluid dynamics. The previous study had shown that reverse flow in the collector could occur with an average suction velocity of 0.0125 m/s due to buoyancy effects under no-wind conditions. This study extended the analysis to cross-wind conditions for multiple building shapes. Under high wind conditions (5 m/s), the study showed that the minimum suctions velocity should be raised to 0.017 m/s for long buildings with a collectors facing into the wind. The transpired wall at Intek had a width to height ratio of almost 15.

Fleck *et al* (2002) looked at the wind effects on performance in a field study. Fleck declares that the wind around a building is much more complicated than a steady unidirectional parallel flow. More detailed measurements were taken in this study, including wind speed and direction near the test site. A sonic anemometer was used to measure the three velocity components about two feet from the collector surface. The distribution of the velocity data suggest that turbulence exists near the wall and Fleck assert that the laminar model may not be an accurate representation of the actual flow patterns observed. Fleck states, "in spite of the apparent accuracy of the efficiency estimates using the laminar parallel flow model, it is quite clear from our observations that such a model is a poor descriptor of the physical phenomena driving UTSC performance." Despite the known limitations to the laminar analysis, the assumption that the convective losses are low compared with solar energy collected still dominates the literature. Since the laminar assumption has been shown to predict efficiency well in previous studies, it will be used for the purpose of modeling the performance of the collector.

The effectiveness of the heat exchanger was defined earlier as the temperature rise in the collector versus the maximum possible temperature rise. The collector surface temperature and outlet temperature are unknown and therefore must be predicted from variables that will be known about the collector and its operating conditions. A definition of the heat exchanger is

$$\varepsilon_{HX} = 1 - \exp(-NTU) \tag{3.4.9}$$

where NTU is the number of heat transfer units from the following equation:

$$NTU = \frac{U_{coll} A}{\rho V_s A_c C_p} = (\frac{A}{A_c})(\frac{U_{coll}}{\rho V_s C_p}) \tag{3.4.10}$$

The ratio of plate area to total collector area, A/A_c, can be expressed in terms of the porosity, σ, also called the open area fraction.

$$\frac{A}{A_s} = 1 - \sigma \tag{3.4.11}$$

U_{coll}, the overall heat transfer coefficient can be calculated from the definition of the Nusselt number.

$$U_{coll} = Nu_D(\frac{k}{D}) \tag{3.4.12}$$

When these equations are combined, the effectiveness of the heat exchanger becomes (Brunger 1999):

$$\varepsilon_{HX} = 1 - \exp\left[\frac{(\sigma - 1)kNu_D}{(\rho V_s C_p)}\right] \tag{3.4.13}$$

The only unknown parameter in this equation is the Nusselt number and several experiments have been performed to determine this correlation Kutscher (1994) carried out experiments on perforated plates to develop a correlation for the heat exchange effectiveness based on hole pitch, hole diameter, suction velocity, porosity, and cross-wind speed. Kutscher conducted experiments for mass flow to collector area ratios down to 0.02 kg/s/m^2 and for test plates that had holes oriented on a triangular pitch. The Nusselt number correlation from his experiments was:

$$Nu_D = 2.75[(\frac{P}{D})^{-1.21}\ \mathrm{Re}_D^{\ 0.430} + 0.0110\sigma\,\mathrm{Re}_D(\frac{U_\infty}{V_s})^{0.480} \tag{3.4.14}$$

$$\mathrm{Re}_D = \frac{V_h D}{\nu} \tag{3.4.15}$$

It is important to note that the measured mass flow ratio for the field tested collector was below the optimal mass flow to collector range, around 0.015 to 0.017 kg/s/m^2 . In addition, the field tested collector had holes on a square pitch.

Van Decker (2001) performed tests on perforated plates with both triangular and square pitch. These results revealed that the Kutscher model can be modified for the square pitch plates by using a pitch scaling factor. His results for the square plate correlate well with Kutscher's model if the pitch used in Kutscher's model is multiplied by 1.6. Therefore, to estimate the effectiveness of the given collector that has holes on a square layout, Kutscher's correlation for the Nusselt number was used with a pitch scaling factor of 1.6.

For a given collector, the only parameters that change in the heat balance are ambient temperature, wind speed, relative humidity, solar radiation, and surface temperature. The first four can be determined from weather data and the equation can be solved for surface temperature.

$$T_{coll} = \frac{\alpha_{coll} I_T A_p + (h_c + h_r) A_s T_{amb} + \dot{m}_{coll} C_p \varepsilon_{HX} T_{amb}}{(h_c + h_r) A_s + \dot{m}_{coll} C_p \varepsilon_{HX}} \quad (3.4.16)$$

Combining the predicted surface temperature and heat exchange effectiveness allows the outlet temperature to be determined and thus the heat gain by the collector.

To compare with Kutscher's correlations and assumptions, an additional model of collector effectiveness from Van Decker (2001) was used. Van Decker makes the assumption that the convective losses are completely negligible and does not include the convective heat transfer coefficient in the equation for collector efficiency. Van Decker (2001) broke the heat transfer up into three components, the heat transfer form the front of the plate, the hole, and the back of the plate. He developed a correlation for the effectiveness of each of these parts for holes on a square pitch. Although the assumption that the convective heat loss is negligible may not be valid, Van Decker's relations were used for analysis because they apply directly to the geometry of the investigated collector and his conclusions were used as a part of the Kutscher model (the pitch scaling factor for triangle pitch versus square pitch). Again, these correlations were based on higher suction velocities than measured. The following relationships defined by Van Decker result in a total effectiveness:

$$\varepsilon_T = 1 - (1 - \varepsilon_f)(1 - \varepsilon_h)(1 - \varepsilon_b) \quad (3.4.17)$$

The back of the plate effectiveness, ε_b, is defined by equation 3.3.18 with a Reynolds number based on hole velocity and pitch shown in equation 3.4.19.

$$\varepsilon_b = \frac{1}{1 + e\,\mathrm{Re}_b^{1/3}} \quad (3.4.18)$$

$$\mathrm{Re}_b = \frac{V_h P}{\nu} \quad (3.4.19)$$

If there is a cross wind, the front of the plate effectiveness, ε_f, is defined by equation 3.4.20. Two Reynolds numbers are used in this equation. Re_w is based on wind and hole pitch and Re_s is based on suction velocity and hole pitch.

$$\varepsilon_f = \frac{1}{(1 + a\gamma_{VD}^{1/2})} \quad (3.4.20)$$

$$\gamma_{VD} = \frac{\mathrm{Re}_s^{\,2}}{\mathrm{Re}_w} = \frac{V_s^{\,2} P}{U_\infty \nu} \tag{3.4.21}$$

$$\mathrm{Re}_w = \frac{U_\infty P}{\nu} \tag{3.4.22}$$

$$\mathrm{Re}_s = \frac{V_s P}{\nu} \tag{3.4.23}$$

For the case when there is no wind the Re_w would be zero and there would be a division by zero in equation 3.4.21 for the dimensionless parameter γ_{VD}. Therefore, the front of the plate effectiveness, ε_f, is defined by equation 3.4.24 based again on the Reynolds number with suction velocity and hole pitch.

$$\varepsilon_f = \frac{1}{1 + f\,\mathrm{Re}_s} \tag{3.4.24}$$

The hole effectiveness, ε_h, is defined by equation 3.4.25 with a Reynolds number based on hole velocity and hole diameter shown in equation 3.4.36.

$$\varepsilon_h = 1 - \exp\left[-4\left(c\frac{P}{D} \right) + \frac{3.66}{\mathrm{Pr}\,\mathrm{Re}_h}\frac{t}{D} \right] \tag{3.4.25}$$

$$\mathrm{Re}_h = \frac{V_s D}{\nu\sigma} = \frac{V_h D}{\nu} \tag{3.4.26}$$

Van Decker experimentally determined the constants e=0.2273, a=1.733, f=0.02136, and c=0.004738. Again, this model assumes that convective losses are completely negligible and therefore the convective heat transfer coefficient is not included in the efficiency equation.

$$\eta = \frac{\alpha_{coll}}{\dfrac{1 + h_r A_c}{\dot{m}_{coll} C_p \varepsilon_{HX}}} \tag{3.4.27}$$

Both the Kutscher and the Van Decker models were used on measured data to estimate predicted collector efficiency and then compared to actual measured efficiency.

3.5 Pressure drop estimation through collector and plenum

Once the heat gain and energy savings are determined, it is important to consider the auxiliary power used to run the fan for operation. Theoretically, the transpired collector will

only be used in buildings where the ventilation system is already required. However, the collector and friction in the plenum will add quite a substantial pressure drop to the ventilation system and the fan must be sized to still provide the minimum amount of ventilation air. Power is related to the total pressure drop in the system that must be overcome by the fan including the pressure drop across the face of the collector, the friction in the plenum, the buoyancy force of the air, and the acceleration of the air in the system.

$$\Delta P_{tot} = \Delta P_{coll} + \Delta P_{fric} + \Delta P_{buoy} + \Delta P_{acc} \tag{3.5.1}$$

Adequate pressure drop across the collector will insure that outflow or flow reversal does not occur in the collector. It has been noted that maintaining a pressure drop of 25 Pa ($0.10 in H_2O$) across the collector is essential to achieving uniform flow and therefore a uniform collector temperature. Summers (1995) notes that for certain plate porosities at the minimum recommended suction velocity of 0.02 m/s (0.0656 ft/s), the pressure drop across the plate may be less than 25 Pa ($0.10 in H_2O$). The suction velocity should be increased to achieve the adequate pressure drop. Although the increased pressure drop helps flow uniformity, it is achieved at the expense of fan power which must be limited to protect savings and energy expenditure in any solar heating system.

There was a lack of data on pressure drop through low porosity perforated plates. Therefore, the pressure drop was experimentally determined by Kutscher for the case of the absence of a cross-wind. The non-dimensional pressure drop is:

$$\zeta = 6.82\,\mathrm{Re}_D^{-0.236}\left[\frac{(1-\sigma)}{\sigma}\right]^2 \tag{3.5.2}$$

The hole orientations tested had similar pressure drops. The pressure drop across the collector can be determined from the following relation:

$$\Delta P_{coll} = \frac{\rho V_S^{\,2}\zeta}{2} \tag{3.5.3}$$

This equation was developed for plates with holes on the triangular pitch, but it was used for the estimating collector pressure drop for the general transpired collector which may have holes on the square pitch.

The other components of pressure drop were outlined by both Summers (1995) and Kutscher (1995). These require some assumptions about the plenum air velocity. Air starts from a zero velocity and goes to the maximum plenum velocity defined by outlet flow

rate divided by the plenum area. In this case, the plenum area is defined by the plenum depth times the width of the collector.

$$V_{plen,\max} = \frac{\gamma Q_{\max}}{A_{plen}} \tag{3.5.4}$$

$$A_{plen} = D_{plen} \times W_{coll} \tag{3.5.5}$$

Since the initial air velocity of the air is zero, the average plenum velocity, $V_{plen,avg}$ is half of the maximum velocity.

$$V_{plen,avg} = \frac{V_{plen,\max}}{2} \tag{3.5.6}$$

The frictional pressure drop in the plenum is defined as:

$$\Delta P_{fric} = f \frac{h_{avg} \rho_{avg} V_{plen,avg}^{\ 2}}{2D_h} \tag{3.5.7}$$

The hydraulic diameter is used in this equation and is found by looking at the ratio of the plenum cross sectional area to its perimeter:

$$D_h = \frac{4A_{plen}}{Per_{plen}} = \frac{4(D_{plen} \times W_{coll})}{2(D_{plen} + W_{coll})} \tag{3.5.8}$$

Summers (1995) defined the acceleration pressure drop by the max plenum velocity. However, this definition will actually underestimate the maximum velocity of the air in the transpired system. Ultimately, the air is accelerated to the velocity at the outlet of the fan, so the acceleration head is better defined in equation 3.5.9.

$$\Delta P_{acc} = \frac{\rho_{avg} V_{out,fan}^{\ 2}}{2} \tag{3.5.9}$$

While its magnitude may be small, the buoyancy force actually acts in direction of the flow. Its contribution is found by looking at the change in density of the ambient air to the outlet air:

$$\Delta P_{buoy} = \frac{(\rho_{out} - \rho_{amb}) gH}{2} \tag{3.5.10}$$

The total fan power required can be calculated from:

$$P_{fan} = \frac{\dot{m}_{out} \Delta P_{tot}}{\rho_{avg} \eta_{fan}} \tag{3.5.11}$$

3.5.1 Example Pressure Drop Calculation

An example pressure drop calculation is done for the parameters shown in Table 3.5.1.

Table 3.5.1 Parameters used to predict static pressure

Suction Velocity	0.02 m/s
Porosity	0.6%
Height (average distance to fan)	8.3 m
Average Density	1.2 kg/m^3
Hole Diameter	0.001588m
Kinematic Viscosity	0.00001589 m^2/s
Plenum Depth	0.2 m
Collector Width	64 m
Outlet Density	1.1575 kg/m^3
Ambient Density	1.2469 kg/m^3
Friction Coefficient	0.05

Combining equations 3.5.2 and 3.5.3, the pressure drop through the collector would be:

$$\mathrm{Re}_D = \frac{(0.02m/s)(0.001588m)}{(0.006)(0.00001589m^2/s)} = 333.1$$

$$\zeta = 6.82(333.1)^{-0.236}\left[\frac{1-0.006}{0.006}\right]^2 = 47526$$

$$\Delta P_{coll} = \frac{(1.2kg/m^3)(0.02m/s)^2 47526}{2} = 11.4Pa$$

The friction as defined by 3.5.7 would be:

$$\Delta P_{fric} = 0.05\frac{(8.3m)(1.2kg/m^3)(0.221m/s)^2}{2(0.3988m)} = 0.0305Pa$$

The buoyancy term action helps push flow in the direction of the fan as defined by equation 3.5.10:

$$\Delta P_{buoy} = \frac{(1.1575 kg/m^3 - 1.2469 kg/m^3)(9.81 m/s^2)(4.34 m)}{2} = -3.81 Pa$$

Again the acceleration term was modified to represent the outlet velocity:

$$\Delta P_{acc} = \frac{(1.2 kg/m^3)(9.71 m/s)^2}{2} = 56.55 Pa$$

Therefore the total pressure drop would become:

$$\Delta P_{tot} = 11.4 Pa + 0.0305 Pa - 3.41 Pa + 56.55 Pa = 64.2 Pa$$

A pressure drop of 64.2 Pa is equal to 0.257 inH_2O. At this static pressure, the manufacturer specifications indicate that the fan outlet flow should be about 6350 cfm close to the design flow rate for the system.

3.6 Results from monitoring data

After installing all the sensors and data acquisition system, data was accessed either by a site visit or via the modem. Calculations to determine air flow, heat collected, and efficiency were performed using Microsoft Excel.

Initial measurements on the air velocity in the duct using the Alnor Velometer indicated that the average velocity in the duct was between 23 and 24 ft/s (7 to 7.3 m/s) or about 8600-9000 cfm (14,610 m^3/hr to 15,290 m^3/hr). Measurements provided by the Fan-E Flow Station confirmed that total air delivered was approximately 8400 to 8600 cfm (14,270 to 14,610 m^3/hr). The design analysis indicated that the system was designed to deliver about 12,000 cfm (20,390m^3/hr). Therefore, actual flow was measured to be lower than design flow. The original control system allowed some recirculated air from the ceiling. Because the recirculated air was included in the total air delivered, the volume of fresh air would be even lower than measured. Similarly, the volume of air actually going through the collector would be lower also, straying even further from the recommended suction velocity of 0.02 m/s (0.0656 ft/s).

Therefore, it appears that the pressure drop equations do not properly estimate the static pressure in the system. Most likely, either the pressure drop across the collector plate or the friction is underestimated. The issue of estimating the static pressure needs to be

address for proper design of the transpired system. The actual flow through the collector was out of the recommended range for the correlations used to obtain the Nusselt number and heat exchange effectiveness.

Examining the actual amount of fresh air heated by the solar collector with the old control system is more complicated. Because some of the air is recirculated, it is more challenging to determine accurately how much air is coming from the wall versus the ceiling. When designing the monitoring system, it was assumed that a thermodynamic balance on the air entering and leaving the fan box fan could be used to determine the relative contributions of air flow from the ceiling and the wall (Equation 3.3.4). To calculate the relative contributions, the two fan inlet temperatures and the fan outlet temperature were measured. However, the balance becomes less reliable as the temperature of the ceiling and wall air are closer. As previously mentioned, the system was not as successful at destratifying the air as anticipated. Therefore, when the system was operating during the day, the temperature between the fan outlet and the ceiling temperature became relatively close. From examining these results, it appears that the system hardly ever only delivers air from the solar wall. Even if the damper is completely closed to the ceiling, it is also possible that the ceiling damper leaks. Because of the uncertainty in the mass flow calculations with the original control system, it is unreliable to report the amount of heat provided strictly from the collector during that time. In addition, the Solar Center requested that the plant operate the system during this time from at least 9am to 4pm. Employees would only sporadically turn the system on due to the cold air being delivered to the room at night and on cloudy days.

3.6.1 Temperatures Measurements

A plot of the temperatures of the fan inlet from the wall, the fan inlet from the ceiling, fan outlet, and ambient outdoor for a three day period is shown in figure 3.5.1 (reference figure 3.1.3 for sensor location). This graph shows data collected in late January with the original control system. During peak sun hours, the system is capable of heating the air up 50^{o}F (28^{o}C) in the collector. It can be seen from this graph that the outlet air temperature is in between the inlet temperatures from the wall and ceiling. During the time period shown, the system is still bringing in fresh air during the nighttime or cloudy hours. At night, the outlet air was between 65-70^{o}F (18.3-21.1^{o}C) . The circulation of this air at room

temperature caused the room to feel colder. An inline auxiliary heater would allow a constant outlet temperature and fixed quantity of ventilation air. When this industrial facility was in full operation, they had three shifts, working 24 hours a day. It is essential to make workers comfortable all the time.

During non-peak sun hours, it is notable that the fan inlet temperature is quite a bit higher than the ambient outdoor temperature. The fan inlet sensor was mounted from the inside of the wall into the wall plenum. As the ventilation damper closes, this temperature reading is influenced by the temperature inside the building. The temperature is also warmer because this plenum is recovering some heat loss from the south wall of the building.

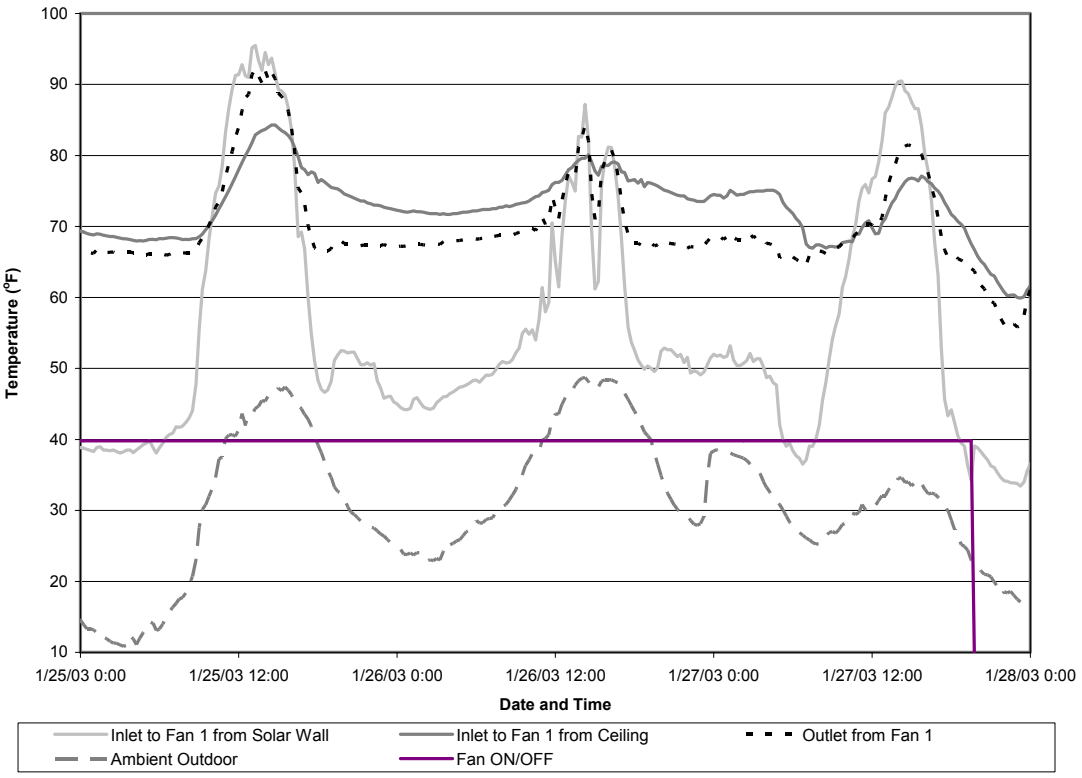

Figure 3.6.1 Temperatures of fan inlets from the wall and ceiling, fan outlet, and ambient outdoor

Of the twenty four days of data that were collected after the new control system was installed, there were twelve days where the system brought in fresh air and heat for at least four hours. For the period after the new control system was installed, the temperature rise in the collector is presented in a different manner. The difference between ambient temperature (collector inlet) and outlet temperature is plotted versus solar radiation incident on the collector in Figure 3.6.2. These points were collected in February and early March on

days with significant solar resources. Although there is not a simple linear relation, this graph shows that the collector heats the air between 20-50^{o}F during peak sun hours.

Employees in the warehouse also complained that the warm air stayed at the ceiling level. This claim was verified by comparing the data on indoor ambient temperature at floor and ceiling levels. The ambient indoor temperature sensor was located halfway between the two fans. Figure 3.6.3 shows the temperature stratification between the floor and ceiling for the same

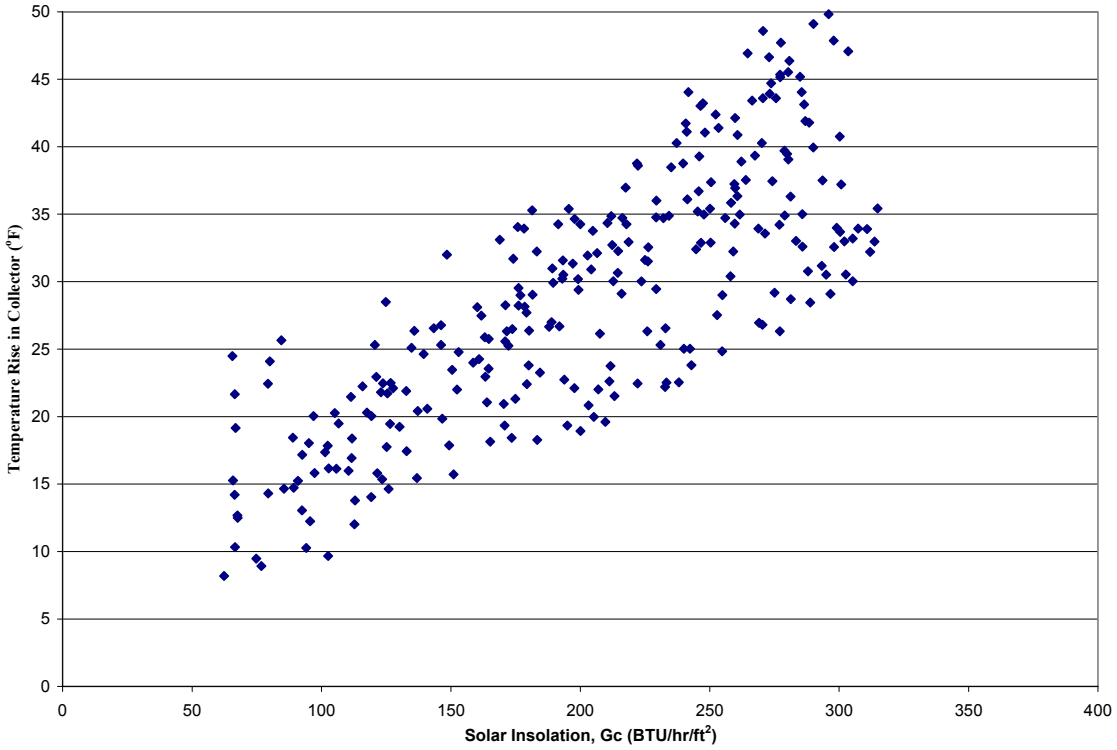

Figure 3.6.2 Temperatures rise in collector compared to solar insolation.

three day period in January. There were wide fluctuations in the temperature stratification; when the solar collector was providing heat, the difference in temperature between the floor and ceiling level was 10-20^{o}F. Some warm air was making it to the ground level, but the system did not provide as much destratification as expected. A different approach to

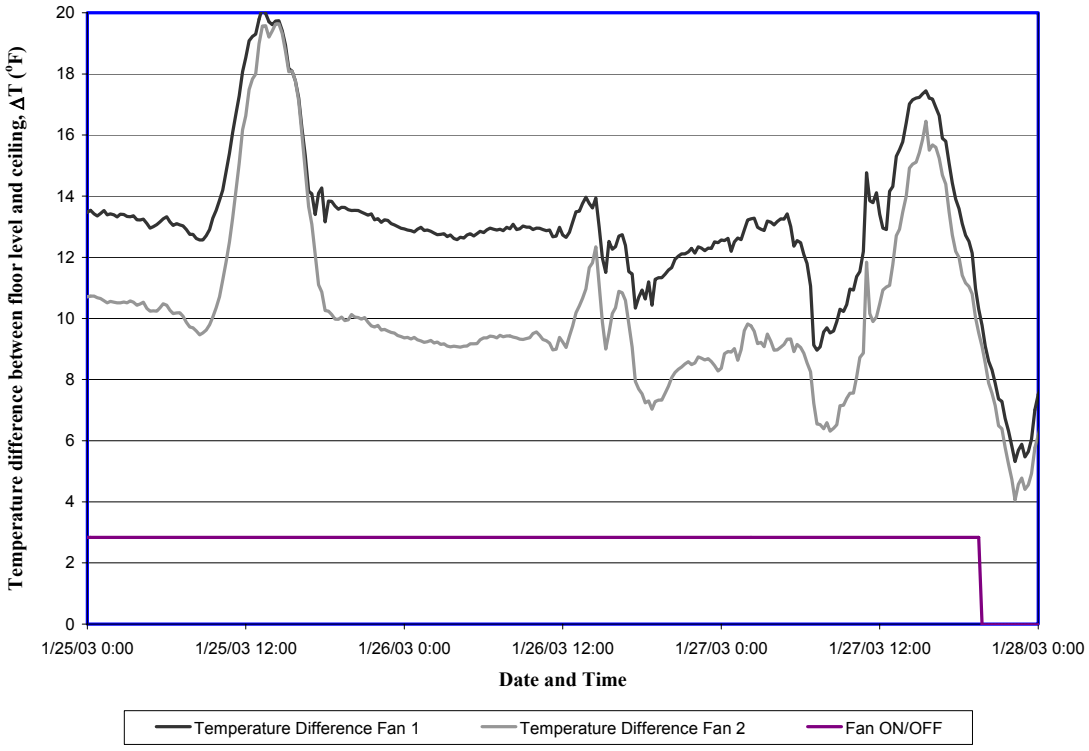

Figure 3.6.3 Temperature difference between ceiling and ambient indoor near floor level.

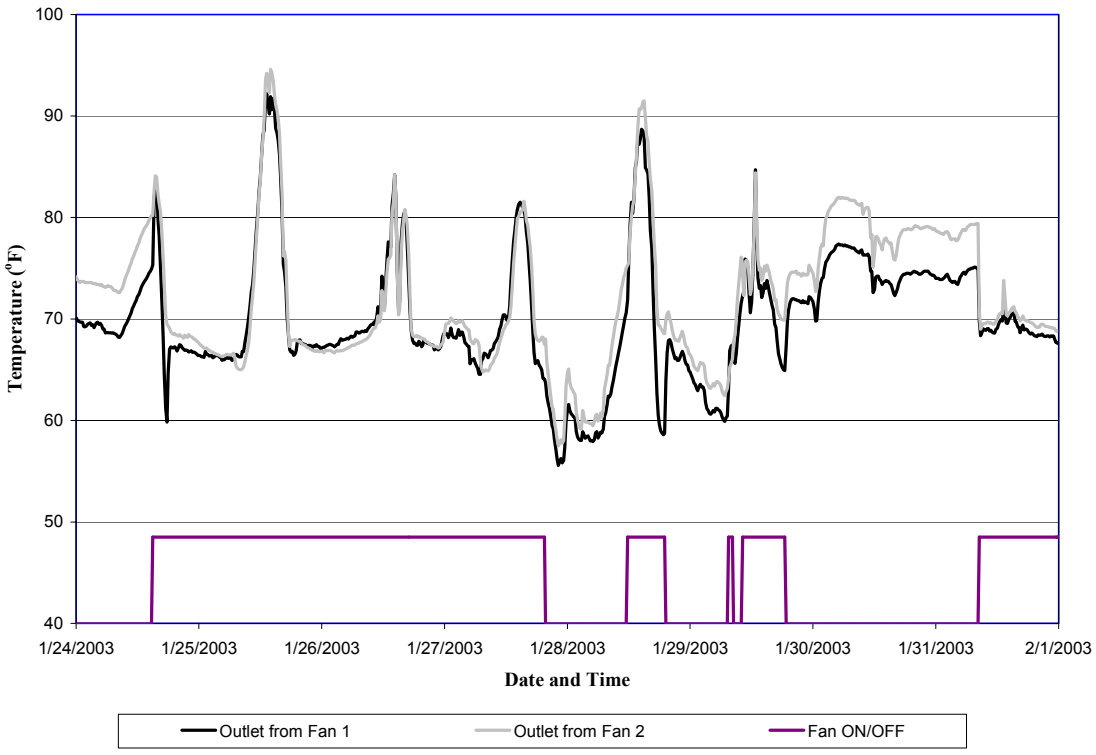

Figure 3.6.4 Temperature on both fan outlets

recirculation would be to draw air from the ground level back through the fan instead of ceiling air. This approach may create better circulation of air. Temperature was monitored on each fan to determine whether the two sections of the wall performed similarly. Figure 3.6.4 shows the outlet temperatures from both fans. The results were surprisingly consistent. When the system is turned on, each side supplies air at about the same temperature. This means that both fans and that each half of the collector performs fairly uniformly.

3.6.2 Experimental and Empirical Efficiency Comparison

Instantaneous efficiency according to equation 3.2.7 was calculated for each data point with the new controls where both fans were operating and the solar radiation was above 200 W/m^2 (63.4 $BTU/hr/ft^2$). The average daily instantaneous efficiency for these data points ranged from 32% to 55%. Previous performance studies of demonstration projects showed that these systems had annual average efficiencies of 57-72% (Brunger 1999). Therefore, the initial results from the 2003 heating season indicate that this system would have a lower annual efficiency than typical systems. The lower efficiency may be due to operating below the design air distribution flow rate (about 8600 cfm instead of 12000 cfm). A lower operating flow results in a higher temperature rise in the collector, but still less total heat delivered to the building.

Figure 3.6.5 shows a plot of the efficiency versus solar radiation for the measured instantaneous efficiency, the Kutscher model and the Van Decker model. Both the Kutscher model and the Van Decker model predict fairly uniform efficiency, but the measured actually varies more. As expected, the measured efficiency is somewhat scattered but has decreasing trend with increasing solar radiation. Whereas this at first may be counterintuitive, as the plate temperature increases under high solar radiation, the radiative and convective losses increase. This trend is not reflected well in either the Kutscher or the Van Decker model. To show this effect more, Figure 3.6.6 reflects the transpired collector data on the typical plotting coordinate for solar collectors. A glazed collector would expect to have a curve with a negative slope. The transpired collector has a positive slope. The efficiency curve for a transpired collector is quite different from a normal glazed solar collector. This is because the ambient air is actually the inlet air, whereas in most solar energy systems, the inlet conditions would come from the storage tank. The normal Hottel Whittlier equation does not

exactly apply because the second term drops out. This means that again, the Kutscher and Van Decker models predict fairly uniform values for the efficiency, while actual operating conditions have a wider range. This plot only includes solar radiation in the range of 275-325 BTU/hr/ft^2. Plots of the same parameters at lower radiation levels, yield very similar results, only matching well at the high end of the graph around a $\Delta T/G$ ratio of 0.15 ^oF-ft^2/BTU/hr. The Kutscher model overpredicts surface temperature, and this plot only represents actual surface temperature, not predicted surface temperature.

Figure 3.6.7 shows an efficiency versus wind speed. The highest wind speed measured during peak operational hours was just under 14 mph (6.3 m/s) and most were under 7 mph (3.1 m/s). Both the Kutscher model and the measured values show the decreasing trend with wind speed, but the Kutscher model overpredicts the efficiency. The Van Decker model stays steady with no noticeable dependence on wind speed. This outcome is to be expected since this model did not include a convective heat loss coefficient in the equation for the heat removal factor. However, wind speed does show up in Van Decker's effectiveness correlation, which affects the efficiency.

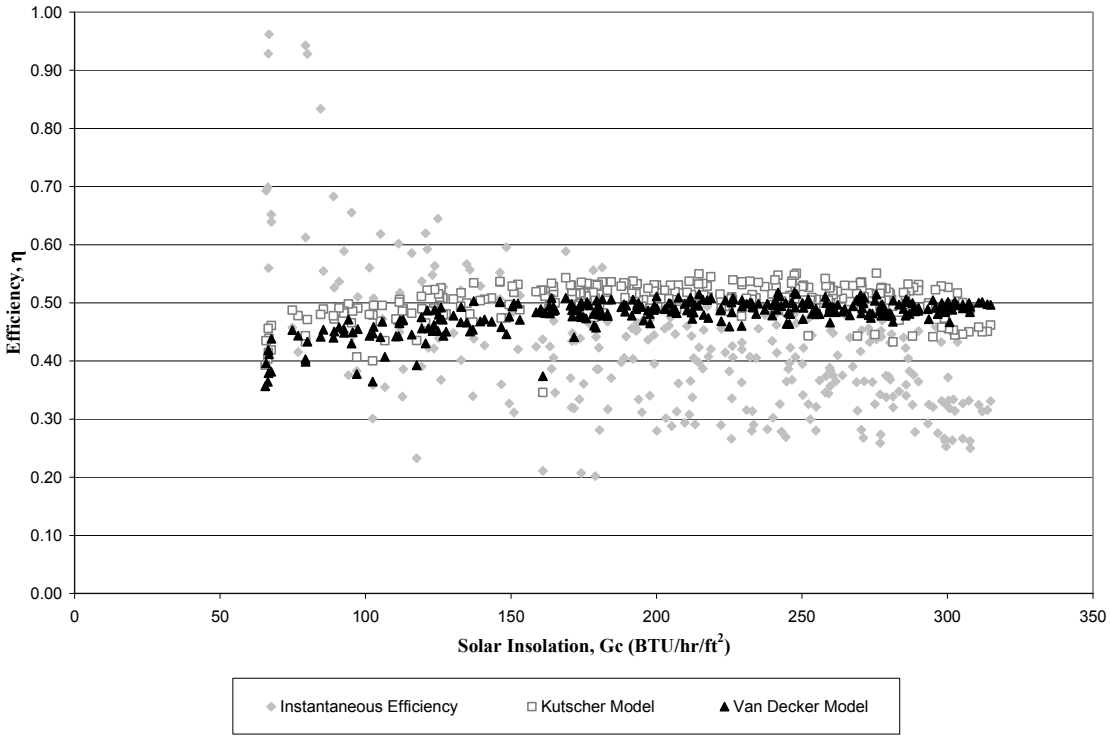

Figure 3.6.5 Efficiency versus solar radiation incident on the transpired collector

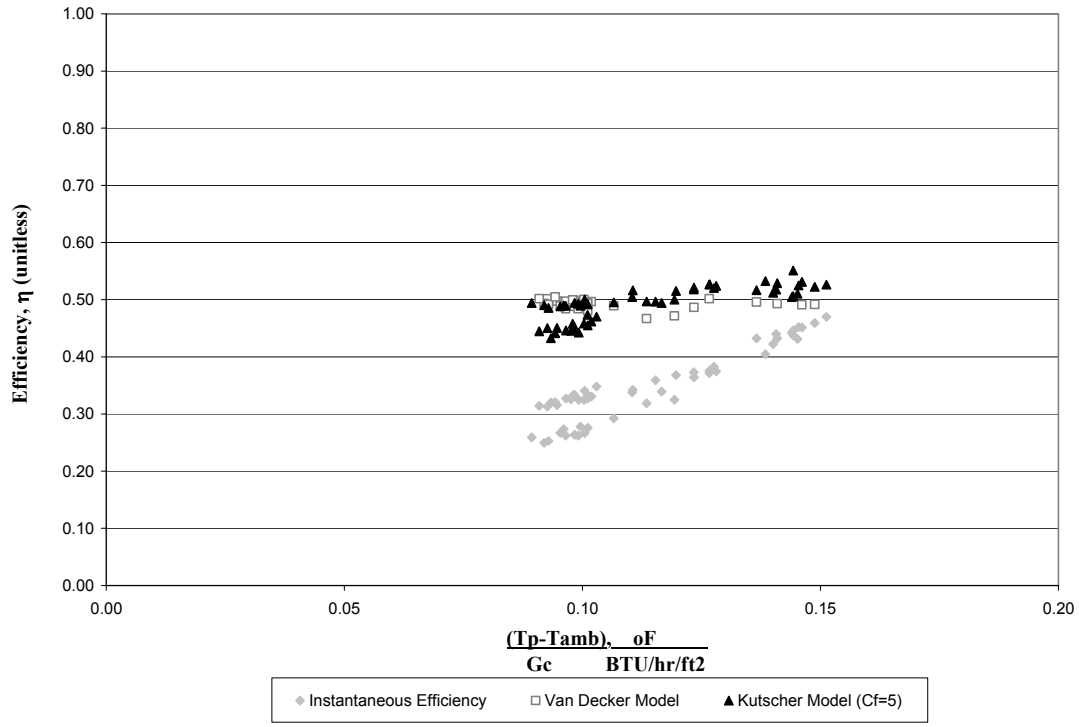

Figure 3.6.6 Efficiency versus measured plate temperature, ambient temperature, and solar insolation

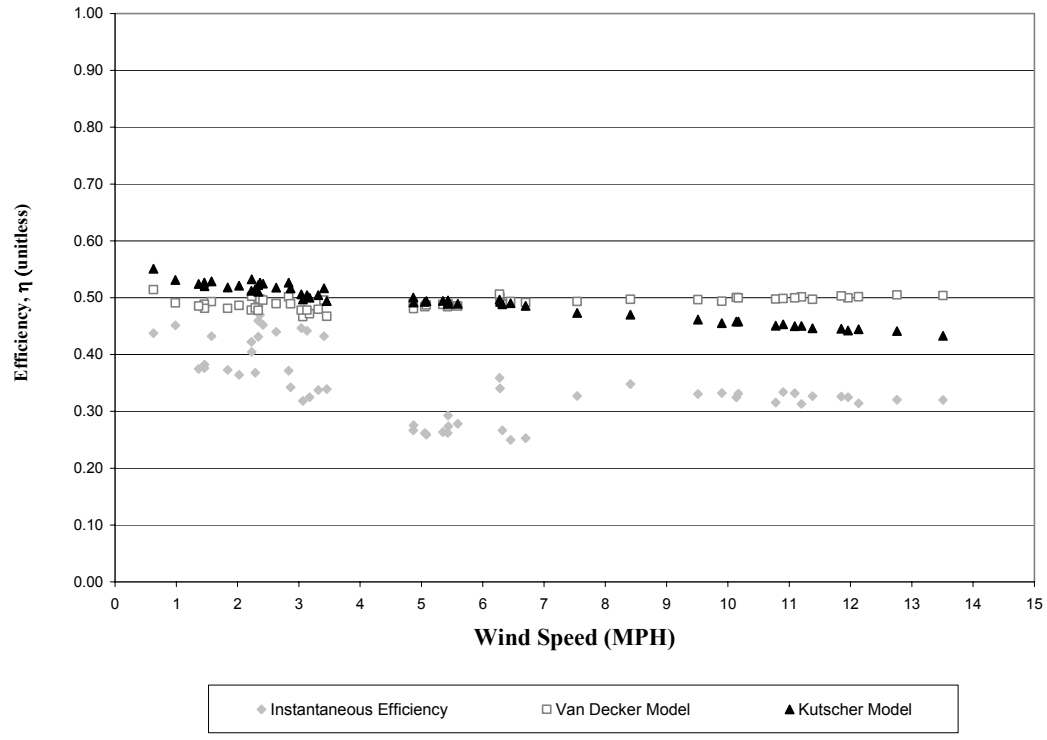

Figure 3.6.7: Measured and modeled instantaneous efficiency versus wind speed

3.7 Economic Evaluation

Most active solar heating systems require conventional electricity to deliver solar energy. A direct power measurement was on the fan distribution system taken with a three phase power meter while the system was operating. The measurements on both fans were between 1070-1100 Watts. Therefore, as a ventilation system operating 24 hours a day, these fans would consume 51-53 kWh each day. Assuming the rate for electricity for an industrial facility is between $0.035 and $0.05 per kWh, the cost to operate the fans would only be between $1.80 and $2.60 per day. For six months of operation, this translates into between $325 to $500 spent to collect and deliver the solar heated air. Operational costs were much lower for the monitored system, since it did not run near 24 hours a day. Transpired collector systems are only supposed to be used for applications where the ventilation would be required. Consequently, the cost of operation of the fans does not necessarily have to be subtracted from the energy savings.

The system delivered between 0.9 MMBTU/day and 2.0 MMBTU/day on the monitoring days in February and March. In the twenty four days that was collected with the new control system, the system delivered a total of 18.6 MMBTU (186 therms). Assuming a conventional gas heating system has a system efficiency of 80%, then the equivalent gas consumption would be 23.3 MMBTU (233 therms). Energy rates vary and natural gas prices in particular are subject to demand swings. An conservative value of $0.80 per therm is used to calculate the offset cost of natural gas heating (PSNC 2004). The estimated fuel savings during this twenty four day period was $212. Since the fans did not operate 24 hours a day, the operation cost was low and only about $7-10 for the same period.

4 TRNSYS Simulation

The Transient System Simulation Software (TRNSYS) was used to predict performance of the transpired collectors using weather data in North Carolina. There are some computer design models already developed, but this software was chosen because it is modular and the standard tool in the solar industry. Systems are built with this software using component models already built into the program. For example, a conventional solar air heating system can be simulated easily using pre-made components using a solar collector, thermal storage, control system, mixing ducts, and auxiliary heaters.

Summers (1995) conducted a similar study of a transpired collector for a Master's thesis with a simulation in TRNSYS. There is not an official component in TRNSYS for the transpired collector, but the FORTRAN code from Summers (1995) was available for the unglazed transpired collector at the official TRNSYS website (TRNSYS). Summers' component uses Kutscher's earlier work in modeling transpired collectors. Based on Kutscher's conclusions, Summers' model completely neglected convective heat loss for suction velocities above 0.02m/s (0.0656ft/s). Kutscher's more recent model (1994) is used in the formulation of a simulation in TRNSYS. Several other studies have claimed that the laminar asymptotic model applies well to these collectors provided the suction velocity is high enough. While most of the formulation of the component is based on the work of Summers, the component developed for this thesis includes the convective losses and a user specified corrugation factor, which may help correct heat losses for additional problems in the model due to the corrugations.

To run a TRNSYS simulation, the user must specify inputs and parameters. Parameters are values which do not change throughout the simulation (such as solar collector area) whereas inputs can change over time (such as weather data). A couple of the parameters in Summers' component were changed to inputs. For example, the room temperature was changed from a parameter to an input so that the room temperature can vary for thermostat setback or seasonally. Also, a separate variable was added to recirculation temperature from room temperature. This separation of room temperature and recirculation temperature would make it possible to evaluate the effect of recirculating air that is stratified,

although there is not currently a component in TRNSYS capable of modeling a building with air stratification.

4.1 Energy balance for TRNSYS simulation

An energy balance was presented previously to predict surface temperature under operating conditions of the transpired collector and was used to examine experimental data. Experimental data was only analyzed during peak operating conditions. This energy balance on the surface did not examine any recovered heat loss through the south wall or heat transfer in the plenum because they were considered insignificant under times of high solar radiation. However, for the TRNSYS simulation, recovered heat loss and heat transfer in the plenum were included in the energy balance. These contribute more during non-peak solar hours. An energy balance on the collector is shown in Figure 4.1 and is defined by equation 4.1.1. The energy balance follows the previous TRNSYS model, except convection losses from the collector are included.

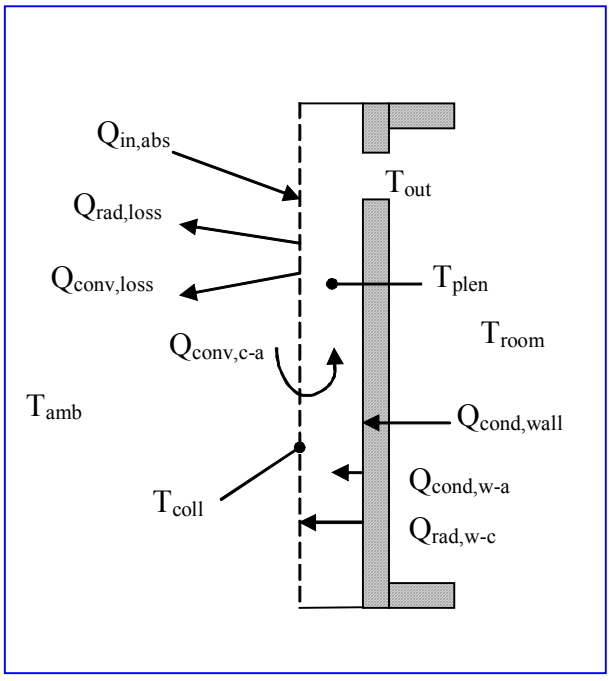

Figure 4.1.1: Energy balance on the collector and the wall.

$$Q_{in,abs} + Q_{rad,w-c} = Q_{conv,loss} + Q_{rad,loss} + Q_{conv,c-a} \qquad (4.1.1)$$

The energy absorbed by the collector, $Q_{in,abs}$, is found from the absorptivity of the collector, the incident solar radiation, and the area of the collector.

$$Q_{in,abs} = \alpha_{coll} I_T A_P \tag{4.1.2}$$

The convection from the collector to the air is the heat gain from the collector. In this model, there is a distinction between plenum temperature and collector outlet temperature.

$$Q_{conv,c-a} = \dot{m}_{coll} C_p (T_{plen} - T_{amb}) \tag{4.1.3}$$

$$T_{plen} = \varepsilon_{hx} (T_{coll} - T_{amb}) + T_{amb} \tag{4.1.4}$$

The radiative and convective losses were explained in detail in section 3.3 and are defined for the component by equations 4.1.5 ad 4.1.6.

$$Q_{conv,loss} = h_c A_s (T_{coll} - T_{amb}) \tag{4.1.5}$$

$$Q_{rad,loss} = \varepsilon_{coll} \sigma_{sb} A_s ({T_{coll}}^4 - {T_{sur}}^4) \tag{4.1.6}$$

The conduction through from the room to the wall is defined can be defined as:

$$Q_{cond,wall} = \left(\frac{1}{\frac{1}{U_{wall}} - \frac{1}{h_{conv,w-a}}} \right) A_{wall} (T_{room} - T_{wall,o}) \tag{4.1.7}$$

$$= (UA)_{wall} (T_{room} - T_{plen}) \tag{4.1.8}$$

Usually the outer wall to air heat transfer coefficient, $h_{conv,w-a}$, is already accounted for when calculating the overall heat loss coefficient for the wall. It has to be subtracted out of this overall coefficient if the outer wall temperature is used to define this conduction. Otherwise, the wall conduction is defined by the second equation using the U_{wall} and the plenum temperature.

There is also radiant exchange between the outer wall and the collector.

$$Q_{rad,w-c} = \sigma_{sb} A_s \frac{({T_{wall,o}}^4 - {T_{coll}}^4)}{\frac{1}{\varepsilon_{wall}} + \frac{1}{\varepsilon_{coll}} - 1} \tag{4.1.9}$$

While the previous equations defined the energy balance on the collector, an energy balance on the wall will leave only two unknowns in the equations, $T_{wall,o}$ and T_{coll}.

$$Q_{cond,wall} = Q_{conv,w-a} + Q_{rad,w-c} \quad (4.1.10)$$

$$Q_{conv,w-a} = h_{conv,w-a} A_s (T_{wall,o} - T_{plen}) \quad (4.1.11)$$

$$= \dot{m}_{coll} C_p (T_{out} - T_{plen}) \quad (4.1.12)$$

The heat transfer coefficient from the outer wall to the air depends on the velocity in the plenum. The correlation for laminar flow across a flat plate is (Incropera and Dewitt 2002):

$$N\overline{u}_L = 0.664 \, \mathrm{Re}_L^{1/2} \, \mathrm{Pr}^{1/3} \quad \text{where } \mathrm{Re_L} < 5\mathrm{x}10^5 \quad (4.1.13)$$

while the following correlation was used for mixed flow

$$N\overline{u}_L = (0.037 \, \mathrm{Re}_L^{4/5} - 871) \, \mathrm{Pr}^{1/3} \quad \text{for } 5\mathrm{x}10^5 < \mathrm{Re_L} < 10^8 \quad (4.1.14)$$

The energy balance was solved in a FORTRAN subroutine in TRNSYS by a trial and error method. These equations reduce down to two unknowns, the wall temperature and the collector temperature. For the transpired collector, the range of these temperatures under operating conditions is predictable. Therefore, guesses were made at the temperature of the wall and collector in the operating conditions. The values which return the least error in the energy balance were assumed to be the appropriate solution to the simultaneous equations.

As previously mentioned, Summers (1995) had previously developed a component for the transpired collector in TRNSYS. While several modifications were made to incorporate new correlations from the literature, most of the same strategies and basic energy balances were followed. The basic equations are also the same, they are presented here for clarification and because there were a few minor modifications. To calculate energy savings from the transpired collector, it is necessary to look at an energy balance on a ventilated building with or without a transpired collector system as shown in figure 4.2.

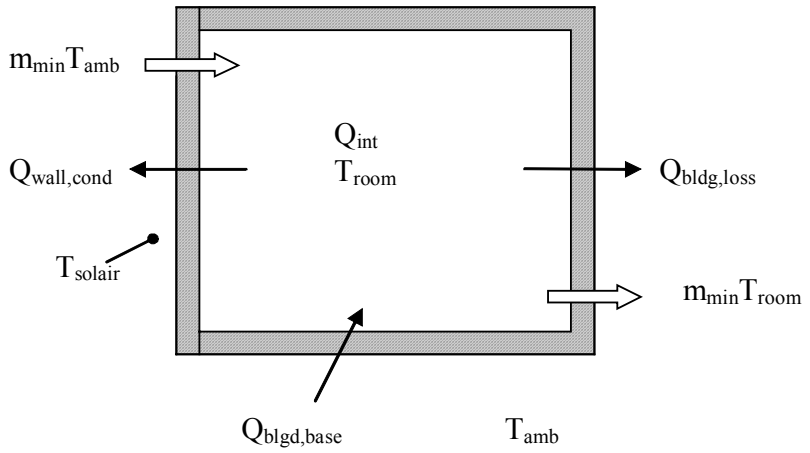

Figure 4.1.2: Energy balance on a building with ventilation system

The heat energy required for the base case building (without a transpired collector) is a function of the conductive heat loss, heating of ventilation air, and the internal gains. The auxiliary heating that would be required for a normal ventilation system on a building without the transpired collector is:

$$Q_{bldg,base} = Q_{bldg,loss} + Q_{cond,wall} + \dot{m}_{\min} C_p (T_{room} - T_{amb}) - Q_{int} \qquad (4.1.15)$$

The conductive heat loss from the building could be characterized by the following equation:

$$Q_{bldg,loss} = (UA)_b (T_{room} - T_{amb}) \qquad (4.1.16)$$

For comparative purposes to the transpired wall case, the heat transfer through the area of the wall where the transpired collector would be installed (usually the south side) is defined separately:

$$Q_{cond,wall} = (UA)_{wall} (T_{room} - T_{solair}) \qquad (4.1.17)$$

The sol-air temperature, $T_{sol\text{-}air}$, is defined by ASHRAE (1997) and is used to look at the heat flux into exterior sunlit surfaces. For vertical surfaces, the equation simplifies to:

$$T_{solair} = T_{amb} + \frac{\alpha_{wall} I_T}{h_o} \qquad (4.1.18)$$

The recommended value from ASHRAE for h_o, the heat transfer coefficient between the outer wall and the air, is 17 W/m^{2}K. Details about the conditions that result in this heat transfer coefficient value are shown in the Section 5.

The third term in equation 4.1.15 defines the energy required to heat the minimum amount of ventilation air for the building. The fourth term is added to the energy balance to take into account any internal gains within the buildings, Q_{int}. Internal heat gains in conditioned spaces can be from people, lighting, electrical motors, or other mechanical equipment.

The addition of the transpired collector system changes the energy balance slightly for the ventilated room as shown in Figure 4.1.3. The transpired collector mounted on the south side of the building changes the heat transfer through that wall. In that case, the heat loss through the transpired wall becomes:

$$Q_{cond,tran} = (UA)_{wall} (T_{room} - T_{plen}) \qquad (4.1.19)$$

Therefore, the difference in conductive heat transfer losses between the situation with or without the transpired collector becomes:

$$Q_{cond,diff} = (UA)_{wall}(T_{plen} - T_{solair}) \tag{4.1.20}$$

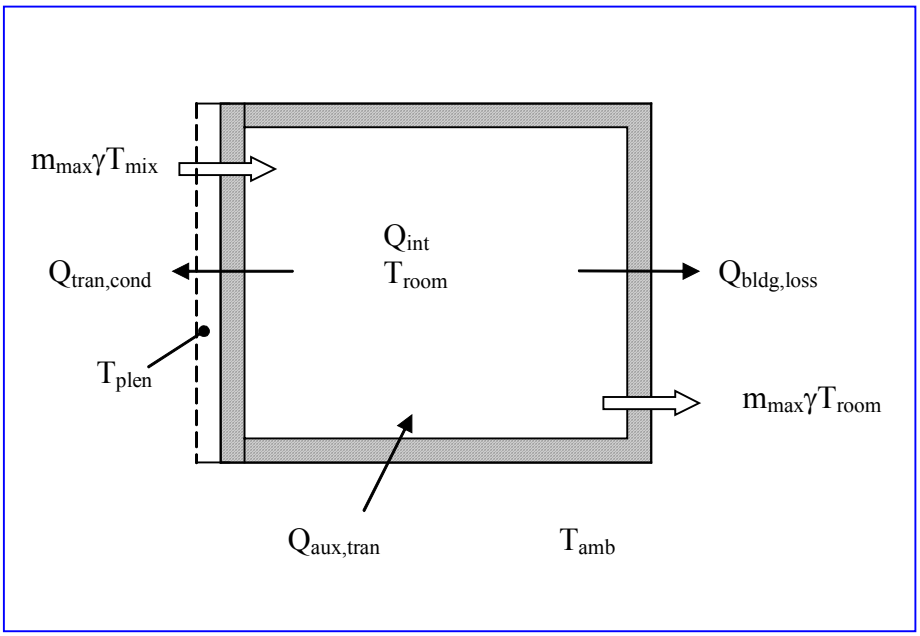

Figure 4.1.3: Energy balance on a building with transpired collector ventilation system

If the plenum temperature is greater than the effective sol-air temperature, then there is a reduced convective loss through this wall. However, since the collector actually shades the wall from solar radiation, it is possible for the conductive losses to increase when the plenum temperature is less than the sol-air temperature. Either way, this difference in the conductive loss must be accounted for in the heat loss from the buildings. The total heating required for the building becomes:

$$Q_{bldg,tran} = Q_{bldg,loss} + Q_{cond,tran} + \dot{m}_{\max}\gamma C_p(T_{room} - T_{amb}) - Q_{\text{int}} \tag{4.1.21}$$

Heated make-up air must at minimum supply enough heat to overcome this building conductive heat loss plus the heat lost because of the air being forced into the building. The $Q_{bldg,tran}$ is defined also as the heat energy into the ventilation air which is supplied to the room at T_{sup}.

$$Q_{bldg,tran} = \dot{m}_{\max}\gamma C_p(T_{\text{sup}} - T_{amb}) \tag{4.1.22}$$

While this is the total heating load of the building, defining the load another way becomes useful to find an optimal supply temperature.

$$Q_{bldg,load} = Q_{bldg,loss} + Q_{cond,tran} - Q_{\text{int}} \tag{4.1.23}$$

Now the supply temperature is calculated based on this heat load divided by the flow and specific heat of the incoming air:

$$T_{\sup} = T_{room} + \frac{Q_{bldg,load}}{\dot{m}_{\max} \gamma C_p} \tag{4.1.24}$$

Because a room has a constant or predictable thermostat setting, from a control standpoint this approach is valid because the auxiliary heating system will maintain the setpoint temperature within a room.

Once this supply temperature is predicted, it can be used to determine the optimal amount of air that is drawn through the collector to provide maximum heat gain and minimum auxiliary heating. The heated air from the collector is mixed with some recirculated air from the room. Therefore, it is necessary to solve the collector outlet and mixed air temperature several times. The mixed air temperature can be defined by a thermodynamic balance:

$$T_{mix} = \gamma T_{out} + (1-\gamma) T_{recirc} \tag{4.1.25}$$

Summers (1995) used a bisection method in the FORTRAN program to address this recirculation within the TRNSYS model. The same strategy was used in the component formulation presented in this text. First the mixed air temperature is found for the minimum amount of air flow through the collector. If the mixed air temperature is less than the supply temperature, the fraction of air flow, γ, remains at the minimum and the auxiliary heating energy is calculated. If the mixed air temperature is greater than the needed supply temperature, then the fraction of airflow is set to one and the collector outlet temperature is found using this maximum flow rate. Note that in this case, the mixed air temperature is equal to the collector outlet air temperature. Then, the mixed air temperature is checked again against the supply temperature. If the mixed temperature is less than the supply temperature the bisection method is used to find the appropriate mass fraction of airflow to minimize auxiliary heating. To calculate savings from the transpired collector, it is necessary to examine the auxiliary heating required. The auxiliary heating with a transpired collector is defined by equation 4.1.26 and shown in Figure 4.1.4.

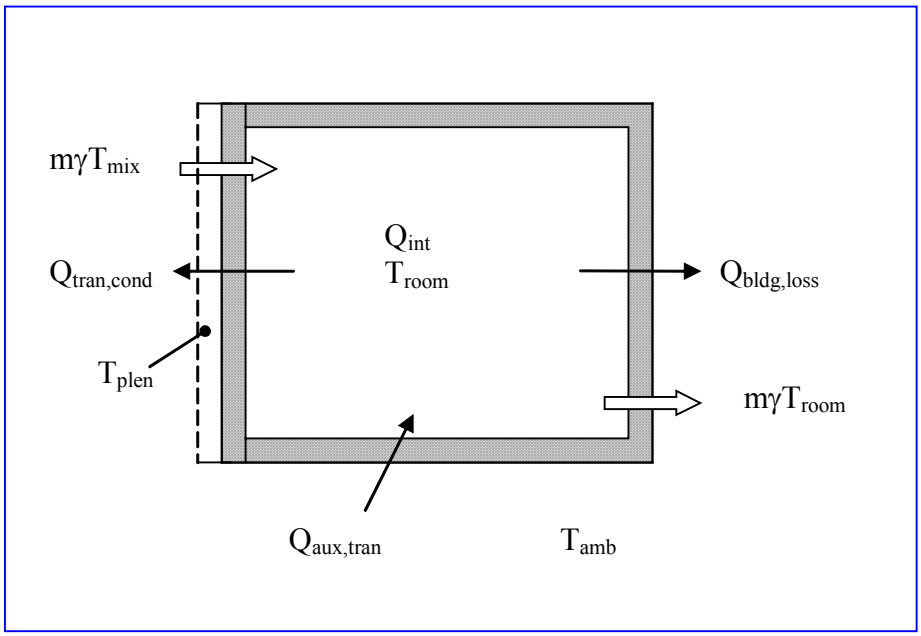

Figure 4.1.4: Redefined energy balance on a building with transpired collector ventilation system to show auxiliary heating

$$Q_{aux,tran} = \dot{m} C_p (T_{sup} - T_{mix}) \tag{4.1.26}$$

The difference between these two auxiliary heating values becomes the energy savings from the transpired collector system.

$$Q_{save} = Q_{aux,base} - Q_{aux,tran} \tag{4.1.27}$$

The energy savings is different from the heat gain from the transpired system defined by the following:

$$Q_{gain,tran} = \dot{m} \gamma C_p (T_{mix} - T_{amb}) \tag{4.1.28}$$

Sometimes the collector will provide more heat than required to provide the supply temperature. While this heat is recovered from the collector, it does not necessarily offset auxiliary heating and therefore cannot be included in the calculation of energy savings. Ultimately, energy and monetary savings only result from offset fuel consumption. The control strategy used in this model will allow more heat into the room than necessary to maintain supply temperature. It is possible though for this strategy to cause overheating of the room.

If the ambient temperature is above the specified bypass temperature, the bypass damper is opened. In this operation, the heat gain, auxiliary heating, heat exchange effectiveness, and solar efficiency are all set to zero. The mixed and outlet temperatures are equal to the ambient air temperature and the program does not solve for the collector, plenum, and outside wall temperatures. In addition, Summers (1995) included an optional feature to bypass the collector at night. Due to radiation and convective heat loss, air may be cooler if it is drawn through the collector. Therefore in night bypass mode, the bypass damper is opened and only the minimum amount of ventilation air required is drawn into the room. This air is mixed with recirculated air from the room and heated with the auxiliary heater. If this feature is enabled, the solar efficiency, heat exchange effectiveness, and heat gain are all set to zero. Again, the mixed air temperature and outlet air temperature are equal to the ambient temperature and the subroutine does not solve for the collector, plenum, and wall temperatures. Nighttime is defined by the times when there is not solar radiation incident on the collector.

The FORTRAN computer program for the component is included in Appendix A.

4.2 TRNSYS Simulation Results

The component appropriate for the transpired collector was developed on the principles in the last section, this component was connected to the following other standard components in TRNSYS:

1) TM2 Weather Data
2) Solar Radiation Processor
3) Lumped Capacitance Building
4) Psychometric Chart
5) Online Plotter

The new component essentially has all of the outputs needed to assess energy savings, but the lumped capacitance building component was used to verify results and evaluate the room temperature change over time.

There were several goals to using TRNSYS to model the transpired collector system. It is a convenient way to model yearly performance of solar thermal systems using Typical

Meteorological Year data. Simulations were done for the collector configuration of the monitored transpired collector to determine the potential heat gain and energy savings for cities in North Carolina. These results were compared to the potential heat gain and energy savings from a collector in a colder climate such as Madison, WI or Buffalo, NY. Table 4.2.11 and Table 4.2.2 shows all the typical operating parameter and inputs used in the simulation. The simulation units are all in metric units, but the results are reported in English Units.

Table 4.2.1 List of Parameter Values in TRNSYS simulation

Collector Area (m^2)	277
Collector Emmissivity	0.89
Collector Absorptivity	0.94
Collector Height (m)	4.34
Hole Diameter (m)	0.001588
Hole Pitch (m)	0.0256
Plenum Depth (m)	0.20
Corrugation Factor	varies (0-5)
Porosity	0.006
Collector Surface to Projected Area Ratio	1.15
UA for wall behind collector (W/K)	157
Emissivity of outside wall behind collector	0.5
Absorptivity of outside wall behind collector	0.5
UA of the building (wall behind collector not included) (W/K)	1232
Summer Bypass Temperature (^oC)	18
Number of Fans	3
Fan Diameter (m)	0.6048

Table 4.2.2 List of Input Values in TRNSYS simulation

Hour		Weather Data
Solar Radiation (W/m^2)		Weather Data
Ambient Temperature (^oC)		Weather Data
Wind Speed (m/s)		Weather Data
Dew Point (^oC)		Weather Data
Max. Flow Rate through Collector (m^3/hr)		32500 (varies)
Min. Flow Rate though collector (m^3/hr)		20400 (varies)
Atmospheric Pressure (Bar)		Weather Data
Room Temperature (^oC)		20 (varies)
Internal Gains (W)		10700
Night Bypass Enabled (0=No, 1=Yes)	No	
Recirculation Temperature (^oC)	Varies	

First, results from a simulation for the same inputs were compared between the component developed as a part of this thesis (new) and the Summers component (old) to verify that the component was working properly. Because of the method of solution, the new component had a longer run time, taking a couple of minutes to run a yearly simulation. However, this component does gain some flexibility since the room temperature does not have to be set as a constant (to allow thermostat setback). Also, the recirculation temperature does not have to be the same as the assumed room temperature for the purpose in the future of using a stratification model for the building. In this case, room air at "ceiling" or "floor" temperature would be mixed with collector air; room temperature used to calculate the heat loss from the building would be some average of these two temperatures.

A comparison of energy savings and potential heat gain for the new and Summers model are shown in Table 4.2.3. It was assumed that the system would need three fans to meet the required ventilation and suction velocity. The minimum flow through the collector would be the 12,000 cfm (20,400 m^3/hr) and maximum flow was assumed to be the flow out of three fans 19,050 cfm (32,2500 m^3hr) at 0.25 inH_20 static pressure. The room ambient temperature was set to 20°C (28°F), the bypass temperature is 18°C (64.4°F). The comparisons are made for cities in North Carolina and two cities with colder climates, Madison, WI and Buffalo, NY.

Table 4.2.3: Comparison of potential heat gain and energy savings between new and Summers TRNSYS component model.

	Potential Heat Gain (MMBTU/yr)			Energy Savings (MMBTU/yr)		
	New Model	Summers Model	Percent Diff	New Model	Summers Model	Percent Diff
Raleigh, NC	374	374	0.0%	199	185	-7.7%
Wilmington, NC	308	304	-1.2%	158	143	-10.4%
Asheville, NC	398	397	-0.2%	226	225	-0.4%
Charlotte, NC	415	414	-0.3%	207	197	-5.1%
Madison, WI	428	426	-0.5%	341	341	0.1%
Buffalo, NY	375	382	2.1%	291	315	7.4%

Because Summers model neglected convective losses, for this comparison, a corrugation factor (for convective heat loss coefficient) of zero was used in the new component. Overall, the yearly energy savings predicted by the two components were comparable. Summers model was considered the standard in the percent difference calculation. The largest difference is energy savings was for Wilmington at 10.4%. In most cases, the new model predicted a higher energy savings than the old model. There are slight differences in the definitions of the radiative heat loss coefficient and heat exchange effectiveness in the two different models, so small differences in the output are expected. From other results reviewed, the difference probably came from the definition of energy savings. As stated earlier, the energy savings is defined as the difference in heating for a regular building with no UTC system and the auxiliary heating for a building with a UTC system. The new model consistently predicted a larger base heating and auxiliary heating than the old model. Slight modifications were made to the equations for base and auxiliary heating which may account for the difference.

Next, the effect of adjusting the corrugation factor for convective losses was examined. The conclusions from the monitoring study showed these convective losses were more significant at lower suction velocities. Therefore, two values of flow rate through the collector will be used in the simulation, one equal to previous specifications and one to represent a suction velocity outside the recommended range. Figure 4.2.1 shows the potential heat gain and energy savings for six cities with the corrugation factor set to zero (no convective losses) and a corrugation factor equal to five. The corrugation factor equal to five was recommended by Brunger (1999) from studies of the effects of the corrugations on heat loss, but is not necessarily a definitive value. Again, the comparison is run for a minimum collector flow rate of 20,400 m^3/hr (12,000cfm) and a maximum collector flow rate of 32,500 m^3/hr (19,050cfm). The inclusion of convective losses for the simulated cities results in a 13-20% reduction in potential heat gain and a 7-18% reduction in energy savings.

The second comparison for the effect of convective losses on the collector is done at a lower flow rate. The minimum flow through the collector was set to 10,200 m^3/hr (6000cfm) (1 ACH) and the maximum was set to approximately the measured flow rate 15,300 m^3/hr (8960cfm). As shown in table 4.5, the lower flow increases the percentage of convective losses slightly. This result is expected because the higher flow rates through the collector

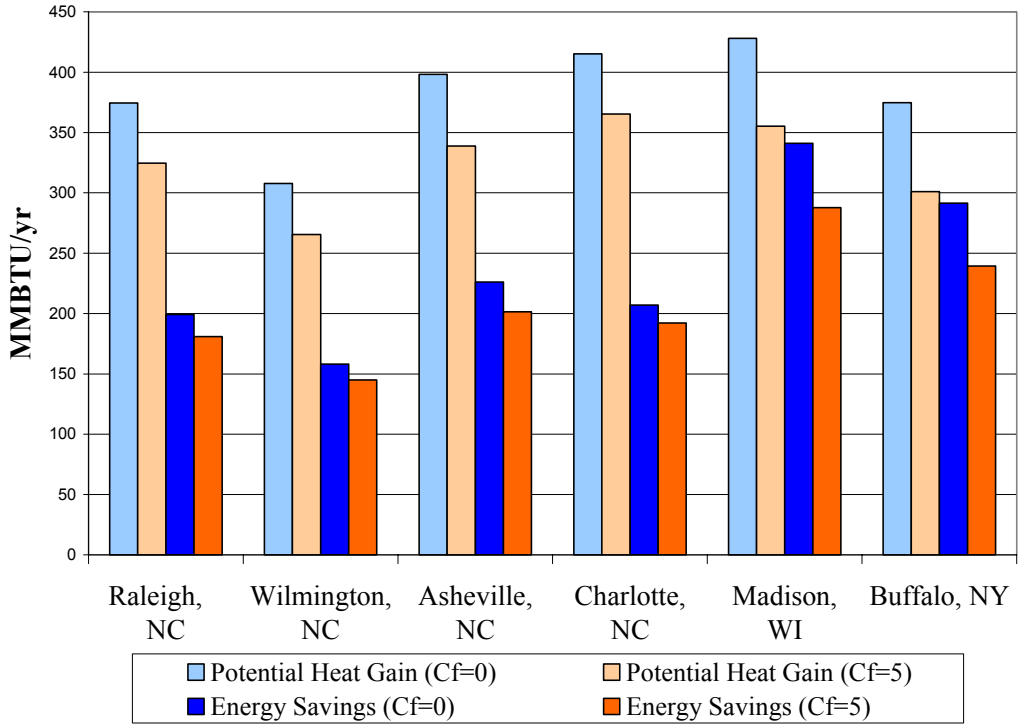

Figure 4.2.1: Comparison of potential heat gain and energy savings for neglected convective losses (Cf=0) and for the inclusion of convective losses through the collector (Cf=5) at a recommended flow rate

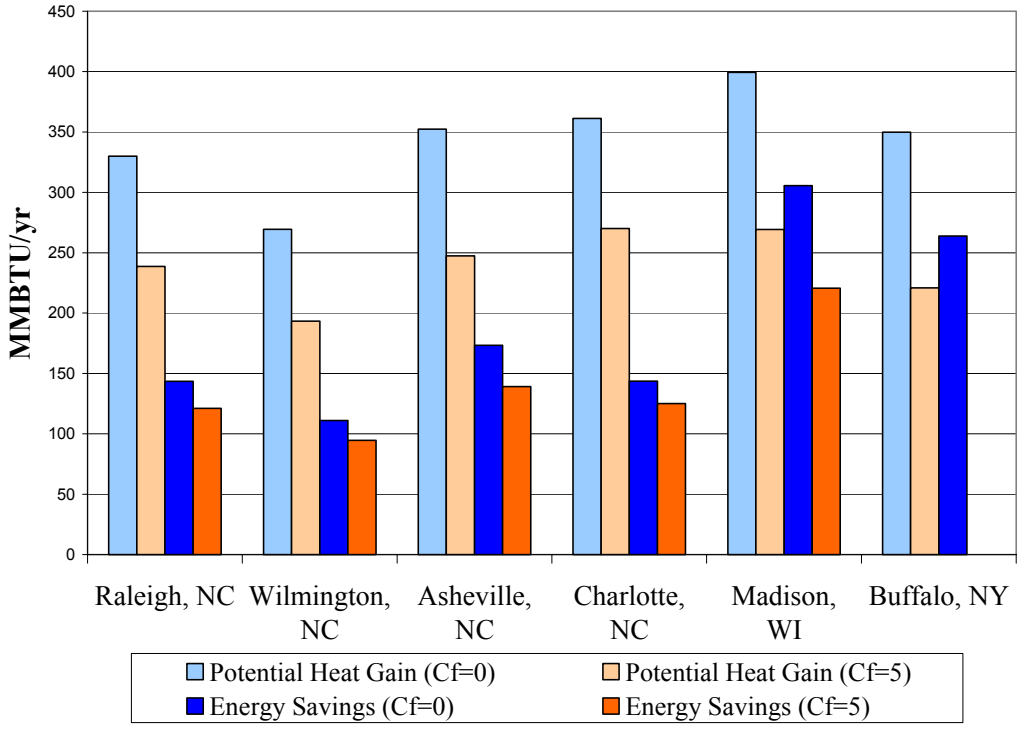

Figure 4.2.2: Comparison of potential heat gain and energy savings for neglected convective losses (Cf=0) and for the inclusion of convective losses at a lower than recommended flow rate

help maintain the asymptotic boundary layer that reduces convective losses. The minimum and maximum flows through the collector are about half of the flows presented in the previous example. However, the energy savings is not reduced by a half from the previous example because the lower flow results in a larger temperature rise in the collector. These flow rates are outside the recommended range for the model and it is probable that the energy savings is overpredicted for the low flow rate.

By leaving all but one variable constant, it is possible to look at how certain operating conditions affect overall energy savings. For a collector with specified physical characteristics (collector area, building size, porosity, etc.), the energy savings is highly dependent on the assumed internal gains in the building, the building set point temperature, and the flow through the collector.

Figures 4.2.3 and 4.2.4 show how setting the minimum and maximum flow through the collector affects energy savings. First, the simulations were run for a minimum collector flow of 20,400 m^3/hr and maximum collector flows of 20,400 m^3/hr, 30,600 m^3/hr, 40,800 m^3/hr, and 51,000 m^3/hr (12,000 cfm to 29,900 cfm) (which correspond to suction velocities of 0.02 m/s to 0.05 m/s or 0.0656 ft/s to 0.164 ft/s). By definition, energy savings should not be affected by the maximum flow and that is shown by the graph in Figure 4.2.3. Increasing the maximum flow through the collector only slightly affects the potential heat gain. Allowing a maximum flow of 30,600m^3/hr (17,900 cfm) only increases the potential heat gain by 9% while the maximum flow of 51,00 m^3/hr (29,900 cfm) provides an additional 15% of potential heat gain. The curve for potential heat gain is asymptotic because at suction velocity of 0.05 m/s, the solar efficiency does not increase. Changing the minimum flow rate does affect energy savings as shown in Figure 4.2.4. For this simulation, the maximum and minimum flow rates were set as the same at 20,400 m^3/hr, 30,600 m^3/hr, 40,800 m^3/hr, and 51,000 m^3/hr (12,000 cfm to 29,900 cfm). Choosing the optimum flow rate for the collector system is dependent on required ventilation rates. The curves for both energy savings and potential heat gain are asymptotic. Therefore, installing a larger system than to meet ventilation standards may not necessarily be economical.

Of course, when the room set point temperature is increased, the transpired collector will provide more energy savings. Figure 4.2.5 shows how the set point temperature can affect energy savings in the range of 64^{o}F and 75^{o}F (17.8^{o}C to 23.9^{o}C). Most thermostat set

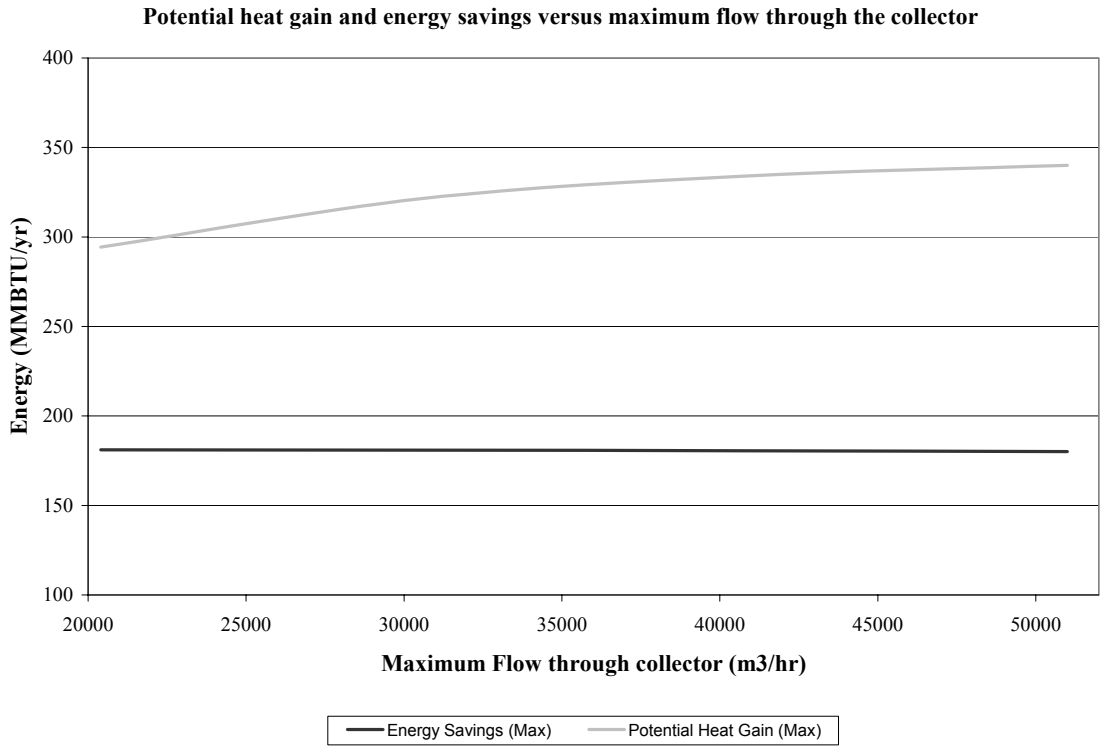

Figure 4.2.3: Potential heat gain and energy savings changing maximum flow through the collector with the minimum flow constant

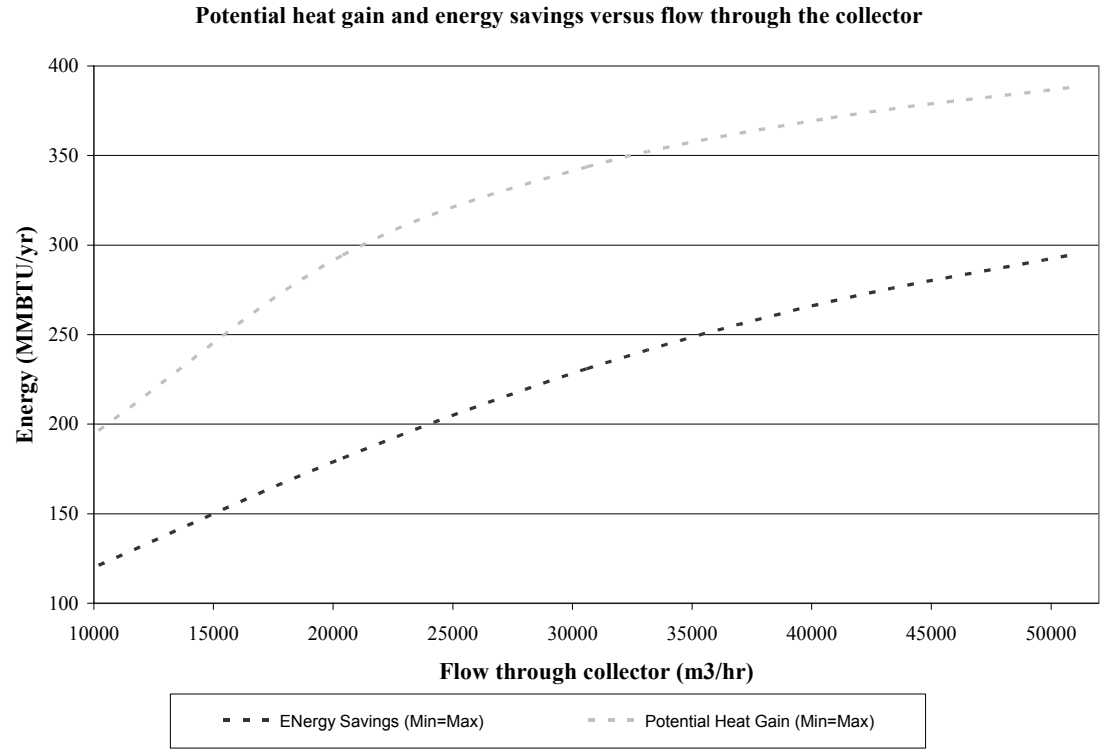

Fig ure 4.2.4: Potential heat gain and energy savings changing flow through the collector

points for a commercial building would most likely be between 66°F and 70°F (18.9°C to 21.1°C) , but possibly lower for some industrial facilities. The low set point temperatures make the energy savings quite marginal for the stated configuration and assumptions.

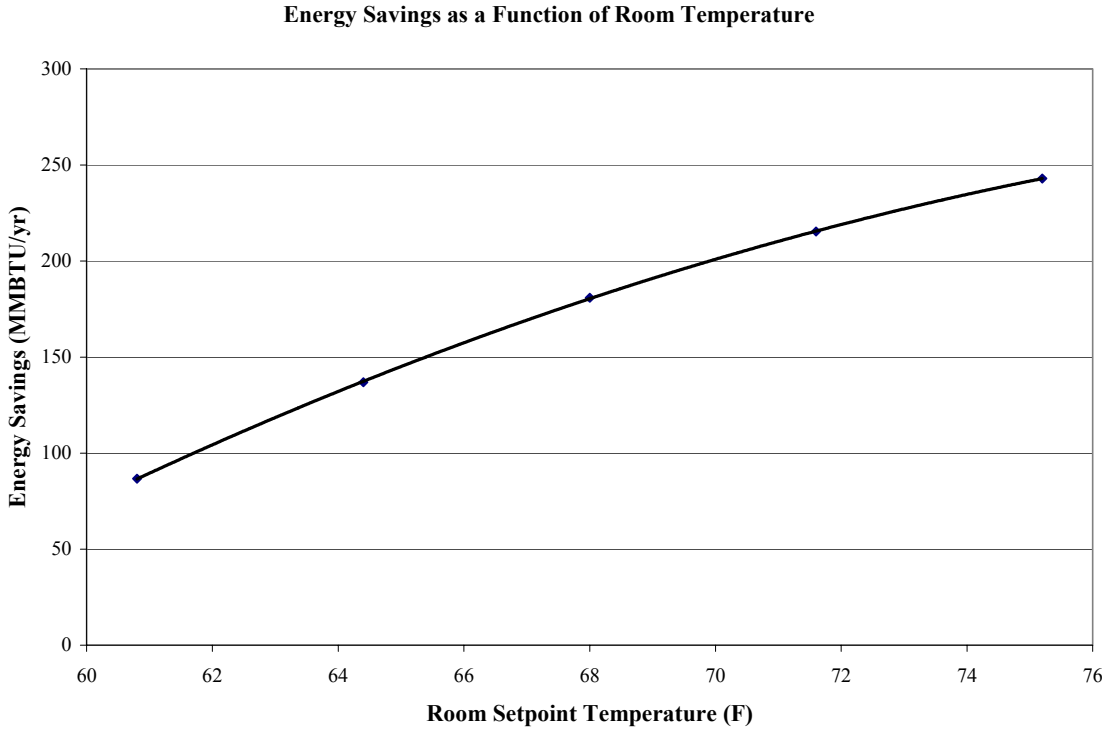

Figure 4.2.5: Energy savings dependent on room temperature

All previous TRNSYS analysis was based on the assumption that the room temperature and temperature of the recirculated air in the fan were equal. Although these systems are supposed to provide destratification of the room, there will most likely be a temperature differential between air at the floor and at the ceiling level. Whereas the distribution fan usually recirculates air from ceiling level, the controls for the heating system would be located at the floor level to maintain the setpoint temperature of the room where the people actually are located. Therefore, as most of the transpired systems are set up, this assumption may not be valid. To truly analyze the effect of temperature stratification on energy savings and room comfort, it would be necessary to use a computational fluid dynamics software appropriate for buildings such as FLUENT. This was beyond the scope of the current study. However, since there are separate inputs in the new TRNSYS component for room temperature and recirculation, it is worth assess whether small

temperature differentials have the potential to affect energy savings. Figure 4.2.6 shows that a recirculation temperature higher than room temperature can impact energy savings.

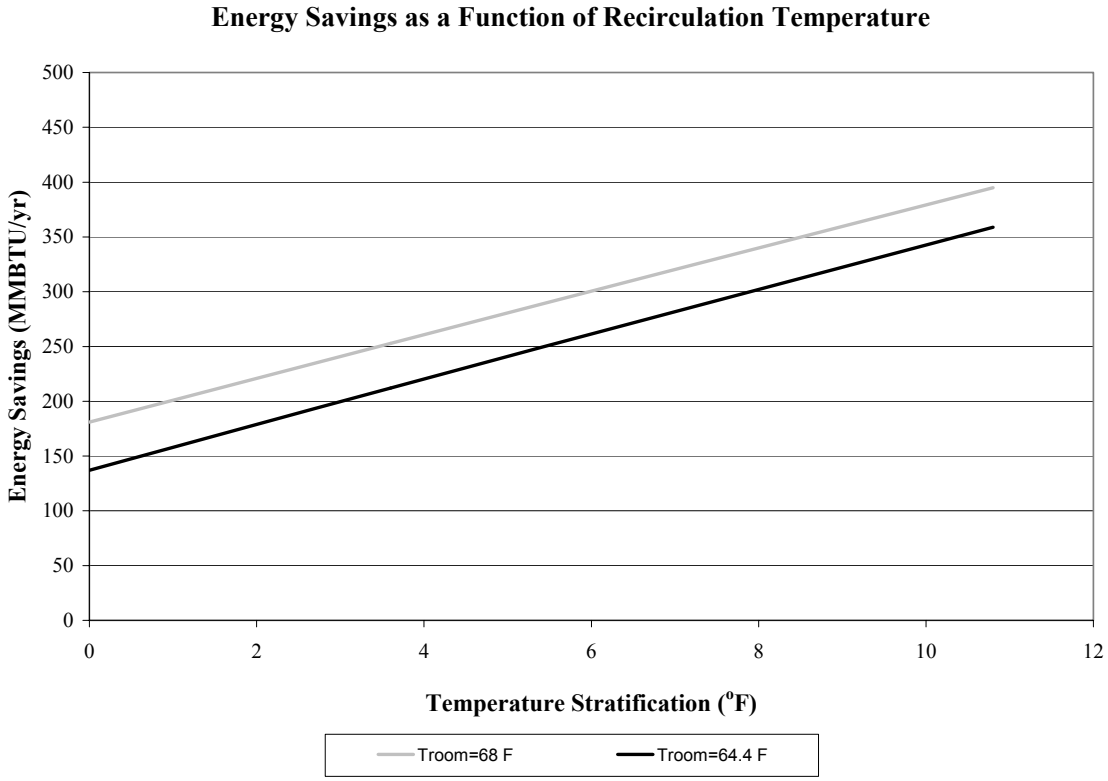

Figure 4.2.6: Energy savings dependent on recirculation temperature

To compare solar energy systems, solar engineers often use the solar fraction, the fraction of the total heating load provided by solar energy. Many solar water or space heating systems are designed to have solar fractions between 0.4 and 0.8, offsetting a percentage of fuel costs. Because it is a low temperature and simple heating system, previous studies have noted that the solar fraction for a transpired system is only about 0.20 As shown in shown in Table 4.6, the solar fraction is about 0.10-0.20 or the solar provides only 10-20% of the total heating load of the building.

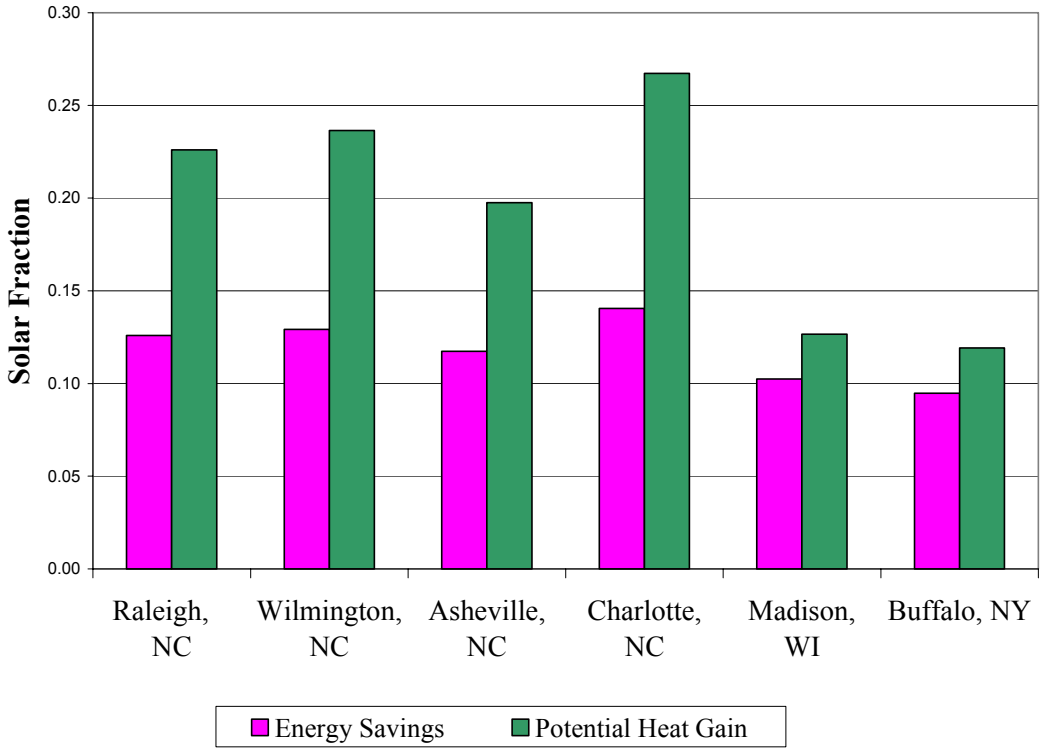

Figure 4.2.8: Solar Fraction for the potential heat gain and energy savings from transpired collector system

5 Heat Transfer Analysis of Plenum during Bypass Conditions

There have been some claims that these collectors can help cool the south wall because of the induced natural convection through the perforations and plenum. Often in North Carolina's climate cooling is more of a concern than heating. There was some concern that there may be some unwanted heat gain because of the collector in the summer. A simple analysis of how this collector might encourage negative heat gain in the summer was done. For this analysis, two cases were considered: 1) A south facing wall without a collector and 2) a south facing wall with a collector.

In Section 3.5, an assumption was made that the heat transfer coefficient from an outer wall (exposed to sunlight) to the air is 17 $W/m^2/K$ when calculating the sol-air temperature. Then, the difference in conduction through the sunlit wall was proportional to the difference between the sol-air temperature and the plenum temperature. In this section, case 1 for a sunlit wall and case 2 for a transpired collector will be compared for relative heat gain in the cooling season. Because of the availability of property data, all inputs and results are reported in metric units.

5.1 Case One: A Sunlit Wall

Case 1. A resistance network analogy was used consisting of conduction through the wall to the room, convective losses from the wall due to natural and forced convection, and radiative losses from the wall. The network analogy is shown in Figure 5.1.1. There is a flux of solar energy on into the outer wall equal to the absorptivity of the wall times the solar radiation.

Using the resistance analogy, equation 5.1.1 can be used to solve for the outer wall temperature.

$$T_{wall,1} = \frac{S'' R_{loss} R_{cond} + T_{amb} R_{cond} + T_{room} R_{loss}}{R_{cond} + R_{loss}} \qquad (5.1.1)$$

The total loss resistance is defined in equation (5.1.2) from the radiative loss coefficient and the total convective loss coefficient. A relation recommended in Incropera and DeWitt is used to find the total convective loss coefficient from the natural and forced convection as shown in equation 5.1.3.

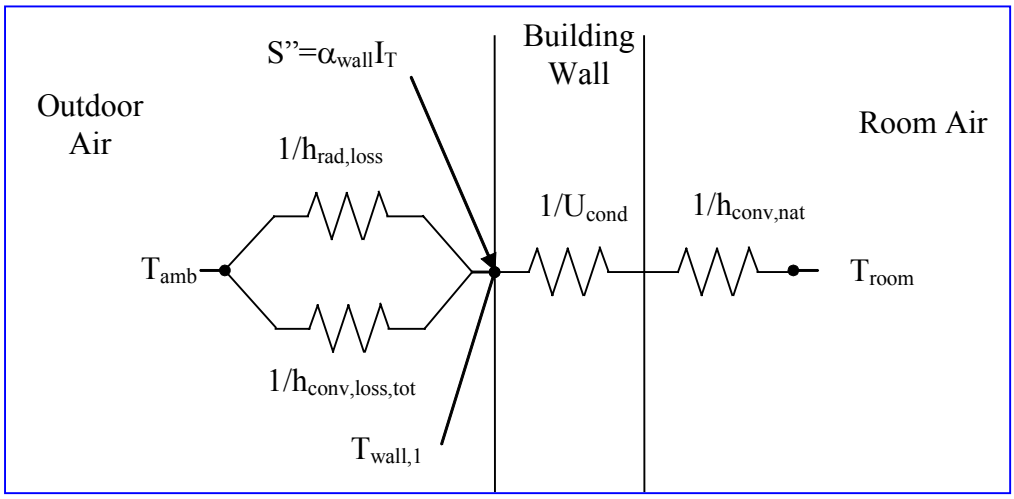

Figure 5.1.1: Resistance analogy network for the heat transfer through wall exposed to solar radiation.

$$R_{loss} = \frac{1}{h_{rad,loss} + h_{conv,loss,tot}} \tag{5.1.2}$$

$$h_{conv,loss,tot} = (h_{conv,nat,out}^{3} + h_{conv,for,out}^{3})^{1/3} \tag{5.1.3}$$

The conduction resistance is defined in equation 5.1.4 and depends on the conduction heat transfer coefficient through the wall, $U_{cond,}$ and the natural convection from the inner wall surface of the room.

$$R_{cond} = \left(\frac{1}{U_{cond}} + \frac{1}{h_{conv,nat,in}} \right) \tag{5.1.4}$$

The U_{cond} is determined from the inverse of the sum of the R-values of the materials of the wall. Equations must be used to find $h_{conv,nat}$ and $h_{conv,for}$ for the regular outside wall and is fairly straight forward. Although $h_{conv,nat}$ was calculated for the temperatures of the outside wall, the same value was used for the heat transfer coefficient for the inside wall. The difference in temperatures between the collector and the inside wall may cause some error,

but this value was used for both case one and case two. Therefore, it is really only used for comparative purposes. For a vertical surface, equation 5.1.5 from Churchill and Chu (1975) is used to find the free convection heat transfer coefficient appropriate for both laminar or turbulent free convection flow on a vertical flat plate (Incropera and Dewitt 2002).

$$\overline{Nu}_{\substack{L,nat,\\ vert}} = \left\{ 0.825 + \frac{0.387 Ra_L^{1/6}}{\left(1+\left(\frac{0.492}{\mathrm{Pr}}\right)^{9/6}\right)^{8/27}} \right\}^2 \qquad (5.1.5)$$

where the Raleigh number is defined by $Ra_{\substack{L,nat,\\ vert}} = Gr_x \,\mathrm{Pr} = \frac{g\beta(T_{wall,o} - T_{amb})L^3}{\nu\alpha}$ (5.1.6)

For the forced convection case, two different correlations were used for laminar and turbulent flow across a flat plate. These correlations both assume an isothermal plate and unidirectional forced flow. In the case of the plain wall, the forced flow across the flat plate would be the wind. As discussed before, the wind is not necessarily unidirectional, but these were the assumptions used to analyze the bypass condition. A more detailed analysis would need to investigate better correlations for the turbulent flow around a building. The correlations defined by equation 4.1.13 were used for laminar flow (low wind speed) and equation 4.1.14 was used for mixed flow (higher wind speeds). Because of the conditions surrounding the wall, the flow across the wall is most likely not laminar. The Reynold's number depends on the length of the wall in the direction of the wind. For collector lengths of 4m and 10m, the transition to turbulence will occur at a wind speed of 1.9 m/s and 0.8 m/s respectively. The last term to define is the radiative heat loss coefficient (Equation 5.1.7). It is derived similarly to the radiative heat loss from collector, only the outer wall temperature is substituted into the equation.

$$h_{rad,loss} \approx \frac{4\varepsilon_{wall}\sigma_{sb}T_{avg,wall}^{\ 3}(T_{wall,1} - T_{sur})}{(T_{wall,1} - T_{amb})} \qquad (5.1.7)$$

5.2 *Case Two: South Facing Wall with Transpired Collector*

Case two. A south wall with a plenum. The network analogy is shown in figure 5.2.1

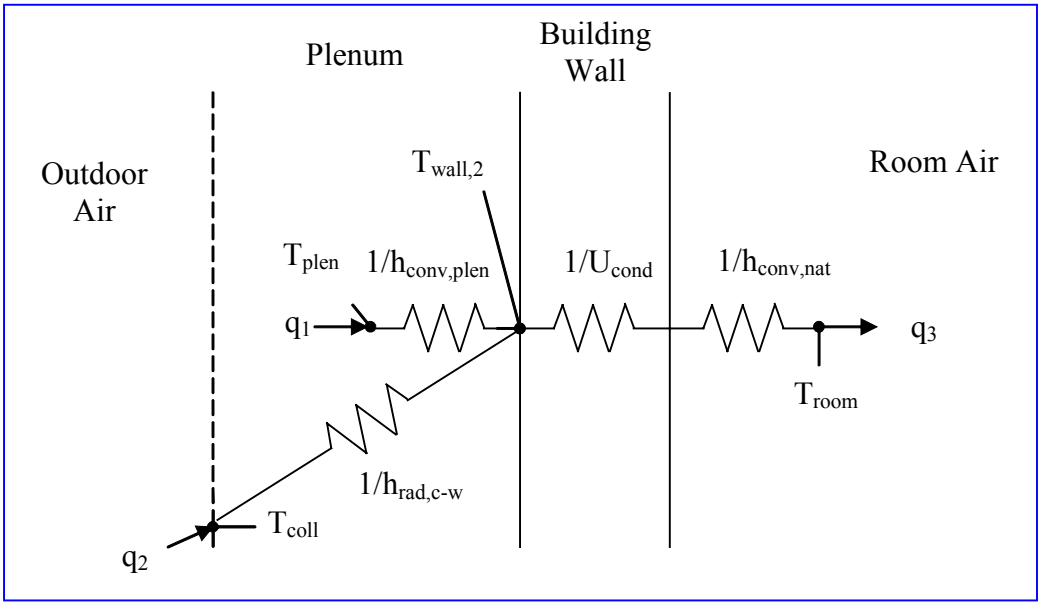

Figure 5.2.1: Resistance analogy network for the heat transfer through wall with transpired collector

The conduction resistance term is the same as in the previous example with equation 5.1.4. The wall to plenum convective resistance is defined in equation 5.1.8 and is used to find the outer wall temperature for case two in equation 5.1.9.

$$R_{plen} = \frac{1}{h_{conv,plen}} \tag{5.1.8}$$

The radiation between the collector and the wall is treated as radiation between infinite parallel plates similar to equation 4.1.9. To simplify analysis, a radiative heat transfer coefficient for parallel plates can be defined as (Duffie and Beckman 1991):

$$h_{rad,c-w} = \sigma_{sb} \frac{(T_{coll}^{\ 2} + T_{wall,2}^{\ 2})(T_{coll} + T_{wall,2})}{\frac{1-\varepsilon_{coll}}{\varepsilon_{coll}} + \frac{1-\varepsilon_{wall}}{\varepsilon_{wall}} + 1} \tag{5.1.9}$$

The radiative resistance then becomes:

$$R_{rad} = \frac{1}{h_{rad,c-w}} \tag{5.1.10}$$

As defined in Figure 5.2.1, the convection and radiation into the outside wall equals the heat transfer to the room or $q_1+q_2=q_3$, the outer wall temperature can be found by equation 5.1.11

$$T_{wall,2} = \frac{T_{coll}R_{plen}R_{cond} + T_{plen}R_{rad}R_{cond} + T_{room}R_{rad}R_{plen}}{R_{rad}R_{plen} + R_{plen}R_{cond} + R_{rad}R_{cond}} \qquad (5.1.11)$$

The challenging part of analyzing the plenum problem is determining the heat transfer coefficient between the plenum air and the outer wall. The flow dynamics in this plenum are not really known. The theory is that some cooling of the south wall will occur driven by natural convection in this plenum. Ambient air should enter the transpired collector at the bottom through the perforations, rise as it is heated and leave through the perforations in the top of the collector. Therefore, it is not straightforward channel flow, free convective flow over a plate plate, forced convective flow over a flat plate, or free convection for an enclosed surface. However, all of these scenarios were examined to estimate a range of heat transfer coefficients that would reasonably represent this configuration. The highest heat transfer coefficient resulted when looking at inverted natural convection between the hot plenum and the cooler wall. The correlation is used in case one for the natural convective heat transfer coefficient for a vertical plate (equation 5.1.5) results in a value of $h_{conv,plen}$=2.5 W/m^{2}K.

Incropera and Dewitt (2002) listed several different correlations to solve for the heat transfer coefficient for channel flow. Case two would be best represented by channel flow between a constant collector temperature which is higher than the constant wall temperature. However, none of the presented correlations for channel flow really matched well to the physical conditions in case two. Two cases were analyzed anyway to obtain a general idea of the heat transfer coefficient: one with symmetric isothermal plates and the other with one isothermal plate and an insulated opposite boundary. For symmetric isothermal plates, equation 5.1.11 was used (Ellenbaas 1942)

$$\overline{Nu}_{\substack{s,nat,\\ chan,1}} = \frac{1}{24}Ra_s\left(\frac{S}{L}\right)\left\{1-\exp\left[\frac{-35}{Ra_s\left(\frac{S}{L}\right)}\right]\right\}^{3/4} \qquad (5.1.11)$$

In these equations, L is the collector height or length in the direction of the flow and S is the plenum depth. The Nusselt number correlation obtained by Cohen and Rohsenow (1984) is given by equation 5.1.11 for channel flow between an isothermal plate and an adiabatic plate.

$$\overline{Nu}_{\substack{s,nat,\\chan,2}} = \left[\frac{C_1}{\left(Ra_s \left(\frac{S}{L} \right) \right)^2} + \frac{C_2}{\left(Ra_s \left(\frac{S}{L} \right) \right)^{1/2}} \right]^{-1/2} \quad (5.1.12)$$

C_1=144 and C_2=2.87

where $Ra_{\substack{s,nat,\\chan}} = \frac{g\beta(T_{wall} - T_{amb})S^3}{\alpha\upsilon}$ for both equations 5.1.10 and 5.1.11 (5.1.13)

The plenum heat transfer coefficient, $h_{nat,plen}$ for both of these situations turned out to be around 0.1 W/m^{2}K.

Assuming that the heating of the collector by the sun actually did not induce flow into the plenum through the perforations, internal free convection would characterize the flow in the plenum. For internal flow in a rectangular cavity, the correlation that covers the widest range of aspect ratios (Collector length in flow direction to plenum depth) is given by equation 5.1.14.

$$\overline{Nu}_{L,enc} = 0.046 Ra_L^{1/3} \quad (5.1.14)$$

for aspect ratios of between 1 and 40, 1<Pr<20, and 10^6<Ra_L<10^9. For the given collector with an aspect ratio of 21.7, the $h_{conv,plen}$= 1.1 W/m^{2}K.

If natural convection creates flow at a velocity in the plenum, the outer wall would be subject to convection over a flat plate at a low velocity. For a given value of the heat transfer coefficient and assuming mixed flow over the wall, equation 4.1.14 can be used to solve for the plenum velocity. Then, the validity of the assumed $h_{conv,plen}$ is checked by calculating the flow associated with that velocity. For a $h_{conv,plen}$=5 W/m^{2}K, the flow through the plenum would be 127,700 m^3/hr which is too high. For a $h_{conv,plen}$=1 W/m^{2}K, the flow through the plenum would be 13,384 m^3/hr, closer to the value when the fans are on. For a $h_{conv,plen}$=0.1 W/m^{2}K, the flow through the plenum would be 133 m^3/hr. Based on this reverse calculation, the predicted plenum heat transfer coefficient should be in the range 0.1 to 1.0 W/m^{2}K.

Even with reasonable estimates of the heat transfer coefficient, the plenum temperature is still unknown and reasonable guesses must be made to analyze the problem. Data was collected over the summer months when the system was not operating and was used to make reasonable guesses at the plenum temperature for a given solar radiation. On high solar radiation days with measured horizontal radiation around 750-850 W/m^2, the

plenum temperature ranged between 40-55^{o} C. Because the sun is high in the sky in the summer months, the incident solar radiation on a vertical surface is significantly less than on the horizontal surface (450-650 W/m^2). In fact, the plenum temperature seemed to be reach a maximum in September, when radiation on the vertical surface is increasing because of the lower sun angles while the ambient temperature is often still high (30-35^{o}C). Analysis on case two was run for these ranges of ambient temperature, plenum temperature, and solar radiation and the results are shown in Section 5.3

5.3 Results from Heat Transfer Analysis during Bypass Conditions

As stated at the beginning of this section, there was some concern that there may be some unwanted heat gain because of the collector in the summer. On the other hand, there have been some claims that these collectors can help cool the south wall because of induced natural convection through the perforations and plenum. Therefore, a comparison was done to predict the outer wall temperature for these two cases because a higher outer wall temperature will result in unwanted heat gain to the building.

The network analogy for case one is shown in Figure 5.1.1. Using equation 5.1.2, R_{loss} was calculated. A total heat transfer coefficient for the heat loss form the wall, U_{loss} is equal to the inverse of R_{loss}. This U_{loss} is comparable to the h_o (coefficient of heat transfer by long-wave radiation and convection at the outer surface of a sunlit wall) defined by ASHRAE (1997) to be 17 W/m^{2}K. The ASHRAE value would compare to a wind speed between 4 and 5 m/s (9.1 to 11.4 mph). Table 5.1.1 lists the assumptions of the parameters for this analysis. Some monitoring data was collected over the summer. Actual measurements of ambient outdoor temperature, solar radiation, and plenum temperature were used for input into equations 5.3.1 and 5.1.9. Three data points with low, medium, and high solar radiation on the vertical surface were chosen with as shown in Table 5.3.2. The FORTRAN computer program is included in Appendix B.

Table 5.3.1: Parameters used in heat transfer analysis of plenum during bypass conditions

Parameter	Value
R_{wall}	1.76 m^2-^oC/W (10 ft^2-hr-^oF/BTU)
U_{wall}	0.568 W/m^2-^oC (0.1 BTU/ft^2-hr-^oF)
α_{wall}	0.44
ε_{wall}	0.9
ε_{coll}	0.9
Collector Height, h	5 m (16.4 ft)
Plenum Depth, D_{plen}	0.20 m (8 in)
T_{room}	22.2 ^oC (72^oF)

Table 5.3.2: Actual data used in heat transfer analysis of plenum during bypass conditions

Day	I_T(W/m^2)	T_{coll}(K)	T_{plen}(K)	T_{amb} (K)
9/20	675	327.8	326.3	306.3
8/3	463	319.3	318.6	305.9
8/1	278	311.4	311.4	303.1

Predicted wall temperature for the two cases is shown in Table 5.3.3. For case two, even though there is uncertainty of the convective heat transfer coefficient, the radiative heat transfer coefficient between the wall and the collector is larger and has more of an effect on the wall temperature. For all three data points, the predicted wall temperature for case one compared with the ASHRAE recommend U_{loss}=17 W/m^2 is lower than the predicted wall temperature for case two. Because the recommended ASHRAE coefficient is only an estimation, the results are not necessarily definitive to show that the collector cause unwanted heat gain. However, the results do suggest that the collector may cause additional cooling load on the building in the summer. Furthermore, the collector does not necessarily provide

cooling of the wall through natural convection in the plenum. This topic could use more investigation to verify theory with measured data on the wall temperature and characterize the flow in the plenum during bypass conditions.

Table 5.3.1 Predicted outer wall temperature versus total heat loss coefficient.

Solar Radiation (W/m2)	278
Collector Temperature (K)	311.4
Plenum Temperature (K)	311.4
Ambient Tempeature (K)	303.1

Case One		
Wind Speed (m/s)	U_{tot} (W/m^2C)	Twall,1 (K)
1	9.66	314.80
2	10.50	313.91
3	13.08	311.86
4	15.83	310.39
ASHRAE	17.00	309.91
5	18.52	309.36
6	21.12	308.60
7	23.66	308.03

Case Two		
$h_{rad,w-c}$ (W/m^2C)	$h_{conv,plen}$ (W/m^2C)	Twall,2 (K)
5.48	0.10	310.19
5.51	0.60	310.29
5.53	1.10	310.37
5.54	1.60	310.44
5.55	2.10	310.50
5.55	2.60	310.55

Solar Radiation (W/m2)	463
Collector Temperature (K)	319.3
Plenum Temperature (K)	318.6
Ambient Tempeature (K)	306.3

Case One		
Wind Speed (m/s)	U_{tot} (W/m^2C)	Twall,1 (K)
1	10.49	324.00
2	11.10	323.04
3	13.43	320.18
4	16.10	317.88
ASHRAE	17.00	317.28
5	18.75	316.24
6	21.34	315.01
7	23.86	314.07

Case Two		
$h_{rad,w-c}$ (W/m^2C)	$h_{conv,plen}$ (W/m^2C)	Twall,2 (K)
5.99	0.10	317.58
5.99	0.60	317.65
5.91	1.10	317.70
5.93	1.60	317.76
5.94	2.10	317.81
5.95	2.60	317.86

Solar Radiation (W/m2)	695
Collector Temperature (K)	327.8
Plenum Temperature (K)	326.3
Ambient Tempeature (K)	306.3

Case One		
Wind Speed (m/s)	U_{tot} (W/m^2C)	Twall,1 (K)
1	11.45	331.46
2	11.94	330.47
3	14.11	326.88
4	16.76	323.72
ASHRAE	17.00	323.50
5	19.45	321.38
6	22.08	319.62
7	24.66	318.26

Case Two		
$h_{rad,w-c}$ (W/m^2C)	$h_{conv,plen}$ (W/m^2C)	Twall,2 (K)
6.47	0.10	325.58
6.47	0.60	325.63
6.47	1.10	325.67
6.47	1.60	325.71
6.38	2.10	325.72
6.40	2.60	325.75

6 Economic Analysis and Application in NC

6.1 Economics

Results from the TRNSYS simulation of yearly energy savings were used to look at monetary savings from the installation of a transpired wall system in North Carolina. While these results did show that energy savings are significantly less than colder climates, the tax incentives in North Carolina help balance the actual payback for the system. North Carolina offers a 35% State Income Tax Credit for Renewable Energy Systems including solar water heating, active solar space heating, photovoltaics, wind energy systems, and biomass systems. For commercial and industrial facilities, the maximum amount of the tax credit is $250,000 and can be taken over 5 years. There is also currently a 10% federal tax credit for renewable energy systems installed on commercial or industrial facilities.

The estimated total system cost with an additional fan to meet minimum flow through the collector was around $63,000. The system cost can include the purchase and installation costs for the ventilation fans, but in most cases the ventilation system would be required. Therefore, only the cost of the installation of the collector will be used when looking at payback. However, the solar energy tax credit does apply to all equipment including distribution fans.

After the 35% North Carolina State Tax Credit and 10% Federal tax credit, the system cost is $34,700. Then the cost of the fan is subtracted from this value and the effective cost to the customer for the solar components is $10,400. Savings are compared to Madison, WI. Wisconsin has a State Rebate Program for solar water heating, solar space heating, photovoltaics, and wind energy for 25 % of the total cost up to $35,000. The reduced system cost with the Wisconsin rebate minus the fan cost around $17,000.

Yearly savings from the UTC system is calculated assuming the conventional gas heating system is 80% efficient. Currently, natural gas prices are fairly high in North Carolina with the industrial service rate at around $0.80/therm or $8.00/MMBTU (PSNC 2004). The savings is used to calculate a simple payback. The simple payback turns out to be around 5 to 7 years. Compared to Madison, WI, the North Carolina Tax Credit helps absorb the reduced savings from the warmer climate.

Table 6.1.1 Yearly monetary savings from the energy saved by using UTC system over conventional gas heating

City	Monetary Savings/yr	Simple Payback Not Including Ventilation Cost (yrs)
Raleigh, NC	$ 1,809	5.9
Asheville, NC	$ 2,014	5.3
Charlotte, NC	$ 1,921	5.6
Wilmington, NC	$ 1,451	7.4
Greensboro, NC	$ 2,139	5.0
Cape Hatteras, NC	$ 1,573	6.8
Madison, WI	$ 2,878	5.9

For a more detailed analysis, it is useful to use the P_1/P_2 method to calculate life cycle savings presented in Duffie and Beckman (1991). For the purposes of this study, this method is only used to determine if the life cycle savings is positive. The life cycle savings defined in term of P_1 and P_2 is:

$$LCS = P_1 C_{F1} L\mathsf{F} - P_2 (C_A A_C + C_E) \qquad (6.1.1)$$

where P_1 is the ratio of life cycle cost savings to first year fuel cost savings and P_2 is the ratio of life cycle expenditures incurred because of additional capital investment. P1 and P2 are calculated according equations outlines by Duffie and Beckman (1991) and the assumptions about interest rates and inflation rates are listed in Appendix C. As shown in figure 6.1.1, for the period of economic analysis of 10 years, there is a positive life cycle savings. However, this is only true for the case where the NC and federal tax credits are taken and the ventilation fans are not included in the initial cost of the system. If the fan cost is included, the life cycle cost is not positive for the estimated fuel savings in NC.

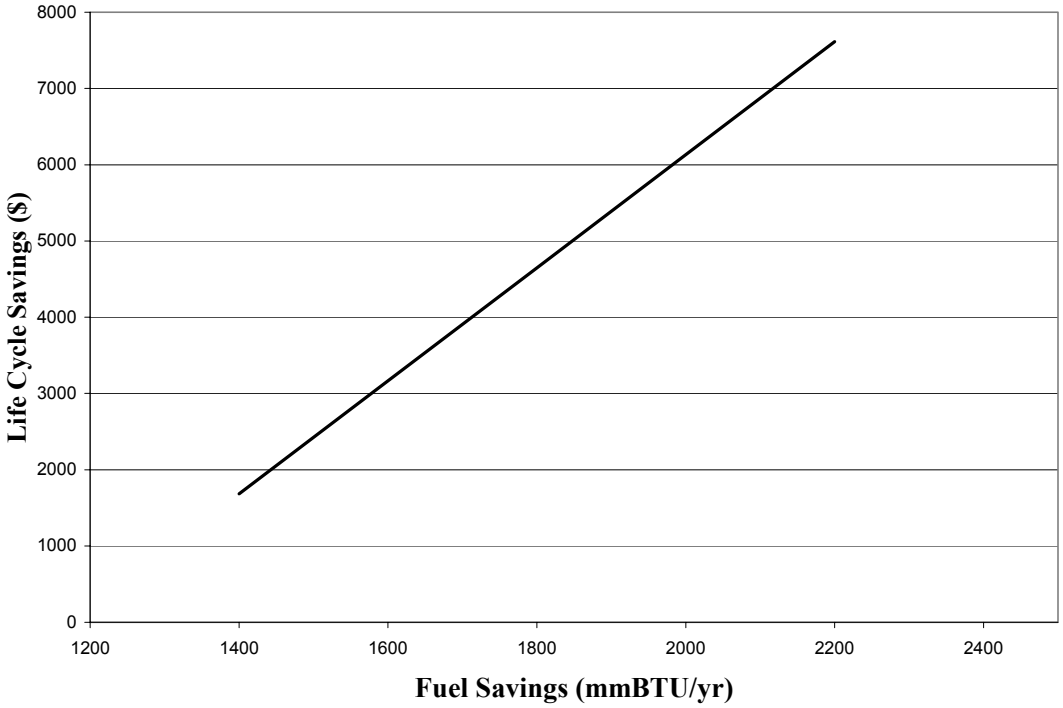

Figure 6.1.1 Estimated life cycle savings based on first year fuel savings for transpired collector system

6.2 Application in North Carolina

Most transpired collectors have been installed at industrial facilities and commercial buildings, but they are also currently marketed for the residential sector. These collector systems can be incorporated into new building design or retrofitted for existing buildings. In general, many industrial buildings have fairly high internal heat gain and therefore a low balance temperature for the building. An analysis was done for the potential of UTC systems in Wisconsin by Summers (1995), it was found that the energy savings only yields a life cycle savings for industrial buildings with a high ventilation rate and electric heating. Since this was an unlikely scenario, it was concluded that there was little potential in Wisconsin for using UTC systems in the industrial sector. As shown in the previous section, it is possible to yield a life cycle savings for a UTC system with auxiliary gas heat. However, it is only valid when the tax credits are taken into account and when the cost of the ventilation system is not included. The industrial sector consumes about 28% the energy use in North Carolina, however only 2.5% of this energy is used for space heating and cooling (State Energy Office

2003). Therefore, even though some facilities may be able to save money, heating is still only a low percentage of their overall energy expenses.

7 Discussion

7.1 Monitoring Results

While the transpired collector at Intek provided a substantial amount of heat compared to the energy expended, it did perform below expectations. The system reflected some shortfalls in the design. Any installation in North Carolina needs to have a properly controlled summer bypass damper, even if the system is only to be used for a portion of the year. The daily swings in temperature in the winter days create times where it may be uncomfortable to use this type of heating system without this element. The collector bypass damper would extend the season of use of the system and would also ensure the proper amount of ventilation air.

There was less destratification of the air than expected; heated air seemed to stay at ceiling level with or without the recirculation damper. Further investigation into air flow patterns in this building or a different air recirculation strategy may help bring more warm air to floor level. Etheridge and Sandberg (1996) provide a through discussion of building ventilation and air flow within rooms. Room air flow can be induced by momentum or buoyancy. The fan distribution system introduces momentum flow to the room. Likewise, the air distribution methods within a room can be classified as either controlled by momentum, buoyancy of the supplied air, or buoyancy of internal sources. Some general factors that will influence the flow pattern in a room include supply velocity, type and location of supply, and geometry of the room and obstacles within the room. In addition, with a non-isothermal supply where ventilation air is at a different temperature than room air, several other factors influence the air flow including the buoyancy flux of the air, the height of supply, whether the supply is positively or negatively buoyant relative to the room, heat loss coefficient for the room, and location of the auxiliary heaters. All of these issues apply to the success of the performance of the transpired collector.

In addition, the original control system allowed cold air to be delivered to the warehouse. Employees complained about the cold air and monitoring of the outlet air temperature confirmed that it was a problem. An inline heater seems essential and any solar heating system is supposed to have a backup or auxiliary heater. While the Intek facility had

some gas heaters, they were not sufficient to meet the heating load of this area of the building. This missing element caused the system to be turned off completely at night, during cloudy days, and even on days with a sufficient solar heating resource.

Another key realization of the monitoring study was about the awareness of this solar heating system. Instead of trying to address issues with this heating system, employees simply did not run the system. It is important that employees treat these systems as anything else in the workplace which requires periodic inspection and maintenance. It is essential to do follow-up studies on technologies for this reason. For systems like this that are not familiar to plant personnel, a higher level of customer support will be required if the supplier wants the customer to be satisfied. There is no payback for solar thermal systems which are not used.

7.2 TRNSYS Analysis

The new TRNSYS compared fairly well the previous model developed by Summers. A couple of minor errors in the old model were found and some improvements were made. First, there was an error in the equation for acceleration pressure drop. The old model assumed the maximum velocity to be the maximum velocity in the plenum. In reality, the air must be accelerated to the velocity at the fan outlet. The outlet velocity is significantly higher than the plenum velocity because the cross sectional area of the distribution duct is much smaller than the cross sectional area of the plenum. In addition, some small discrepancies were found in the Summers' equations for the difference in heat conduction through the south wall because of the installation of the transpired collector and were corrected in equations 4.1.17, 4.1.19, and 4.1.20.

There is still room for improvement to accurately model these collectors in TRNSYS. First, the run time for the new model is much longer because of the method used to solve the energy balance equations. Also, the improvements of making room temperature and recirculation temperature separate inputs cannot realize their full potential without a stratified building model. TRNSYS is wonderful for doing systems analysis, but certain aspects of the performance of these systems could be modeled better in other programs. Using a standard computational fluid dynamics software such as FLUENT would be extremely beneficial to understanding how the introduction of the warm make-up air affects the temperature

stratification in the room. Working out these issues are equally important to the performance of the transpired collector system and are worth evaluation in the future.

The previous results show that the difference between potential heat gain and energy savings is much larger for the warm climates of North Carolina, than for the colder climates of the Northeastern U.S. These results imply that the potential for overheating is much greater. One major assumption in the TRNSYS model is that the building remains at a constant temperature or has negligent capacitance. While this may be true for a building that remains at a constant setpoint temperature, without a capacitance model, the effect of overheating cannot properly be investigated. Ultimately, it may be better to separate the transpired collector component in TRNSYS from a building model.

7.3 Heat Transfer During Bypass Conditions

Initially, there was concern that the installation of the black surface on the south side of the building might actually increase the heat gain through this wall in the summer months. For the assumptions made, it seems that the presence of the collector does increase the wall temperature. This effect is due more to the radiation exchange between the collector and the wall than convective heating from the air in the plenum. While there was some speculation that natural convective airflow through perforations in the collector would cause cooling of the outer wall, the results seem to contradict this claim. The results are partly based on collected field data and theory. They are dependent on some of the assumptions made about the flow in the plenum, the temperature of the collector and plenum, the radiative properties of the collector and plenum (emmisivity and absorptivity), and the conductive properties of the wall.

To answer this question definitively, this topic would need further study. Experimentally, the question could be answered by taking measurements of the outer wall temperature exposed to solar radiation and a wall behind the collector exposed to the same solar radiation. To be able to analyze the effects of this for any application, it is necessary to know the velocity of the flow induced by natural convection and the flow in the plenum would have to be characterized.

7.4 Economics and Application in North Carolina

Despite the short heating season, transpired collectors may still be an acceptable investment in North Carolina. If a facility is required to have ventilation system, the cost of the ventilation system can be excluded from the overall cost of adding the solar heating system. With the NC State Tax Credit and the Federal Tax Credit, the cost to the customer becomes only 55% of the original cost. Based on these assumptions, the fuel savings can payback on a similar schedule to those of a cooler climate. However, the fuel savings is highly dependent on characteristics of the building such as ventilation requirements, desired room temperature, internal gains, etc. This fact leads to the conclusion that the application of these will have to be considered on a case by case basis.

8 Conclusions

The North Carolina Solar Center is responsible for outreach to the public about solar technologies and their application. The center has an industrial and commercial program to assist in evaluating the potential for integrating renewable energy systems into these sectors. There has been increasing interest in using unglazed transpired collector systems in this climate. North Carolina has a short heating season and long cooling season and consequently the energy savings will be less than in the Northeastern US and Canada where these collector systems are more common. A case study of a transpired collector system in North Carolina was done to understand the components of the system and evaluate the performance.

A data acquisition system was installed at an industrial facility in Aberdeen, NC and the system was monitored in 2003. There were some problems with the system design and operation to prevent it form working at its full potential. Measured flow through the collector was low causing the convective losses to be more significant. The collector did deliver warm air to the building, but often the air within the building remained stratified.

A TRNSYS component was built based on a model previously created by a student at the Solar Energy Laboratory at University of Madison Wisconsin. More recent studies of the transpired collector show that convective losses are more important on field installed corrugated collectors. Therefore, convective losses were included in the component. Some other changes were made to the component. To accurately predict and guarantee performance of the transpired collector, the model should be combined with simulation of flow dynamics and temperature stratification in a building.

A heat transfer analysis was done to look at the possibility of the collector causing additional heat gain to the building in the summer. The results show that it is possible that the collector causes unwanted heat gain in the summer. Additional investigation could be done to characterize the flow conditions in bypass mode and validate theory with experimental data.

Despite the short heating season, some industrial or commercial buildings could still benefit from the technology. The success of the technology depends on site characteristics and building conditions; therefore, transpired collector systems must be considered on a case

by case basis. Even if the system works well, space heating is only a minor portion of the energy used in industrial facilities in North Carolina.

References

Arulanandam, S. J., K.G.T. Hollands and E. Brundett. (1999). A CFD Heat Transfer Analysis of the Transpired Collector Under No-Wind Conditions. *Solar Energy* **67**(1-3), 93-100.

Brunger, A.P. (Ed.) (1999). Low-Cost, High Performance Solar Air Heating Systems Using Perforated Absorbers: A Report of Task 14 Air Systems Working Group. International Energy Agency.

Duffie, J.A. and W.A. Beckmann. (1991). Solar Engineering of Thermal Processes. New York: John Wiley and Sons.

Dymond C. and Kutscher C. F. (1995). A computer design model for transpired solar collector systems. Proceedings of the ASME,JSME,JSES International Solar Energy Conference, Maui, HA, USA. ASME. Vol. **2**, 1165-1174.

Dymond, C. and C. Kutscher. (1997). Development of a Flow Distribution and Design Model for Transpired Solar Collectors. *Solar Energy* **60**, 291-300.

Etheridge, D.W. and M. Sandberg. *Building ventilation: theory and measurement.* New York : John Wiley & Sons.

Fleck, B.A., R.M. Meier and M.D. Matovic. (2002). A Field Study of the Wind Effects on the Performance of an Unglazed Transpired Solar Collector. *Solar Energy* **73** (3), 209-216.

Golneshan, A.A. and K.G.T Hollands. (2000). Forced Convection Experiments on Slotted Transpired Plates.

Gunnewiek, L. H., E. Brundett, and K.G.T. Hollands. (1996). Flow Distribution in Unglazed Transpired Plate Solar Air Heaters of Large Area. *Solar Energy* **58**, 227-237.

Gunnewiek, L. H., E. Brundett, and K.G.T. Hollands. (2002). Effect of Wind in Flow Distribution in Unglazed Transpired Plate Collectors. *Solar Energy* **72**(4), 317-325.

Hollick, J. C. (1990) Conserval Solarwall: Air Heating Design Manual. Buffalo, NY: Conserval Engineering, Inc.

Incorpera, F.P. and D.P. Dewitt (2002) Introduction to Heat Transfer. *External Flow* (pp.364-375) *Free Convection* (pp.496-533) New York: John Wiley and Sons.

Kutscher, C.F. and C.B. Christensen. (1993). Unglazed Transpired Solar Collectors. Advances in Solar Energy: An Annual Review of Research and Development, Vol. 7. Boulder, CO: ASES.

Kutscher, C.F., C.B. Christensen, and G.M. Barker. (1993) Unglazed Transpired Solar Collectors: Heat Loss Theory. *Journal of Solar Energy Engineering* **115**, 182-188.

Kutscher, C.F. (1994). Heat Exchange Effectiveness and Pressure Drop for Air Flow Through Perforated Plates With and Without Crosswind. *Journal of Heat Transfer* **116**, 391-399.

PSNC Energy (2004) Commercial Gas Service Rates. Accesses April 2004 **www.scana.com/PSNC+Energy/In+Business/Commercial+Gas+Services/Rates.htm**

Schlichting, H. (1979). Boundary-layer theory. New York: McGraw Hill.

Solar Energy Laboratory. (2002) Transient Systems Simulation Program. Accessed April 2004 from **http://sel.me.wisc.edu/trnsys/**

State Energy Office, North Carolina Department of Administration and Appalachian State University Energy Center. (2003). North Carolina State Energy Plan.

Summers, D. (1995). Thermal Simulation and Economic Assessment of Unglazed Transpired Collector Systems. M.S. Thesis. University of Wisconsin at Madison.

Van Decker, G.W.E., K.G.T Hollands, and A. P. Brunger. (1996). Heat Exchange Effectiveness of Unglazed Transpired-Plate Solar Collector in 3-D Flow. Proceedings from EuroSun. pp. 130-135.

Van Decker, G.W.E. and K.G.T. Hollands. (1999). An Empirical Heat Transfer Equation for the Transpired Collectors Including No-Wind Conditions. Proceedings from Solar World Congress.

Van Decker, G.W.E. Hollands, K.G.T. and A.P. Brunger. (2001). Heat Exchange Relations for Unglazed Transpired Collectors with Circular Holes on Square or Triangular Pitch. *Solar Energy* **71** (1), 33-45.

Appendix A

```
SUBROUTINE TYPE99 (TIME,XIN,OUT,T,DTDT,PAR,INFO,ICNTRL,*)
C**********************************************************************
C Object: Type99-UTC
C IISiBat Model: Type99-UTC
C
C Author: C.C. Maurer based on work by Summers
C Editor: C.C. Maurer
C Date:   30/1/2004 last modified: 30/1/2004
C
C
C ***
C *** Model Parameters
C ***
C                       1)Area   m^2 [-Inf;+Inf]
C                       2)Collector Emissivity      - [-Inf;+Inf]
C                       3)Collector Absorptivity    - [-Inf;+Inf]
C                       4)Height            m [-Inf;+Inf]
C                       5)Diameter          m [-Inf;+Inf]
C                       6)Pitch   m [-Inf;+Inf]
C                       7) Plenum Depth m [0,+Inf]
C                       8)Corrugation Factor        dimensionless [-Inf;+Inf]
C                       9)Porosity          dimensionless [-Inf;+Inf]
C                       10)Ratio - [-Inf;+Inf]
C                       11)UA Wall        W/K [-Inf;+Inf]
C                       12)Emissivity Inside Wall - [-Inf;+Inf]
C                       13)Absorptivity Inside Wall
C                       14)UA Building   W/K [-Inf;+Inf]
C                       15)Bypass Temperature     C [-Inf;+Inf]
C ***
C *** Model Inputs
C ***
C                       1) Hour  - [-Inf;+Inf]
C                       2) Solar Radiation            W/m^2 [-Inf;+Inf]
C                       3) Amb Temp      C [-Inf;+Inf]
C                       4) Wind m/s [-Inf;+Inf]
C                       5) Dew Point       C [-Inf;+Inf]
C                       6) Max. Flow Rate through Collector           kg/s [-Inf;+Inf]
C                       7) Min. FLow Rate though collector            kg/s [-Inf;+Inf]
C                       8) Atm Pressure   Pa [-Inf;+Inf]
C                       9) Room Temp    C [-Inf;+Inf]
c                       10) Internal Gains kJ/hr [0,+Inf]
C                       11) Night Bypass = 0 if none, = 1 if enabled
C ***
C *** Model Outputs
C ***
C                       1) Surface Temperature C [-Inf,+Inf]
C                       2) Plenum Temperature C [-Inf,+Inf]
C                       3) Outlet Temperature       C [-Inf;+Inf]
C                       4) Mix Temperature          C [-Inf;+Inf]
C                       5) Mass Fraction of Outside Air [0,1]
C                       6) Mass Fraction of Recirculated Air [0,1]
```

```
C                       7) Effectiveness   - [-Inf;+Inf]
C                       8) Efficiency      - [-Inf;+Inf]
C                       9) Total Pressure Drop      Pa [-Inf;+Inf]
C                       10) Heat Gain      W [-Inf;+Inf]
C                       11) Auxilliary Heat to Transpired Collector  W [-Inf;+Inf]
C                       12) Base heating for regular ventilation [-Inf,+Inf]
C                       13) Savings of auxilliary heating
C                       14) Reduced Conduction Heat Loss
C                       15) Fan Power
c                       16) Bypass Output
C ***
C *** Model Derivatives
C ***

C (Comments and routine interface generated by IISiBat 3)
C**********************************************************************

C               STANDARD TRNSYS DECLARATIONS
                        DOUBLE PRECISION XIN,OUT
                        INTEGER NI,NP,ND,NO
                        PARAMETER (NI=12,NP=17,NO=16,ND=0)
                        INTEGER*4 INFO,ICNTRL
                        REAL T,DTDT,PAR,TIME
                        DIMENSION XIN(NI),OUT(NO),PAR(NP),INFO(15)
                        CHARACTER*3 YCHECK(NI),OCHECK(NO)

C       Inputs
        real*8 mflow,minflow,pamb,lowg,hig,oldg, prair,nuht
        real*8 pcoll,pfric,pbuoy,pacc,ptot,perp
        real*8 gamma, gmin, check, dif
        real*8 qaux1, qbldgbase, qbldgloss, qbldg
        integer hr,j, jmax, bypnite,bypout



C---------------------------------------------------------------------

C               IF ITS THE FIRST CALL TO THIS UNIT, DO SOME BOOKKEEPING
                        IF (INFO(7).GE.0) GO TO 100

C               FIRST CALL OF SIMULATION, CALL THE TYPECK SUBROUTINE TO CHECK
THAT THE
C               USER HAS PROVIDED THE CORRECT NUMBER OF INPUTS,PARAMETERS,
AND DERIVS
                        INFO(6)=NO
                        INFO(9)=1
                        CALL TYPECK(1,INFO,NI,NP,ND)

                        open (unit=99,file='debug99.dat',status='replace',buffered='no')


                        RETURN 1

C               END OF THE FIRST ITERATION BOOKKEEPING

C---------------------------------------------------------------------
```

```
C                GET THE VALUES OF THE PARAMETERS FOR THIS COMPONENT
100      CONTINUE

                         area=PAR(1)
                         ecoll=PAR(2)
                         absor=PAR(3)
                         ht=PAR(4)
                         Diam=PAR(5)
                         Pitch=PAR(6)
                         depth=PAR(7)
                         CF=PAR(8)
                         Por=PAR(9)
                         Ratio=PAR(10)
                         UAw=PAR(11)
                         EWall=PAR(12)
                         awall=PAR(13)
                         UAb=PAR(14)
                         Tbypass=PAR(15)
                         Fans=PAR(16)
                         diafan=PAR(17)
C                GET THE VALUES OF THE INPUTS TO THIS COMPONENT
                         Hour=XIN(1)
                         rad=XIN(2)
                         Tamb=XIN(3)
                         Wind=XIN(4)
                         Tdp=XIN(5)
                         flow=XIN(6)
                         flowmin=XIN(7)
                         AtmPres=XIN(8)
                         Troom=XIN(9)
                         Qint=XIN(10)
                         bypnite=XIN(11)
                         Trecirc=XIN(12)
C-----------------------------------------------------------------------
C****
C****Define constants
C****
          cp=1007
          hfilm=17
          fric=0.05
C*****Define other geometric parameters of plenum/collector***
          width=area/ht
          Ap=width*depth
          Perp=2*width+2*depth
          Dh=4*Ap/Perp
          areasur=area*ratio
          aduct=3.14*(diafan**2)/4
C*****Convert Solar Radiation from kJ/hr/m2 to W/m2**********
          rad=rad*1000/3600
C*****Convert Temps to Kelvin and Calculate Sky Temp**********
          Tamb=Tamb+273.15
          Pamb= atmpres*1000
          Tbypass=Tbypass+273.15
          Tsky=(Tamb)*(0.689+0.0056*Tdp+0.000073*(Tdp**2)+
     +                         0.00012*Pamb)**0.25
```

```
      Tgr=Tamb
      Tsur=(Tsky+Tgr)/2
      Troom=Troom+273.15
      Trecirc=Trecirc+273.15
      Tsolair=Tamb+awall*rad/hfilm
      Troomavg=(Trecirc+Troom)/2
C****
C****Convert volumetric flow to mass flow
C****
      dens=atmpres*100000/287/Tamb
      mflow=flow/3600*dens
      minflow=flowmin/3600*dens
C****
C****Introduce variables to check equation validity and convergence
C****
      tiny=0.01
      jmax=100
C*************************************************************************
C     Solve heat balance equations for collector operation. First, solve for
C     collector,plenum, and outlet temperatue for minimum flow rate through
C     collector. For the minimum flow rate, the heat loss from the building
C     and required ventilation supply temperature is calculated.  Based on
C     the outlet temperature and fraction of the mass flow, a mixed air
C     temperature is calculated. If the mixed air temperature is greater than
C     needed supply temperature, then collector outlet temperature and needed
C     supply temperature are solved for case where collector flow is equal
C     to maximum collector flow.  Then, a bisection method is used to minimize
C     auxiliary heating.  This strategy is based almost completely on the
C     previous transpired collector model in TRNSYS developed by Summers (1995).
C*************************************************************************
C
C*****SOlve for heating load on building*******
      Qbldgloss=UAb*(Troomavg-Tamb)
      Qwallloss1=UAw*(Troomavg-Tsolair)
C*****Solve temperatures for minimum flow rate*******************************
      if(Tamb.lt.Tbypass) then
            bypout=0
            gmin=minflow/mflow
            gamma=gmin
      call colltemp (wind,dens,ht,vel,por,diam,pitch,cp,cf,red,ap,
     +ewall,ecoll,area,UAw,Troom,Tsur,areasur, mflow,Tamb,rad,
     +gamma, absor, Tcollnew, Twallnew,Tplennew,Toutnew,err,Qin,effhx)
            Qwallloss2=Uaw*(Troomavg-Tplennew)
            Qbldg=Qbldgloss+Qwallloss2-Qint
            Qconddiff=UAw*(Tplennew-Tsolair)
            Tsup=Troomavg+Qbldg/(mflow*cp)
            Tmix=gamma*Toutnew+(1.0-gamma)*Trecirc
            if(tmix.lt.Tsup) then
                  qaux1=mflow*cp*(Tsup-Tmix)
            else
C*****Solve temps provided by maximum flow rate through collector************
                  qaux1=0.0
                  gamma=1.0
      call colltemp (wind,dens,ht,vel,por,diam,pitch,cp,cf,red,ap,
     +ewall,ecoll,area,UAw,Troom,Tsur,areasur, mflow,Tamb,rad,
     +gamma, absor, Tcollnew, Twallnew,Tplennew,Toutnew,err,Qin,effhx)
```

```
                        Tmix=Toutnew
                        Qconddiff=UAw*(Tplennew-Tsolair)
C*****Use Bisection method to minimize auxiliary heating**********************
                        if(Tmix.lt.Tsup) then
                                j=0
                                lowg=gmin
                                hig=1.0
                                gamma=(lowg+hig)/2.0
 150                            continue
                                j=j+1
        call colltemp (wind,dens,ht,vel,por,diam,pitch,cp,cf,red,ap,
    +ewall,ecoll,area,UAw,Troom,Tsur,areasur, mflow,Tamb,rad,
    +gamma, absor, Tcollnew, Twallnew,Tplennew,Toutnew,err,Qin,effhx)
                                tmix=gamma*Toutnew+(1.0-gamma)*Trecirc
                                Qconddiff=UAw*(Tplennew-Tsolair)
                                if(tmix.lt.tsup) then
                                        hig=gamma
                                else
                                        lowg=gamma
                                endif
                                oldg=gamma
                                gamma=(lowg+hig)/2.0
                                check=gamma-oldg
                                dif=ABS(check)
                                if(dif.gt.tiny.and.j.lt.jmax) go to 150
                                if(j.ge.jmax) then
                                write (99,*) time,'**no convergence in j loop**'
                                end if
                        end if
                end if
C*****Calculate auxiliary heating and heat gain for collector*********
                if(Tsup.gt.Tmix) then
                Qaux1=mflow*Cp*(Tsup-Tmix)
                end if
                Qgain=mflow*gamma*Cp*(Toutnew-Tamb)
                If(Qgain.lt.0) then
                        Qgain=0
                end if
        end if
        if(rad.gt.0) then
                effic=mflow*gamma*Cp*(Toutnew-Tamb)/rad/area
                qabs=qin
                If(effic.lt.0) then
                        effic=0
                end if
        else
                qabs=0
        end if
C*************************************************************************
C    Define ouputs for bypass conditions where outlet temperature is equal
C    the ambient temperature.  Air is not drawn through collector, therefore
C        solar efficiency, heat gain, auxiliary heating are zero.
C*************************************************************************
        if(Tamb.ge.Tbypass) then
                gamma=gmin
                Tmix=Tamb
```

```
                effhx=0
                effic=0
                Toutnew=Tamb
                Qgain=0
                Qaux1=0
                bypout=1
                Tcollnew=273.15
                Tplennew=273.15
                qconddiff=0
        end if
C*****************************************************************
C       Calculate efficiency of collector.  For case with low solar radiation,
C       efficnicy is zero.
C       Look at case with bypass damper enabled for nightime.  Air is not
C       drawn through collector and only minumum amount of air is drawn
C       into the room directly from outside.
C*****************************************************************
        if(bypnite.ge.0.99) then
        if(rad.lt.1) then
                effic=0
                effhx=0
                Tplennew=Tamb
                Toutnew=Tamb
                Tmix=Tamb
                Tcollnew=273.15
                Twallnew=273.15
                bypout=1
                qconddiff=0
                gamma=gmin
        end if
        end if
        if(bypnite.le.0.01) then
        if(rad.le.1) then
                qconddiff=UAw*(Tplennew-Tamb)
                bypout=0
                if(Tamb.ge.Tbypass) then
                        gamma=gmin
                        Tmix=Tamb
                        effhx=0
                        effic=0
                        Toutnew=Tamb
                        Qgain=0
                        Qaux1=0
                        bypout=1
                        Tcollnew=273.15
                        Tplennew=273.15
                        qconddiff=0
                end if
        end if
        end if

C*****************************************************************
C       Calculate energy savings.  First, calculate heat required for base
C       case, a building with no transpired collector.  Then subtract auxiliary
C       heating from the base heating.  This approach is different from
C       looking only at collector heat gain because sometimes collector will
```

```
C       provide more heat than is needed.
C*************************************************************************
        If(Tamb.lt.Tbypass) then
                Qbldgbase=Qbldgloss+Qwallloss1+minflow*Cp*(Troomavg-Tamb)-Qint
        else
                Qbldgbase=0
        end if
        Qsave=Qbldgbase-Qaux1
C       Setup output for mass flow
        flow1=mflow*gamma
        flow2=mflow*(1-gamma)
C*************************************************************************
C       Calculate total pressure drop by adding up the collector pressure drop,
C       friction pressure drop, buoyancy pressure drop, and acceleration
C       pressure drop.  The method outlined by either Kutshcer (1995) or
C       Summers (1995) was used.  With total pressure drop, fan power is
C       estimated.   Note: the correlation for nondimensional
C       pressure drop across the collector was developed for a plate with holes
C       on a triangular pitch.
c*************************************************************************
        zi=6.82*(((1-por)/por)**2)*red**(-0.236)
        pcoll=dens*(vel**2)*zi/2
        dens2=atmpres*100000/287/Toutnew
        densavg=(dens+dens2)/2
        Vplenmax=gamma*mflow/dens/ap
        Vfanout=mflow/dens/aduct
        Vplenavg=Vplenmax/2
        pfric=fric*ht*densavg*(Vplenavg**2)/2/Dh
        pbuoy=(dens2-dens)*9.81*ht
        pacc=densavg*(Vfanout**2)/2
        ptot=pcoll+pfric-pbuoy+pacc
        Fanp=mflow*gamma*ptot/dens
C*************************************************************************
C       Although all equations were solved in Watts, outputs with power units
C       will be changed to kJ/hr.  The output temperatures will be changed from
C       Kelvin to Celcius
C*************************************************************************
        Tcollnew=Tcollnew-273.15
        Tplennew=Tplennew-273.15
        Toutnew=Toutnew-273.15
        Tmix=Tmix-273.15
        Trecirc=Trecirc-273.15
        Qgain=Qgain*3600/1000
        Qaux1=Qaux1*3600/1000
        Qbldgbase=Qbldgbase*3600/1000
        Qsave=Qsave*3600/1000
        Qconddiff=Qconddiff*3600/1000
        Qabs=Qabs*3600/1000
        Fanp=Fanp/1000
C               SET THE OUTPUTS
200     CONTINUE
C               Surface Temperature
                        OUT(1)=Tcollnew
C               Plenum Temperature
                        OUT(2)=Tplennew
C               Outlet Temperature
```

```
                        OUT(3)=Toutnew
C                   Mixed Air Temperature
                        OUT(4)=Tmix
C                   Mass Fraction of Outside Air
                        OUT(5)=flow1
C                   Mass fraction of recirculated air
                        OUT(6)=flow2
C                   Effectiveness
                        OUT(7)=Effhx
C                   Solar Efficiency
                        OUT(8)=Effic
C                   Energy Absorbed by Collector
                        OUT(9)=Qabs
C                   Heat Gain
                        OUT(10)=Qgain
C                   Auxiliary Heat to transpired collector
                        OUT(11)=Qaux1
C                   Base heating for regular ventilation
                        OUT(12)=Qbldgbase
C                   Savings on Auxiliary Heating
                        OUT(13)=Qsave
C                   Difference in Building heat loss because of collector
                        OUT(14)=Qconddiff
C                   Fan Power
                        OUT(15)=fanp
C                   Bypass Output
                        OUT(16)=BYPOUT
                        RETURN 1
                        END
C-------------------------------------------------------------------
        subroutine colltemp (wind,dens,ht,vel,por,diam,pitch,cp,cf,red,ap,
     +  ewall, ecoll,area,UAw,Troom,Tsur,areasur,mflow,Tamb,rad,gamma,
     +  absor,Tcollnew, Twallnew,Tplennew,Toutnew,err,Qin,effhx)
C       Inputs
        real*8 mflow,minflow,pamb,lowg,hig,oldg, prair,nuht
        real*8 pcoll,pfric,pbuoy,pacc,ptot,perp
        real*8 gamma, gmin, check, dif
        integer hr,j, jmax, bypnite,bypout
C*********************************************************************
C       Define constants and flow velocities
C*********************************************************************
        vis=(0.0000171)*((Tamb/273)**0.7)
        tc=(0.00008)*tamb+0.0026
        sigma=0.0000000567
        vel=gamma*mflow/dens/area
        Vplenmax=gamma*mflow/dens/ap
        Vplenavg=Vplenmax/2
C*********************************************************************
C       Estimate Heat Loss Coefficients/Effhx with Kutscher model
C*********************************************************************
        if(vel.gt.0) then
                hc=cf*0.82*wind*vis*dens*cp/vel/ht
                Red=vel/por*diam/vis
                dnu=2.75*(((pitch/diam)**(-1.21))*red**0.43+
     +          0.011*por*red*(wind/vel)**0.48)
                U=dnu*tc/diam
```

```
                units=(1-por)*U/dens/vel/cp
                effhx=1-exp(-units)
C*************************************************************************
C       Find heat transfer coefficient for wall to air to determine
C       additional heating that occurs in plenum
C*************************************************************************
                prair=0.7
                replen=vplenavg*ht/vis
                if(replen.gt.500000) then
                        nuht=(0.037*(replen**0.8)-871)*(Prair**(1/3))
                else
                nuht=0.664*(replen**0.5)*(Prair**(1/3))
                end if
                hconvwa=nuht*tc/ht
C*************************************************************************
C       Estimate Surface Temp/Efficiency from Model.  Guess Collector and wall
C       temperature and solve heat balance equations.  The solutions are wall
C       and collector temperatures that minimize error in the solving of the
C       heat balance.
C*************************************************************************
                err=1000000000
                Do Twall=250,330,0.5
                        Do Tcoll=250,330,0.5
                                Uw=UAw/area
                                Unew=(1/((1/Uw)-(1/hconvwa)))
                                Qconvwa=hconvwa*area*(Twall-(effhx*(Tcoll-Tamb)+Tamb))
                                Qradwc=sigma*area*(Twall**4-Tcoll**4)/(1/ewall+1/ecoll-1)
                                Qcondwall=Unew*area*(Troom-Twall)
                                Qconvloss=areasur*hc*(Tcoll-Tamb)
                                Qradloss=ecoll*sigma*areasur*(Tcoll**4-Tsur**4)
                                Qconvca=mflow*gamma*cp*(effhx*(Tcoll-Tamb))
                                Qin=area*rad*absor
                                f1=Qconvwa+Qradwc-Qcondwall
                                f2=Qconvloss+Qradloss+Qconvca-Qin-Qradwc
                                errnew=(f1**2+f2**2)**0.5
                                Tplen=effhx*(Tcoll-Tamb)+Tamb
                                Tout=Qconvwa/mflow/gamma/Cp+Tplen
                                if(errnew.lt.err) then
                                        err=errnew
                                        Twallnew=Twall
                                        Tcollnew=Tcoll
                                        Tplennew=Tplen
                                        Toutnew=Tout
                                end if
                        End do
                End do
        end if
        return

        end
```

Appendix B

```
C ***********************************************************************
C       This program is for analyzing heat transfer in the plenum when
C       a trasnpired collector is operating in bypass mode.  Natural
C       convection will be induced in the plenum from heating of the heating
C       of air in the collector
***********************************************************************
        real*8 k, Nuwnat, Nuwfor, Nuplnat, pr, num
        real*8 dens, visd, visk, alp, pamb, patm, psat, prat
        open (unit=13,file='heatxfer3.dat',status='replace',buffered='no')
C
C*****Enter plenum and collector assumptions**********
        depth=0.203
        ht=5
        patm=101325
        Troom=295.4
        sigma=0.0000000567
        absw=0.44
        ewall=0.9
        ecoll=0.9
        uw=0.5675
        ho=17
C
C*****Enter Inputs (Variables) for collector**********
        Tcoll=327.8
        Tplen=326.3
        Tamb=306.3
        Tdp=14
        rad=695
        twall1=Tcoll
C
C*****Calculate other needed variables*********************
        S=rad*Absw
        tgr=Tamb
        pAMB=patm/100
        Tsky=(Tamb)*(0.689+0.0056*Tdp+0.000073*(Tdp**2)+
   +                    0.00012*Pamb)**0.25
    Tsur=(Tgr+Tsky)/2
C
C*****Write assumptions to output file*********************
        Write(13,*) 'Ewall=', Ewall
        Write(13,*) 'Solar=',rad,'height=', ht
        write(13,*) 'Tplen=', Tplen, 'Tamb=', Tamb,'Tcoll=',Tcoll
        write(13,*) 'Case 1:'
        write(13,*) 'Utot       Wind         Twall       Tsolair'
C
C***********************************************************************
C       Calculate the wall temperature for case one based on forced
C       convection for various wind speeds. Establish film temperature
C       and calculate Air Properties.  Intially, outer wall temperature
C       is assumed to be the same as the collector temperature. The program
C       iterates for the wall temperature.
C***********************************************************************
```

```
      Do wind=1,7,1
      Do j=1,50
      Tf=(Twall1+Tamb)/2
      Tavg=(Twall1+Tsur)/2
      Beta=1/Tf
      g=9.81
      Cp=1007
      Pr=0.71
      dens=patm/287/Tf
      visd=(0.0000171)*((Tf/273)**0.7)
      visk=visd/dens
      k=(0.00008)*tf+0.0026
      alp=k/dens/Cp
C
C*****Calculate Nusselt Number/HTC for Natural Convection for case one
      Rawnat=g*beta*(Twall1-Tamb)*(ht**3)/visk/alp
      Nuwnat=(0.825+((0.387*(rawnat**(0.16667)))/((1+((0.492/Pr)
     +      **(0.5625)))**(0.2963))))**2
      hconvnat=Nuwnat*k/ht
C
C*****Calculate forced convection coefficient, radiative loss coefficient,
C     and overall loss coefficient.  Calculated the outer wall temp.
      Rewin=dens*wind*ht/visd
      if(Rewin.lt.500000) then
            Nuwfor=0.664*(Rewin**0.5)*(Pr**0.333333)
      end if
      if(Rewin.ge.500000) then
            Nuwfor=(0.037*(Rewin**0.8)-871)*(Pr**0.333333)
      end if
      hconvfor=Nuwfor*k/ht
      hradloss=4*sigma*ewall*(Tavg**3)*(Twall1-Tsur)/(Twall1-Tamb)
      hconvtot=(hconvnat**3+hconvfor**3)**(0.3333333)
      Rcond=1/Uw+1/hconvnat
      Rloss=1/(hradloss+hconvtot)
      Utot=(Hradloss+hconvtot)
      Two1=(S*Rloss*Rcond+Tamb*Rcond+Troom*Rloss)/(Rcond+Rloss)
C*****Check assumption about wall temperature to find properties and iterate
      if(abs(Twall1-Two1).lt.0.001) then
            go to 100
      end if
      Twall1=Two1
100   end do
C
C*****Calculate the Sol-air temperature for the outer wall based on the
C     calculated overall heat transfer coefficient
      Tsolair=Tamb+absw*rad/Utot
      write(13,*) Utot, wind, Two1, Tsolair
      end do
C****Calculate the Sol-air temperature for the outer wall based on the
C     ASHRAE recommended outer wall total heat trasnfer coefficient of
C      17 W/m2 and the wall temperature for thsi overall heat trasnfer
C     coefficient
      Tsolairbase=Tamb+absw*rad/ho
      Twallbase=(S*(1/ho)*Rcond+Tamb*Rcond+Troom*(1/ho))/(Rcond+(1/ho))
      write(13,*) ho,'ASHRAE', Twallbase, Tsolairbase
C*********************************************************************
```

```
C       Calculate Wall Temperature for case 2 for assumed values of the
C       heat transfer coefficient between the wall and the air in the plenum.
C       An intial guess is made at the radiative heat trasnfer coefficient
C       to predict a wall temperature.  The program then checks the assumption
C       and iterates.
C*********************************************************************
        write(13,*) 'Case 2:'
        write(13,*) 'hradcw       hconvplen       hconvnat       Twall2'
        Do hconvplen=0.1,2.6,0.5
        hradcw=1.0
                Do k=1,100
                Rplen=1/hconvplen
                Rrad=1/hradcw
                Two2=(Tcoll*Rplen*Rcond+Tplen*Rrad*Rcond+Troom*Rrad*Rplen)/
   +     (Rrad*Rplen+Rplen*Rcond+Rrad*Rcond)
                hradnew=sigma*(Tcoll**2+Two2**2)*(Tcoll+Two2)/
   +     (((1-ewall)/ewall)+1+((1-ecoll)/ecoll))
                if(abs(hradnew-hradcw).lt.0.1) then
                        go to 200
             end if
                hradcw=hradnew
200             end do
                write(13,*) hradcw, hconvplen, hconvnat, Two2
        end do
        write(13,*)
        Write(13,*)
        end
```

Appendix C

Calculations and Assumptions used for P1,P2 Method

Income or Non Income Producing (1 or 0)	C	0
Effective Income Tax Rate	tbar	40%
Period of Economic Analysis	Ne	10.0
Fuel Inflation Rate	iF	5%
Discount Rate	d	10%
Inflation Rate	i	3%
Annual Mortgage	m	8%
Ratio of Down Payment to Initial Investment	D	20%
Years over which mortgage payment contribute to analysis	Nmin	10.0
Years over which depreciation contribute to analysis	N'min	10.0
Term of Loan	NL	10.0
Depreciation Lifetime	ND	10.0
Ratio first year Miscellaneous Costs to initial Investment	Ms	3%
Ratio of assessed Valuation of Solar energy System in first year to initial investment in the system	V	1
Ratio of resale value at end of period to initial investment	Rv	0.4
Property Tax Rate based on Assessed Value	t	2%

Present Worth Factor (Nmin,0,d)		6.14
Present Worth Factor (Nmin',0,d)		6.14
Present Worth Factor (Nmin,m,d)		8.38
Present Worth Factor (NL,0,m)		6.14
Present Worth Factor (Ne,i,d)		6.88
Present Worth Factor (Ne,if,d)		7.41
Ratio of Life Cycle Cost Savings to First Year Fuel Cost Savings	P1	7.41
Ratio of Life Cycle Expenditures Incurred because of Additional Capital Investment	P2	0.9

	Without Tax Credit	With Tax Credit
First Year Fuel Savings	$ 2,000.00	$ 2,000.00
Cost of Area dependent	$132	$72.60
Area of Collector	277	277
Cost of Shipping/Miscellaneous	1900	1900
Cost of equipment independent of collector	$24,000	$13,200
Total System Cost	$62,464	$34,355
Life Cycle Cost Savings (incuding ventilation in initial cost)	($41,720)	($16,277)
Life Cycle Cost Savings (not incuding ventilation in initial cost)	($19,314)	$6,130

P1/P2 Ratio	7.9
(CE+CA*A)/(CFFQtrad) (inc vent, no tax)	31.2
(CE+CA*A)/(CFFQtrad) (inc vent, tax cred)	17.2
(CE+CA*A)/(CFFQtrad) (no vent, no tax)	19.2
(CE+CA*A)/(CFFQtrad) (no vent with tax cred)	5.2